

Recent Development of Sandwich Assay Based on the Nanobiotechnologies for Proteins, Nucleic Acids, Small Molecules, and Ions

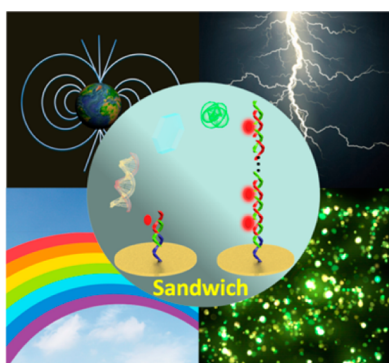
Juwen Shen,^{II,†} Yuebin Li,^{†,§,‡} Haoshuang Gu,[§] Fan Xia,^{*,†} and Xiaolei Zuo^{*,‡}

[†]Key Laboratory for Large-Format Battery Materials and System, Ministry of Education, School of Chemistry and Chemical Engineering, Huazhong University of Science and Technology (HUST), Wuhan 430074, China

[‡]Division of Physical Biology and Bioimaging Center, Shanghai Synchrotron Radiation Facility, Shanghai Institute of Applied Physics, Chinese Academy of Science, Shanghai 201800, China

[§]Hubei Collaborative Innovation Center for Advanced Organic Chemical Materials, Faculty of Physical and Electronic Sciences, Hubei University, Wuhan 430062, China

^{II}Key Laboratory of Systems Biology, Shanghai Institutes for Biological Sciences, Chinese Academy of Sciences, Shanghai 200031, China



CONTENTS

- 1. Introduction
- 2. Principles of the Sandwich Assay
- 3. Sandwich Assay for Protein Detection
 - 3.1. Sandwich Radioimmunoassay
 - 3.2. Sandwich Colorimetric Assay
 - 3.2.1. Colorimetric Assay Based on a Traditional Enzyme
 - 3.2.2. Colorimetric Assay Based on Biomimetic Nanomaterials
 - 3.3. Fluorescence Sandwich Immunoassay
 - 3.3.1. Organic Dyes as Fluorophores
 - 3.3.2. Nanomaterials as Fluorophores
 - 3.3.3. Conjugated Polymers as Fluorophores
 - 3.4. Electrochemical Sandwich Immunoassay
 - 3.4.1. Application of a Redox Label
 - 3.4.2. Application of Enzyme-Based Amplification
 - 3.4.3. Application of Nanomaterials
 - 3.5. Other Sandwich Assays
 - 3.5.1. Giant Magnetoresistive (GMR) Sandwich Assay
 - 3.5.2. Localized Surface Plasmon Resonance (LSPR) Sandwich Assay
- 4. Sandwich Assay for Nucleic Acids Detection
 - 4.1. Fluorescence Nucleic Acid Sandwich Assay
 - 4.1.1. Organic Dyes as Fluorophores
 - 4.1.2. Nanomaterials as Fluorophores

A	4.2. Electrochemical Nucleic Acid Sandwich Assay	R
B	4.2.1. Application of Redox Labels	R
C	4.2.2. Application of Enzyme-Based Amplification	S
D	4.2.3. Application of Nanomaterials	X
E	4.3. Colorimetric Nucleic Acid Sandwich Assay	Y
F	4.3.1. Colorimetric Assay Based on Gold Nanoparticles	Z
G	4.3.2. Colorimetric Assay Based on Traditional Enzymes	AA
H	4.3.3. Colorimetric Assay Based on DNAzyme	AA
I	4.4. Other Nucleic Acid Sandwich Assays	AB
J	4.4.1. Sandwich Assay Based on the QCM	AC
K	4.4.2. Sandwich Assay Based on SPR	AD
L	4.4.3. Sandwich Assay Based on the Microcantilever	AD
M	4.4.4. Sandwich Assay Based on SERS	AD
N	5. Sandwich Assay for Small-Molecule and Ion Detection	AF
O	5.1. Sandwich Assay for Small Molecules	AF
P	5.2. Sandwich Assay for Ions	AG
Q	6. Sandwich Assay for Pathogens and Cells	AI
R	7. Supersandwich Assay	AK
S	8. Portable Diagnostic Devices Based on the Sandwich Assay	AM
T	9. Conclusions and Outlook	AN
U	Author Information	AN
V	Corresponding Authors	AN
W	Author Contributions	AN
X	Notes	AN
Y	Biographies	AO
Z	Acknowledgments	AP
AA	Abbreviations	AP
AB	References	AP

Received: June 18, 2012

1. INTRODUCTION

For decades, the sandwich assay has been a mainstay in the fields of biodetection, clinical diagnostics, environmental monitoring, and quality control in various industries. By eliminating the requirement of labeling the molecular target, the sandwich assays usually require the simultaneous binding of the recognition probe and signaling probe, which makes them extremely specific. Likewise, because signaling is typically coupled to an enzyme catalytic or amplified signaling mechanism, the sandwich assay usually achieves impressive sensitivity of detection.

Along with progress in chemistry, biotechnology, and nanotechnology, the sandwich assay has been extensively developed. For example, the sandwich assay has been employed successfully for the detection of a spectrum of targets, including pathogens, proteins, nucleic acids, small molecules, and ions. The signaling mechanism has also been extensively expanded from radiolabeling to more readily detectable readouts such as enzyme catalysis, fluorescence, or electricity. Furthermore, the basic sandwich architecture has been adapted into a super-sandwich platform, which usually further amplifies the signal and pushes the detection limit down.

To date, thousands of papers have been published on the sandwich assay. However, to our best knowledge, no such review paper summarizing the developments and future goals of this field yet exists. Thus, we present a critical review of the literature on the sandwich assay in the past 10 years to summarize and comment upon its development and advances, concentrating mainly on recent developments in nanobiotechnology.

2. PRINCIPLES OF THE SANDWICH ASSAY

The detection of proteins, nucleic acids, small molecules, and ions is of great importance in both the study of their fundamental functions and the development of molecular diagnostics. These biological molecules and ions not only are involved in the construction of living organisms, but also carry out most biological functions, including storage and transmission of genetic information, regulating biochemical activities and reactions, storing and transporting energy, and providing mechanical support.¹ Measurement of these biomolecules and ions in complex biological systems requires assays with extraordinary analytical specificity and sensitivity. As shown in Figure 1, the assays mentioned above are theoretically composed of three basic elements: analytes, recognition molecules, and the signal marker. In the measuring process, the signal marker, for example, radioactive isotopes, enzymes, fluorescein, and redox tags, is coupled to the recognition molecules, so that, upon or in response to binding of the analyte to the recognition molecules, the signal marker outputs a readily detectable signal, providing the assay with a sensitive measurable, radioactive, colorimetric, fluorescence, and electrochemical signal to indicate the presence and concentration of the target analyte.

This specific, biomimetic recognition of target analytes was initially performed by applying specific binding between antibody–antigen pairs. Such immunoassays can be applied to both competitive and noncompetitive platforms. In a competitive immunoassay, unlabeled analyte (usually native targeting antigen, Ag) in the test sample is measured by its ability to compete with prelabeled antigen (Ag^*) (Figure 2A). The unlabeled antigen competes with the labeled antigen to

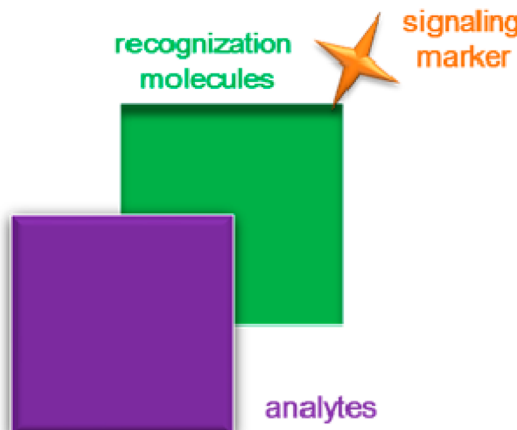


Figure 1. Illustration of the basic components of a biomolecule assay, which include analytes (purple) and recognition molecules (green) labeled with a detectable signaling marker (orange).

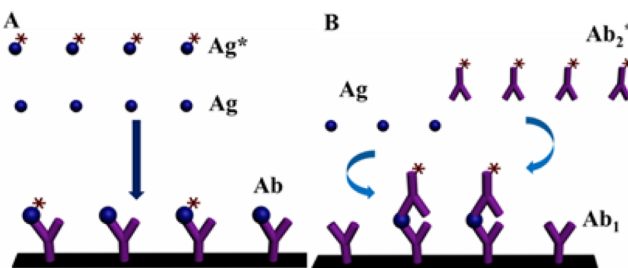


Figure 2. Scheme of competitive (A) and noncompetitive (B) immunoassays.

bind the affixed antibody; thus, the antigen in the test sample is inversely related to the amount of labeled antigen measured in the competitive format. Although these antigen-based assays work well and are considered a clinical mainstay for diagnostics, labeling the wide variety of relevant antigens and maintaining their bioactivity are generally complicated, onerous, and expensive.² Figure 2B shows the commonly used two-site noncompetitive immunoassays: the analyte in the test sample is first bound to the primary antibody (Ab_1), and then signaling-marker-labeled secondary antibody (Ab_2^*) is bound to the analyte, forming a sandwich-like immunocomplex. The concentration of the analyte is directly proportional to the signaling intensity of the immunocomplex proved by the label marked with Ab_2^* . This platform is also known as the sandwich assay as the analyte is “sandwiched” between two antibodies. The sandwich format immunoassay generally provides a high level of sensitivity and specificity to the protein because the protein is sandwiched between two highly specific antibody reagents.

As demonstrated by Figure 3, the most important process for the sandwich assay is analyte sandwiching between recognition molecule 1 and recognition molecule 2 with a signaling marker. With the development of biotechnology, different recognition molecules, such as antibodies, oligonucleotide sequences, and aptamers, have been applied to specifically and selectively recognize protein, DNA, small molecules, and ions. At the same time, the feasibility of modifying the antibody with different signaling markers, such as fluorescein, radionuclides, enzymes, and redox tags, in turn allows for a broader variety of readouts in a sandwich-structured assay. Herein, we focus mainly on the

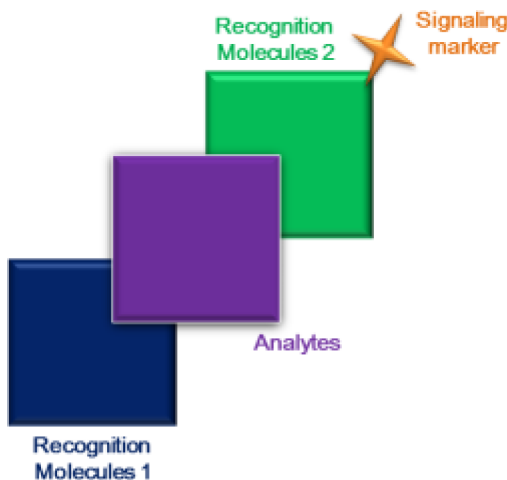


Figure 3. Scheme of sandwich assays.

recent developments of nanotechnology and biotechnology that stimulate the further growth and prosperity of the sandwich assay.

3. SANDWICH ASSAY FOR PROTEIN DETECTION

Given that proteins are the basic functional materials for living organisms, it is not surprising that specific proteins play a crucial role in biotechnology as important biomarkers serving as

indices for health- and physiology-related assessments, such as disease diagnosis, substance abuse, pregnancy, cell line development, and epidemiologic studies.³ Specifically, the quantification of target proteins in patient media can be used to diagnose and monitor early-stage diseases. However, the disease-related protein in the patient's blood or other tissue is often presented at an ultralow level, which demands a highly sensitive detection strategy. Inspired by this basic research and clinical importance, a great number of signaling-technique-based immunoassays, such as radioimmunoassay (RIA), colorimetric assay (CMA), fluorescence immunoassay (FLIA), electrochemical assay (ELCA), giant magnetoresistive assay (GMRA), and localized surface plasmon resonance assay (LSPRA), have been explored in the sandwich format to enhance the trace detection of target analytes.

Figure 4 and Table 1 summarize the detection parameters of the sandwich format assay with different signaling strategies, which confer different advantages and limitations. The giant magnetoresistive assay is the most rapid with an analysis time of only about 10 min. The electrochemical assay achieves the lowest detection limit, as low as 0.001 ng/mL, due to the sensitivity of electrochemical signaling. The colorimetric assay achieves a good detection limit, but a long analysis time of up to 2 h. Generally, Figure 4 and Table 1 imply that lowering the detection limit to the femtomolar level and reducing the analysis time to 10 min are the major development trends in the next generation of sandwich protein assays.

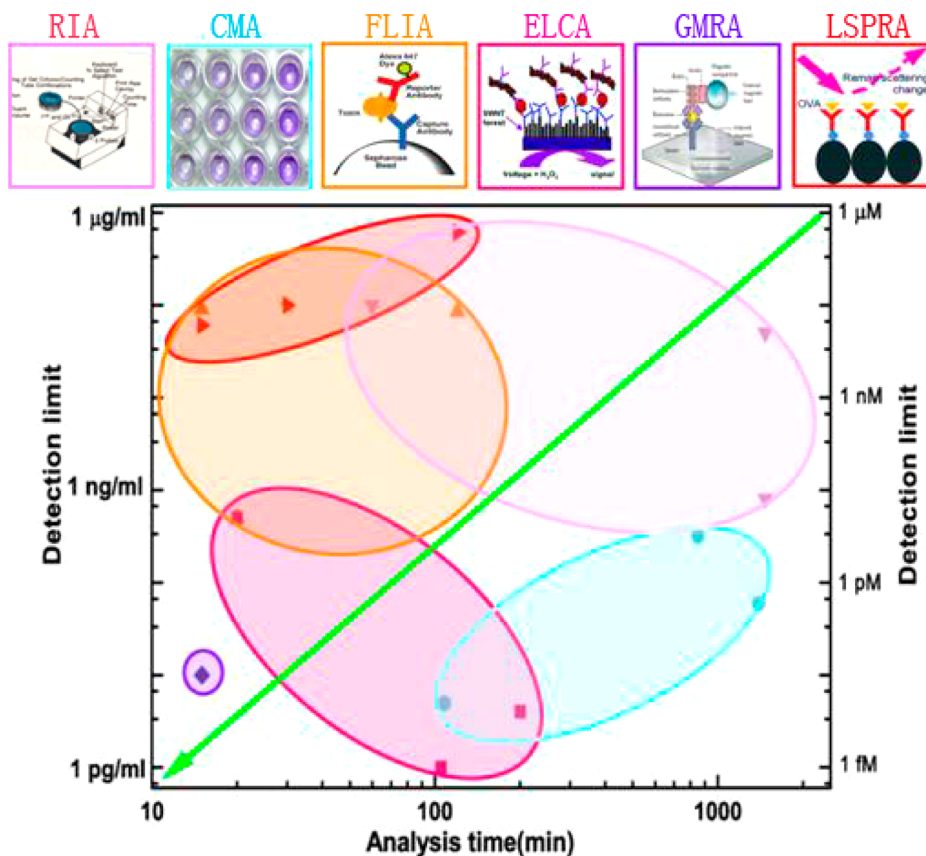


Figure 4. The panels at the top represent the configuration for sandwich-structured RIA, CMA, FLIA, ELCA, GMRA, and LSPRA. RIA: Reprinted from ref 4. Copyright 1977 American Chemical Society. CMA: Reprinted from ref 5. Copyright 2012 American Chemical Society. FLIA: Reprinted with permission from ref 6. Copyright 2009 The Royal Society of Chemistry. ELCA: Reprinted from ref 7. Copyright 2006 American Chemical Society. GMRA: Reprinted with permission from ref 8. Copyright 2009 Nature Publishing Group. LSPRA: Reprinted from ref 9. Copyright 2011 American Chemical Society. The bottom chart profiles the detection limit and analysis time of different types of sandwich assays.

Table 1. Comparison of the Analysis Time and Limit of Detection for RIA, ELISA, and Different Types of Sandwich Assays

category	protein	detection conditions	analysis time (min)	limit of detection	ref
RIA	HCG	phosphate buffer		100 ng/mL	10
	LH	phosphate buffer	1470	50 ng/mL	11
	Ig-G	phosphate buffer	1470	0.8 ng/mL	11
CMA	IGF-1	buffalo milk	850	0.32 ng/mL	12
	p53	PBS buffer	108	0.005 ng/mL	13
	HbsAg	serum	1395	0.06 ng/mL	14
	hGH	serum		6 pg/mL	15
FLIA	thyroxine	serum	1200	90 ng/mL	16
	toxin	PBS buffer	20	0.5 ng/mL	6
	myoglobin	serum	120	85 ng/mL	17
ELCA	protective antigen	PBS buffer	15	90 ng/mL	18
	IgG	PBS buffer	20	0.5 ng/mL	19
	PDGF-BB	PBS buffer		0.001 ng/mL	20
GMRA	PSA	calf serum	200	0.004 ng/mL	7
	IL-1 α	PBS buffer	15	0.01 ng/mL	21
LSPRA	OVA	milk	30	100 ng/mL	9
	PDGF receptor- β	PBS buffer	120	608 ng/mL	22
	h-IgG	PBS buffer	15	60 ng/mL	23

3.1. Sandwich Radioimmunoassay

Radioactive-isotope-labeled antigen (Ag^*) was first applied as a signaling marker in immunoassay to measure the insulin in plasma by Yalow and Berson in 1959, representing a milestone in the history of the application of radionuclide methodology to biomedicine investigation and practice.²⁴ There are two types of radioimmunoassay (RIA), competitive and sandwich (immunoradiometric) assays. As shown in Figure 5, in

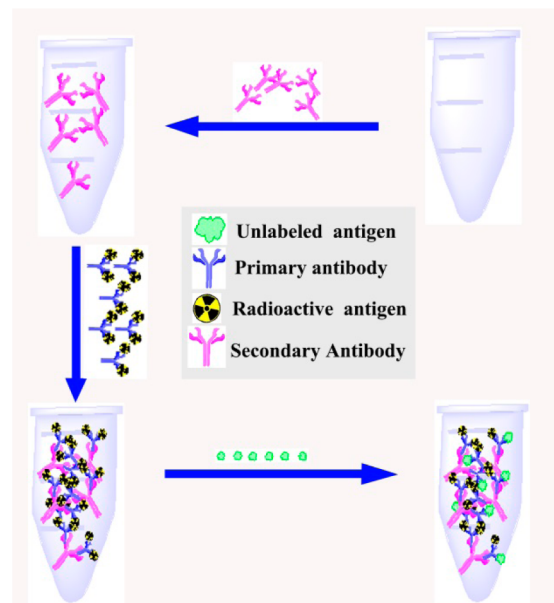


Figure 5. Principle of RIA. Unlabeled antigens compete with radioactively labeled antigens for the binding sites of a specific first antibody.

competitive assays the radiolabeled antigen “competes” with the unlabeled antigen in the sample for a limited number of binding sites on the reagent antibody. Following incubation, the free radiolabeled antigens are removed by decanting or washing, and the radioactivity of the antibody–antigen complexes is measured. RIA can detect the antigen with a concentration as low as several picograms per milliliter due to the detection sensitivity of the radioactive labeling.²⁵

Sandwich radioimmunoassay was developed by Miles and Hales in 1968.²⁶ As shown in Figure 6, two antibodies are used,

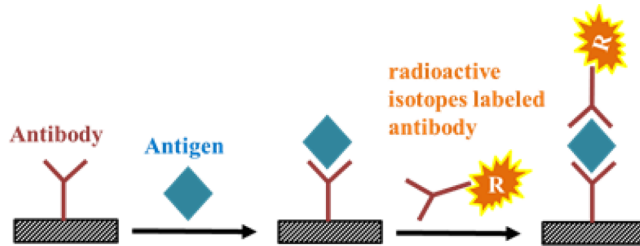


Figure 6. Principle of sandwich radioimmunoassay.

and one is radiolabeled. In the test system, the sample is incubated with a specific antibody usually attached to a solid phase such as a plastic bead or the wall of a plastic test tube. After the antibody–antigen complex is washed to remove unbound sample components, a radioactively labeled antibody is added. The second antibody may be directed against a different part of the antigen molecule to form an immune complex. The second antibody binds to the immune complex, making an antibody–antigen–antibody “sandwich”. After the sandwich complex is washed to remove the unbound radiolabeled antibody, the radioactivity is measured. The amount of radioactivity is directly proportional to the antigen concentration. Compared to those in competitive RIA, the antibodies are larger biomolecules which are feasible to mark with radioactive isotopes and retain bioactivity. Sandwich radioimmunoassays have been widely applied in the clinic determination of various proteins due to their high specificity and sensitivity.²⁷ Iodine (^{125}I) isotope is a common radiolabel due to its high specific activity and short half-life (60 days). These properties result in minimal disposal problems with leftover radioactive reagents. γ -rays emitted by the immune complexes are usually measured following removal of unbound (free) radiolabel. Since background radiation is very low and the counting time can be extended if needed to generate more counts, RIA is a very sensitive immunoassay. The major advantages of sandwich RIA when compared to other immunoassays are higher sensitivity, easy signal detection, and well-established, rapid assays. However, the utilization of hazardous radioactive nuclides requires specialized equipment and an operator with authorized licensing.²⁸ For these reasons, RIA has been largely replaced in routine clinical laboratory practice by enzyme-based colorimetric immunoassay. However, it is still the gold standard to which other immunochemical methods are compared and is still performed in reference laboratories for analytes such as 11-deoxycortisol, for which other methods cannot be used.

Table 2. Commonly Used Enzymes for Protein Detection

enzyme	substrate	protein	signal	detection limit	ref
ALP	pNPP	SR protein kinase 1	$\lambda_{abs} = 405 \text{ nm}$	0.55 mg/mL	36
		human interleukin-8	$\lambda_{abs} = 405 \text{ nm}$	16 pg/mL	34
HRP	TMB	τ -protein	$\lambda_{abs} = 450 \text{ nm}$	5 pg/mL	37
		insulin-like growth factor	$\lambda_{abs} = 450 \text{ nm}$	0.32 ng/mL	12
		coconut milk proteins	$\lambda_{abs} = 450 \text{ nm}$	0.39 ng/mL	37b
		carcinoembryonic protein	$\lambda_{abs} = 370 \text{ nm}$	0.02 ng/mL	38
		α -fetoprotein	$\lambda_{abs} = 490 \text{ nm}$	0.02 ng/mL	38
		chymotrypsin	$\lambda_{abs} = 405 \text{ nm}$	127 ng/mL	39

3.2. Sandwich Colorimetric Assay

To apply the basic principles of the radiolabeled sandwich assay with a less hazardous, more accessible detection scheme, in 1971, Engvall and Perlman developed a user-friendly, enzyme-driven colorimetric assay, now known as the enzyme-linked immunosorbent assay (ELISA).²⁹ The platform of the sandwich colorimetric assay is similar to that of the sandwich radioimmunoassay as shown in Figure 6. As with the sandwich assay, the target first binds to a surface-bound capture antibody; next, a second enzyme-labeled antibody is added to form the sandwich-like immunocomplex. After introduction of the substrate of the labeled enzyme, visible color occurs, which is used for quantification of the target antigen.^{29,30} The sandwich format colorimetric assay could enhance not only the sensitivity but also the specificity.³¹

3.2.1. Colorimetric Assay Based on a Traditional Enzyme.

Sandwich colorimetric assays are typically based on the observable color change in the presence of enzyme-labeled antibody.^{30b,32} As shown in Figure 6, sandwich colorimetric assays utilize a monoclonal antibody directed against a distinct antigenic determinant on the intact protein molecule and used for solid-phase immobilization. A secondary antibody conjugated to an enzyme is used as a signal generator. The target proteins in the test sample are allowed to react sequentially with the two antibodies, resulting in the antigen molecules being sandwiched between the solid-phase and enzyme-linked antibodies. These linked enzymes are able to react with a variety of substrates added to the reaction to generate a measurable spectroscopic signal which can be utilized to deduce the amount of target protein present in a sample.

As listed in Table 2, alkaline phosphatase (ALP) and horseradish peroxidase (HRP) are commonly used enzymes for sandwich colorimetric assays. ALP is a hydrolase enzyme responsible for dephosphorylating several types of phosphomonoesters, such as phenyl phosphate, *p*-aminophenyl phosphate, *p*-nitrophenyl phosphate (PNPP), 1-naphthyl phosphate, and 2-phospho-L-ascorbic acid. As the name suggests, alkaline phosphatases are most effective in an alkaline environment around pH 8–10.³³ Dephosphorylation frequently causes the reagent to change color, in turn providing an optical signal indicating the presence and concentration of the target protein. For example, PNPP is a common alkaline phosphatase substrate which is dephosphorylated by ALP into a yellow water-soluble product with a maximum absorption peak at around 405 nm.³⁴ HRP is an oxidase responsible for catalyzing the oxidation of a wide variety of organic and inorganic substrates with H₂O₂. The most commonly used substrates for HRP are 3,3',5,5'-tetramethylbenzidine (TMB), *o*-phenylenediamine (OPD), and 2,2'-azinobis(3-ethylbenzothiazoline-6-sulfonic acid) (ABTS). Among these enzymes, HRP is the most commonly used one due to its smallest molecular structure,

highest stability, and fastest catalytic rate.³⁵ As demonstrated in Table 2, the detection limit of these conventional sandwich colorimetric assays is as low as 5 pg/mL. However, the 1:1 enzyme–antibody conjugation in this method inherently limits its further improvement in detection limit.

Although sandwich colorimetric assays have been well-developed, immunological detection of small haptens is generally mostly carried out in the competitive format, which requires corresponding competitor molecules labeled with a signaling reporter. To reduce the need to label small molecules and enhance the detection of low molecular weight substances, Ueda et al. constructed an open sandwich immunoassay (OS-IA) utilizing antigen-dependent stabilization of the antibody variable region to quantify various antigens, enabling noncompetitive detection of small molecules.¹⁶ As shown in Figure 7, OS-IA is conceptually constructed on the

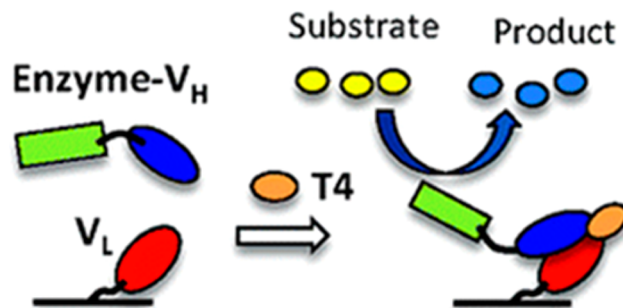


Figure 7. Principle of OS-ELISA. Reprinted from ref 16. Copyright 2011 American Chemical Society.

interaction between the separated enzyme-labeled heavy chain (V_H) and light chain (V_L) of an antibody variable region dependent on the presence of antigen. In the absence of antigen, many of the two V region fragments are prone to dissociation, while in the presence of antigen, these V region fragments turn to bridging the antigen and form a sandwich structure. The labeled enzyme will catalyze the following added substrate to introduce a color change, which in turn indicates the presence and concentration of the antigen. OS-IA has achieved detection limits of 0.1 and 0.01 ng/mL in the detection of thyroxine (T4) and 11-deoxycortisol, respectively.⁴⁰

For the past few years, nanomaterials have shown great promise to enhance the sensitivity of protein sandwich colorimetric assays due to their high surface area to volume ratio, which enables a multienzyme-carrying capability.^{14,42} It is worth noting that Au nanoparticles (Figure 8) are the most practical multienzyme carriers for the immobilization of multienzymes due to their narrow size distribution, good biocompatibility, and ease of modification with functional

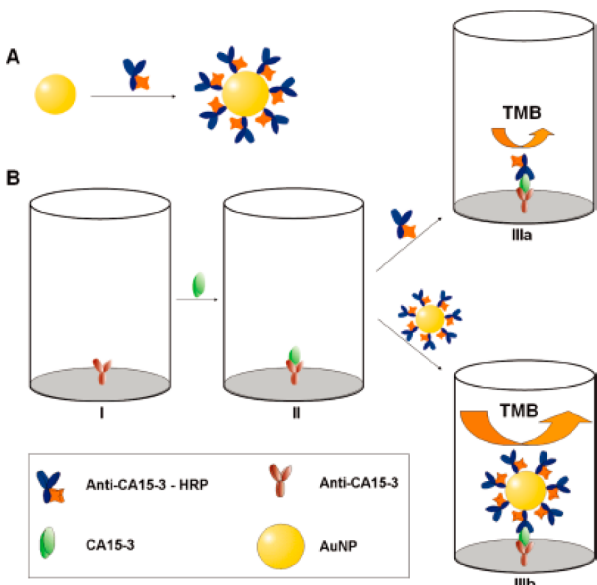


Figure 8. (A) Preparation of the complex Au–anti-CA15-3–HRP. (B) Sandwich-type ELISA procedure without (IIIa) and with (IIIb) the application of Au NPs as the signal enhancer. Reprinted from ref 41. Copyright 2010 American Chemical Society.

groups.^{14,43} Gold–multienzyme–nanocarrier-based sandwich colorimetric assays have been utilized to detect HIV-1 capsid (p24) antigen,⁴⁴ human fetuin A/AHSG,⁴⁵ human IgG,^{42b} CA15-3 antigen,^{42a} and carcinoembryonic antigen.^{42c} Theoretically, the excellent carrying capability of Au nanoparticles could offer an amplified detection limit lowered to about 0.1 pg/mL, which is an about 100–150-fold enhancement in the detection limit over that of the 1:1 enzyme–antibody conjugation method.⁴⁴ These results indicate that the universal labeling technology based on NPs and its application could provide a rapid and sensitive testing platform for clinical diagnosis and laboratory research.

Compared to sandwich radioimmunoassays, sandwich colorimetric assays provide a more convenient and environmentally friendly readout. The development of modern multienzyme nanocarrier technology will likely improve the sensitivities and also shorten the assay time to minutes for sandwich colorimetric assays, which have closer to the required high accuracy for medical evaluations.^{42a}

3.2.2. Colorimetric Assay Based on Biomimetic Nanomaterials. Nanomaterial-based enzymes have attracted great interest as they have numerous improved advantages relative to natural enzymes, such as stability over a wide range of pH and temperature and inertness to several proteases.⁴⁶ As shown in Figure 9, several kinds of nanoparticles, including Pt nano-

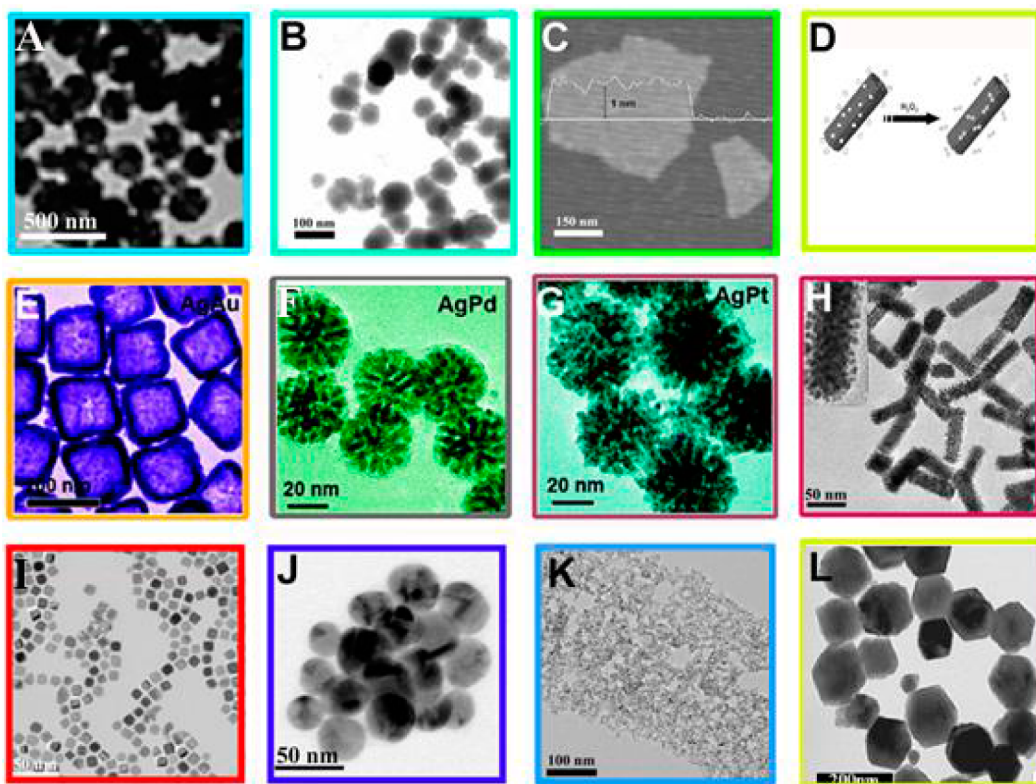


Figure 9. Nanomaterials mimic enzymes. (A) Peroxidase-like Fe₃O₄ nanoparticles. Reprinted with permission from ref 46a. Copyright 2007 Nature Publishing Group. (B) FeS nanoparticles. Reprinted with permission from ref 46c. Copyright 2009 Wiley-VCH Verlag GmbH & Co. KGaA. (C) Graphene oxide. Reprinted with permission from ref 51. Copyright 2010 Wiley-VCH Verlag GmbH & Co. KGaA. (D) Single-wall carbon nanotubes. Reprinted with permission from ref 46b. Copyright 2010 Wiley-VCH Verlag GmbH & Co. KGaA. (E) AgAu nanoparticles, (F) AgPd nanoparticles, and (G) AgPt nanoparticles. Reprinted from ref 53. Copyright 2010 American Chemical Society. (H) Au@Pt nanostructures. Reprinted with permission from ref 48. Copyright 2011 Elsevier. (I) Pt nanoparticles. Reprinted with permission from ref 53. Copyright 2011 Elsevier. (J) CuO nanoparticles. Reprinted with permission from ref 46d. Copyright 2009 Wiley-VCH Verlag GmbH & Co. KGaA. (K) CeO₂ nanoparticles. Reprinted with permission from ref 54. Copyright 2010 IOP Publishing Ltd. (L) α -Fe₂O₃ nanoparticles. Reprinted with permission from ref 55. Copyright 2012 The Royal Society of Chemistry.

particles,⁴⁷ Au@Pt nanoparticles,⁴⁸ Fe₃O₄ magnetic nanoparticles,^{46a,49} CeO₂ nanoparticles,⁵⁰ FeS nanosheets,^{46c} graphene oxide nanoparticles,⁵¹ single-wall carbon nanotubes,^{46b} and cupric oxide nanoparticles,^{46d} have recently been found to exhibit novel performance with horseradish peroxidase (HRP) and show great potential in sandwich colorimetric assays. Among these nanostructured mimic enzymes, Fe₃O₄ magnetic nanoparticles (MNPs) have attracted abundant attention not only because of their intrinsic peroxidase-like properties,^{46a} but also because their magnetic properties facilitate separation.⁵² Gao et al. demonstrated that MNPs that mimic enzymes have several advantages over traditional enzymes: (a) they retain peroxidase activity over a wide range of pH and temperature, (b) they have dual functionality, as a peroxidase and magnetic separator, (c) they have size-dependent catalytic properties, and (d) preparation of Fe₃O₄ MNPs is simple and economical. As a trial, chitosan-modified Fe₃O₄ MNPs were used to mimic peroxidase for the detection of thrombin over a linear range from 1 to 100 nM, and the lowest limit of detection was estimated to be 1 nM.⁵² Pt-nanodot-coated Au nanorods (Au@Pt nanostructures) exhibit interesting intrinsic oxidase-like, peroxidase-like, and catalase-like activity, catalyzing oxygen and hydrogen peroxide reduction and the dismutation decomposition of hydrogen peroxide to produce oxygen. These Au@Pt nanostructures have been utilized to detect mouse interleukin 2 (IL-2) with a detection limit lowered to 1 pg/mL.⁴⁸

Nanostructured enzyme mimics have several advantages over traditional natural enzymes, such as easy preparation, robustness, stability in rough conditions, tunable catalytic properties, and multiple functions, which in turn enhance the detection sensitivity and efficiency of sandwich colorimetric assays. These nanostructured-enzyme-mimic-based sandwich colorimetric assays may find potential applications in the detection not only of protein but also of many other biomolecules.

3.3. Fluorescence Sandwich Immunoassay

Fluorescence immunoassay was first conceptualized to detect pneumococcus by Albert H. Coons in the early 1940s.⁵⁶ Fluorescence sandwich immunoassay, wherein the fluorophore substitutes for the enzyme and introduces a fluorescence signal, could be monitored to investigate the existence and concentration of target proteins.⁵⁷ The commonly used fluorophores include fluorescent organic dye,^{6,58} fluorescent nanoparticles,⁵⁹ and fluorescent conjugated polymers.⁶⁰ Fluorescence immunoassay has been widely used both in research and in clinical diagnostics due to its high sensitivity.⁶¹

3.3.1. Organic Dyes as Fluorophores. Organic dyes are a kind of organic molecule capable of absorbing energy and emitting it as fluorescence for signaling in fluorescence sandwich assay. Originally, organic dyes such as fluorescein isothiocyanate (FITC),⁶² Ru(bpy)₃Cl₂,⁶³ rhodamine,^{62b} Alexa,⁶⁴ cyanine dyes,⁶⁵ and lanthanide chelate⁶⁶ were chosen as major fluorophores in fluorescence sandwich immunoassay due to their industrial tunable emission wavelength ranges, brightness, and commercial availability.⁶⁷ In solid-phase fluorescence sandwich assay, the fluorescence signal detection was performed after additional purification, and this purification could get rid of the interference of the background of the media.⁶⁸ Microbeads show great potential in the applications of solid-phase sandwich assay due to their wide material resources, easier centrifugal separation, and feasible functionalization.⁶⁸ Until today, the microbead-based sandwich immunoassay and

flow cytometer have been widely explored and utilized to detect proteins.^{6,69} As shown in Figure 10, a renewable surface

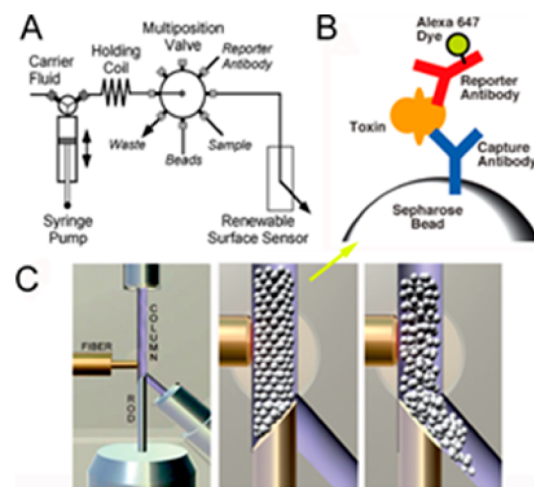


Figure 10. Schematic diagram for the sandwich immunoassay complex for botulinum toxin detection (A), the sequential injection system with the rotating rod renewable surface sensor flow cell as the separator/reactor/detector (B), and the rotating rod flow cell (C). Reprinted with permission from ref 6. Copyright 2009 The Royal Society of Chemistry.

fluorescence sandwich immunoassay biosensor uses a microbead-trapping flow cell to capture antibody-coupled beads with subsequent sequential perfusion of the sample, wash, dye-labeled reporter antibody, and final wash solutions.⁶ Optical fibers coupled to the rotating rod flow cell at a 90° angle to one another deliver excitation light from a HeNe laser (633 nm) using one fiber and collect fluorescent emission light for detection with the other. After each measurement, the used Sepharose beads are released and replaced with fresh beads. The toxin simulant was detected to concentrations of 10 pM in less than 20 min. Using this system, the sensitivity of fluorescence sandwich assay could be enhanced up to 2–4-fold compared to that of traditional assays, and the procedure could be shortened to 20 min.⁶⁹

Parallel detection of biomarkers is essential to clinical validation due to their coexistence in the serum of a patient. The microfluidic purification chip (MPC) has shown great potential to serve as a rapid, point-of-care, ultrasensitive, real-time, multiplexed assay of proteins. Stern et al. designed a novel detection system which combined an MPC and a sensing reservoir.⁷⁰ As shown in Figure 11, MPC captures cancer biomarkers from physiological solutions and, after washing and exposure to UV light, releases the antigens into a pure buffer suitable for sensing. The devices show specific and quantitative detection of two model cancer antigens from a 10 mL sample of whole blood in less than 20 min.

Generally, the combination of fluorescence sandwich assay and other technologies such as a surface renewable flow cytometer and MPC could automatically isolate the detector from the complex environment of whole blood, which in turn enhances the purification process and provides sensitive and rapid detection of protein.

3.3.2. Nanomaterials as Fluorophores. Efforts to improve the performance of fluorescence sandwich immunoassay by incorporating different kinds of novel fluorescent nanostructures such as fluorophore-doped nanoparticles,^{62b,71}

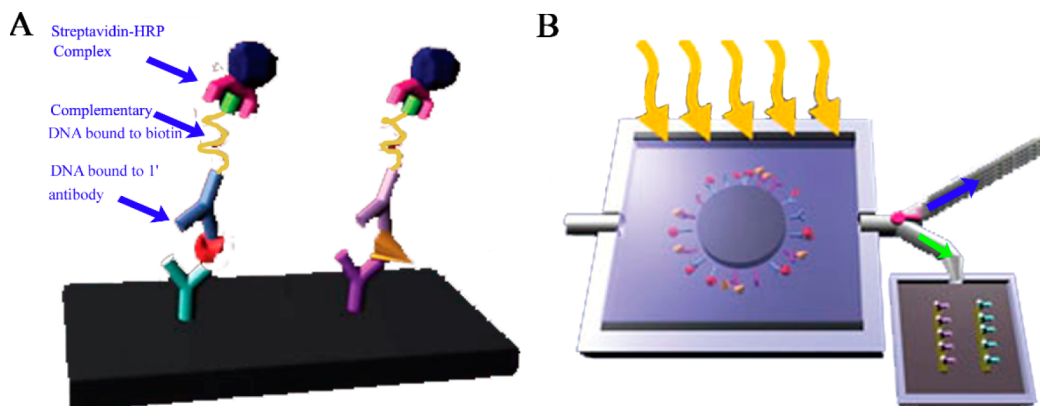


Figure 11. Platform of antiprostate-specific antigen and carbohydrate antigen 15.3 detection using a modified fluorescence sandwich immunoassay (A). Schematic of MPC operation (B). Reprinted with permission from ref 70. Copyright 2009 Nature Publishing Group.

semiconductor quantum dots,^{59b,72} and up-conversion nanoparticles and other inorganic and organic fluorescence nanoparticles⁷³ have gained a lot of attention in recent years. It is worth noting that the emerging fluorescence semiconductor nanocrystals (quantum dots, QDs) exhibit novel fluorescent properties such as size- and composition-dependent narrow emission,⁷⁴ broad absorption,^{59b} single-wavelength excitation with emission at multiple fluorescence colors,^{59b} and long-term photostability and high-quantum yield.^{34,67a,72a,74a} These excellent fluorescent properties make them a good candidate for the fluorescence marker in sandwich immunoassay. Wang et al. utilized ZnO quantum dots as fluorescent labels in a sandwich-type sensitive immunoassay to detect carbohydrate antigen 19-9 (CA 19-9), which is a preferred label for pancreatic cancer.⁷⁵ As shown in Figure 12, the immobilization

of ZnO QDs achieved a detection limit of 0.25 U/mL and a linear response range of 1–180 U/mL.

Clinical diagnosis of disease requires accurate detection of a suite of biomarkers present in a patient's serum and urine simultaneously, so it is important to develop multiplex detection strategies for biomarkers. B. I. Swanson and his co-workers developed a fluorescence QD-based multiplex detection sandwich immunoassay on multichannel waveguides for a limited suite of disease biomarkers in complex samples.^{18,76} As shown in Figure 13, photostable and tunable quantum dots were utilized as the fluorescence reporters for the sensitive, quantitative, multiplex detection of protective antigen (PA) and lethal factor (LF) in serum. This platform allows for the sensitive, specific, and rapid (15 min) detection of lethal factor and protective antigen in complex biological samples with a detection limit of 1 pM, and this assay shows great potential in the future evaluation of these biomarkers in the actual patient.

Crucial for fluorescence sandwich assay applications was the development of surface modifications that make nanoparticles water-soluble,⁷⁷ reduce toxicity,⁷⁸ and allow conjugation to protein-targeting molecules such as antibodies and streptavidin.⁷⁹ The fluorescence properties of nanoparticles show great potential in immunoassay, but efforts still need to explore the surface modification technique to reduce its toxicity and enhance its dispersibility.

3.3.3. Conjugated Polymers as Fluorophores. Conjugated polymers (CPs) are polyunsaturated organic compounds with alternating single and double bonds along the polymer chain.⁸⁰ The interaction of electrons in the polymer chain provides CPs with novel photoelectric properties which exhibit great potential applications not only in electronic devices,⁸¹ but also in biochemical sensors.^{60a,82} Water-soluble CPs have been widely used for protein detection on the basis of their environmentally sensitive optical properties.^{82b,e,g,83} Fan et al. utilized fluorescence quenching resulting from electron transfer to detect protein cytochrome *c*.^{83b} As shown in Figure 14A, the electron transfer between cytochrome *c* (Cyt *c*) and poly[lithium 5-methoxy-2-(4-sulfonylbutoxy)-1,4-phenylenevinylene] (MBL-PPV) induced CP fluorescence quenching, which was reported to detect protein itself at a concentration as low as 10^{-11} M.^{83b} This super fluorescence quenching resulting in high sensitivity is attributed to the electron transfer, which is amplified by the polymeric backbone and causes collective features called the "molecular wire effect".⁸⁴ As shown in Figure

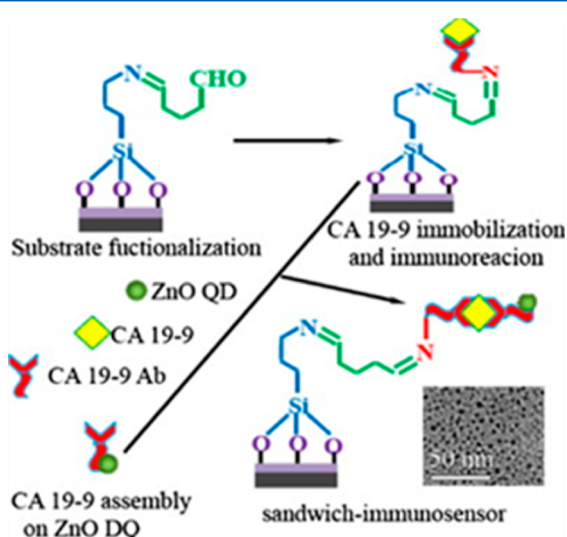


Figure 12. Schematic protocol of ZnO-QD-based fluorescence sandwich immunoassay. Reprinted with permission from ref 75. Copyright 2011 Elsevier.

process was mainly carried out through electrostatic adsorption based on the high isoelectric point of ZnO, and the sandwich platform was constructed through the immunoreaction between CA 19-9 antibodies and antigens. The detection of CA 19-9 was converted into measurement of the amplified signals of intrinsic photoluminescence of the labeled ZnO QDs. The fluorescence sandwich immunoassay based on fluorescence

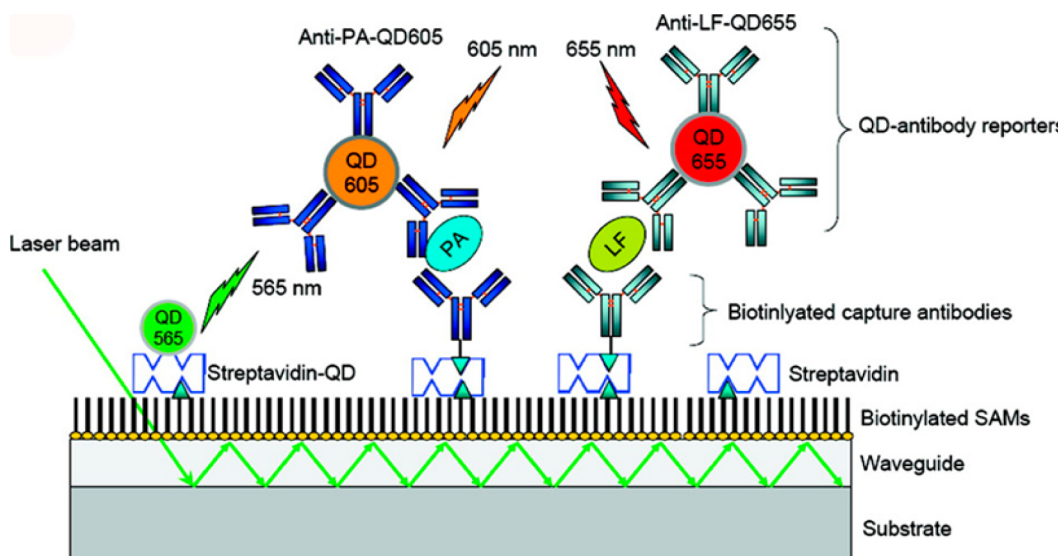


Figure 13. Schematic representation of the multiplex fluorescence sandwich assay on a functionalized single-channel waveguide surface. Reprinted from ref 18. Copyright 2010 American Chemical Society.

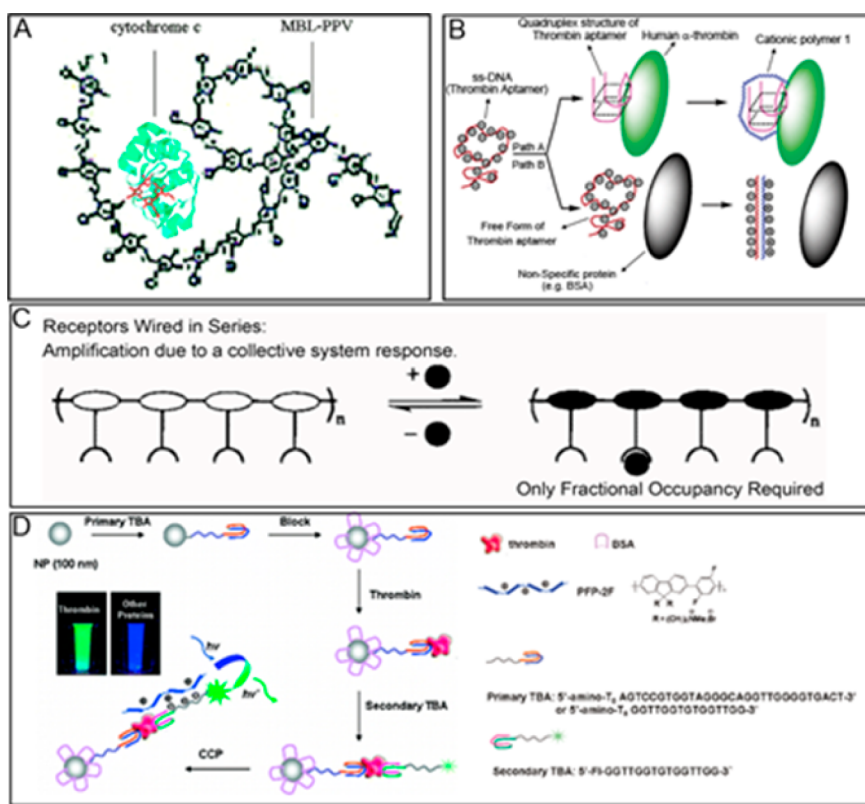


Figure 14. Protein detection based on conjugated polymers. (A) Schematic description of detection of cytochrome *c* by conjugated polymer poly[lithium 5-methoxy-2-(4-sulfonylbutoxy)-1,4-phenylenevinylene]. Reprinted from ref 83b. Copyright 2002 American Chemical Society. (B) Schematic description of the specific detection of human α -thrombin by use of ss-DNA thrombin aptamer and cationic polymer. Reprinted from ref 83c. Copyright 2004 American Chemical Society. (C) Schematic description of the molecular wire effect. Reprinted from ref 85a. Copyright 1998 American Chemical Society. (D) Working principle of CCP-amplified NP-based thrombin detection. Reprinted from ref 87. Copyright 2009 American Chemical Society.

14C, this novel molecular wire effect makes CPs capable of detecting analytes at ultralow content, due to their improved sensitivity, typically better than that of conventional, small-organic-dye-based sensing.^{83b,84b,85} Single-stranded DNA (aptamer) can specifically bind potassium ions or human α -thrombin. When binding takes place, the aptamer undergoes a

conformational transition from an unfolded to a folded structure, resulting in a fluorescence change. Meanwhile, the fluorescence of CPs is not only sensitive to the surrounding quencher or acceptor, but also sensitive to the minor perturbation of conformation due to the possibility of intra- and interchain electron transfer.⁸⁶ On the basis of this

mechanism, as shown in Figure 14B, Ho et al. designed a new selective and highly sensitive method (as few as 2×10^{-15} mol) to detect human α -thrombin by using hybrid anionic aptamer/cationic polythiophene complexes.^{83c}

Fluorescence resonance energy transfer (FRET) between CPs and fluorophores was also utilized to detect protein and other biomolecules due to the excellent light-harvesting properties of CPs.^{82g,85a,87,88} FRET-based sandwich assays have been developed for optical detection of protein in complex biological media with high sensitivity.⁸⁷ As shown in Figure 14D, after the formation of the traditional fluorescence sandwich complex, signal amplification is achieved by the addition of positively charged conjugated polymer. Under optimization, the detection limit of thrombin could be as low as 1.06 nM, and the detection process could be visualized by the naked eye assisted by external UV excitation. Generally, the molecular structures of typical water-soluble CPs are shown in Figure 15.⁸⁸ CP-based biosensors could work via three sensitive

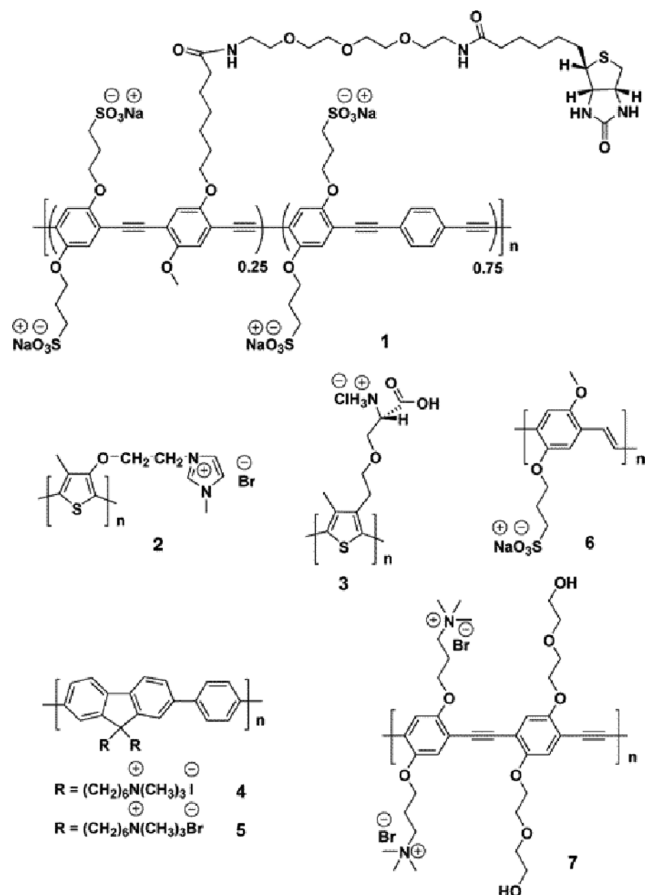


Figure 15. Examples of water-soluble CPs used in biosensor applications. Reprinted from ref 88. Copyright 2004 American Chemical Society.

means: (1) super fluorescence quenching,^{83b,84b} (2) fluorescence resonance energy transfer,^{82g,89} and (3) conformational perturbation.^{60b} The intrinsic collective effect of CPs and the multimode potential provides CPs with a promising future in the development of the next generation of biosensors.

3.4. Electrochemical Sandwich Immunoassay

Electrochemical assay is normally based on the electronic communication between the transducer and biomolecules. As

shown in Figure 16, in the electrochemical sandwich immunoassay, primary antibodies are immobilized onto a supporting surface and target antigens are recognized by a labeled secondary antibody. The following electrochemical quantification is generally performed by the measurement of the electronic signal introduced by the redox-active label.⁹⁰ Electrochemical assay is very attractive for protein detection due to its unique advantages such as high sensitivity, rapid and economic properties, inherent miniaturization, and robust instrumentation.⁹¹

Biomaterials and electronic transducers are foreign components in respect to one another, leading to a lack of electronic coupling or communication between them.⁹² Different strategies have been explored for amplifying the transducing signals of antibody–antigen interactions. To date, different kinds of labels, such as small redox molecules,⁹³ enzymes,⁹⁴ and nanomaterials,^{7,92,95} have been investigated as labels for signal amplification in the process of electrochemical sandwich assay.⁹⁶

3.4.1. Application of a Redox Label. The use of redox label could enhance the sensitivity of electron transduction in the electrochemical reaction. Generally, the sensitivity of electrochemical sandwich assay is majorly based on the electrochemical signal of the biorecognition reaction, but mostly, the direct electron transduction between the protein and the support electrode is hindered because the active redox group is embedded deep within the protein structure.^{90,97} As shown in Figure 17, K. W. Plaxco et al.⁹⁸ explored a methylene blue (MB) labeled, thrombin-binding DNA-aptamer-based (E-AB) sandwich sensor for thrombin detection. The thrombin binding with the aptamer resulted in the formation of a G-quadruplex conformation of the aptamer and release of the MB-tagged oligonucleotide to collide with the electrode surface, producing a readily detectable faradic current with a detection limit lowered to ~ 3 nM.^{98b} Moreover, this assay is selective enough to be performed directly in blood, crude cellular lysates, and other complex sample matrixes. Because the high specificity of the aptamer and the high sensitivity of the redox label, these platforms show great promise in future clinical immunoassays.

3.4.2. Application of Enzyme-Based Amplification. The utilization of enzyme could provide a novel signal amplification to enhance the sensitivity of electrochemical sandwich immunoassay.^{94,99} In enzyme-labeled electrochemical sandwich assay, an enzyme-labeled antibody probe is directly biconjugated to a second binding site on the antigen. At this point, the antigen is sandwiched between two antibodies. The enzyme can generate electroactive products by enzymatic hydrolysis of substrates, and additional signal amplification by redox cycling of the products can offer higher electrochemical signals.⁹⁹ Akanda et al. designed an ultrasensitive phosphatase-based electrochemical sandwich immunoassay to detect cardiac troponin I in human serum using redox cycling by a reducing agent.⁹⁴ As shown in Figure 18, the assay is based on an ITO electrode with an immunosensing layer of passive adsorption of avidin. After the formation of the sandwich complex on the immunosensing layer, the following enzymatic reaction could provide the electronic signal for detection. Under the optimization of substrates and redox cycling, the detection limit of troponin I could be lowered to 10 fg/mL. From a clinical point of view, it is of great importance that ultralow detection limits can be obtained with these simply prepared enzyme-amplified electrochemical sandwich immunoassays.

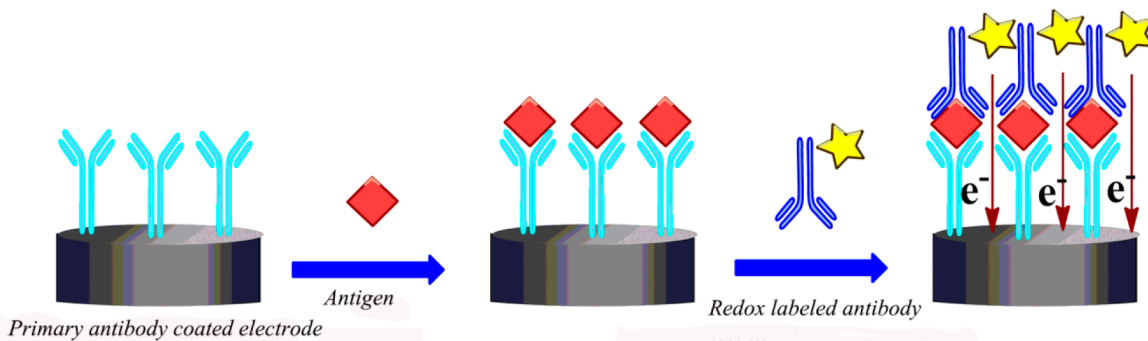


Figure 16. Schematic description of the electrochemical sandwich assay.

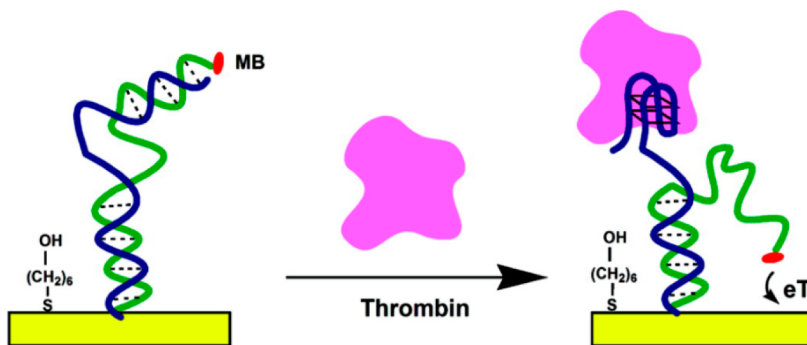


Figure 17. Scheme of the proposed mechanism of the signal-on electronic, MB-labeled, thrombin-binding E-AB sensor. Reprinted from ref 98b. Copyright 2009 American Chemical Society.

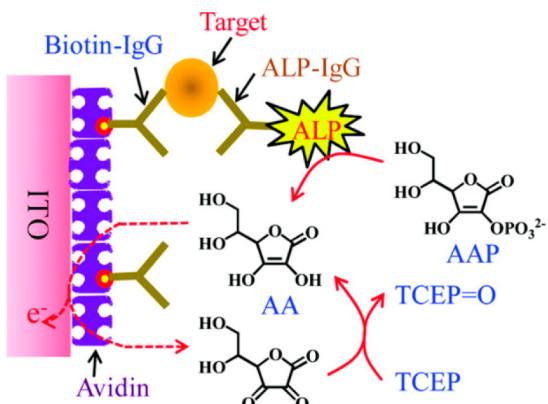


Figure 18. Schematic representation of an electrochemical immuno-sensor using the generation of L-ascorbic acid by alkaline phosphatase and the redox cycling of L-ascorbic acid by tris(2-carboxyethyl)-phosphine. Reprinted from ref 94. Copyright 2011 American Chemical Society.

3.4.3. Application of Nanomaterials. Nanomaterials have shown great potential in the applications of electrochemical sandwich immunoassay due to their unique physicochemical properties.^{19,92,95,100} There are two strategies to realize the enhancement of sensitivity for nanomaterial-based electrochemical immunoassay. One strategy (strategy I) utilizes the multienzyme-carrying capability of the nanocarrier to amplify the signal. Generally, nanomaterials have high surface to volume ratios, allowing each nanoparticle to carry many enzymes to catalyze the redox reaction of the substrate. As shown in Figure 19, gold nanoparticles,¹⁰¹ carbon nanotubes (CNTs),^{7,102} graphene oxide (GO),¹⁰³ magnetic beads,¹⁰⁴ and silica nanoparticles¹⁰⁵ have been used as carriers for multi-

enzymes. Under optimal conditions, these nanocarrier-based electrochemical sandwich immunoassays achieve 29.5-fold increases in detection signals in comparison with the traditional sandwich immunoassay. In conclusion, the nanocarrier-based electrochemical sandwich assay provides a promising approach in clinical applications due to their good reproducibility and selectivity and acceptable stability.

As mentioned in section 3.4.1, in general, the efficiency of direct electron communication between the protein and electrodes is very low. Thus, a second strategy (strategy II) in applying nanomaterials to improve sandwich assays uses nanomaterials to provide a good pathway for electron transfer between the redox center of the enzyme and the electrodes. Recently, many kinds of nanostructured materials have been explored to promote direct electron transfer between the enzyme and the electrode.^{92,95,109} Notably, carbon-based nanostructure materials, such as carbon nanotubes,¹⁰⁷ carbon nanowires or fibers,¹⁰⁹ and graphene,¹¹⁰ have attracted great attention in electrochemical assay, not only due to their sensitive conductivity in promoting the electron-transfer reactions of proteins, but also due to the feasibility of their surface modification to enhance the accumulated absorption of important biomolecules.^{109,111} To take advantage of the remarkable properties of carbon-based nanomaterials in such electrochemical assay applications, these nanomaterials need to be properly functionalized and assembled.

As shown in Figure 20, there are different ways to confine carbon nanomaterials onto electrochemical transducers. Early CNT-based transducers are commonly accomplished using CNT-modified electrodes¹¹² or using CNT/binder composite electrodes.¹¹³ Furthermore, nanoparticles have been added into the CNT/binder composite electrodes to enhance the sensitivity.¹¹⁴ Later, another effective strategy was performed

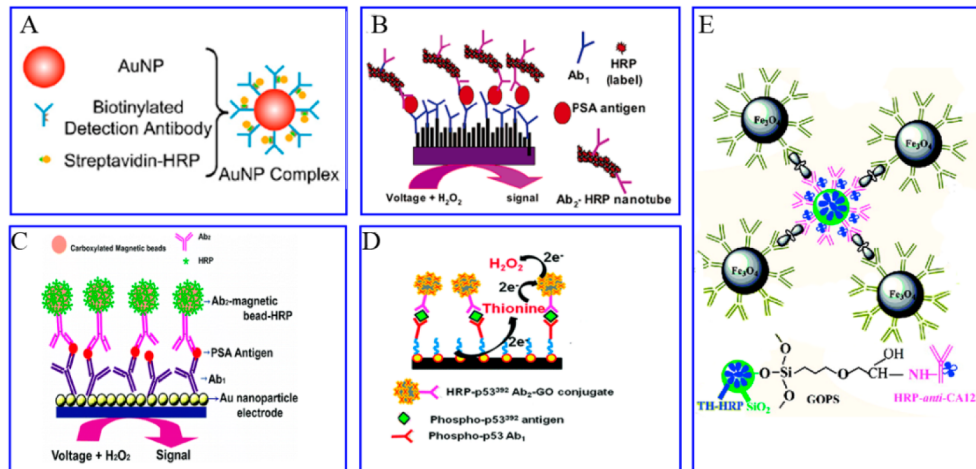


Figure 19. Different nanocarriers for multienzymes. (A) Gold nanoparticles. Reprinted with permission from ref 101. Copyright 2010 Elsevier. (B) Carbon nanotubes. Reprinted from ref 7. Copyright 2006 American Chemical Society. (C) Magnetic beads. Reprinted from ref 104. Copyright 2009 American Chemical Society. (D) Graphene oxide nanoparticles. Reprinted from ref 103. Copyright 2011 American Chemical Society. (E) Silica nanoparticles. Reprinted from ref 105a. Copyright 2010 American Chemical Society.

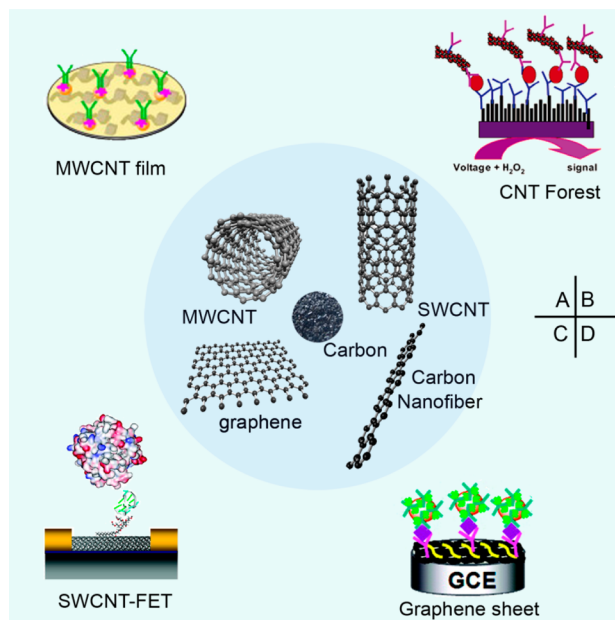


Figure 20. Different ways to confine carbon-based nanomaterials onto electrochemical transducers. (A) CNT-film-based assay. Reprinted with permission from ref 106. Copyright 2010 Elsevier. (B) CNT-forest-based assay. Reprinted from ref 7. Copyright 2006 American Chemical Society. (C) SWNT-FET-based assay. Reprinted from ref 107. Copyright 2005 American Chemical Society. (D) Graphene-sheet-based assay. Reprinted from ref 108. Copyright 2010 American Chemical Society.

by aligning short CNTs normal to the electrodes to form forest-like arrays (Figure 20B).¹¹⁵ Such vertically aligned SWCNTs act as molecular wires to favor electrical communication between the underlying electrode and a redox enzyme.^{7,109} As shown in Figure 20C, a sandwich assay based on an aptamer-modified carbon nanotube FET was developed for label-free detection of thrombin with a detection limit of 10 nM.¹⁰⁷ Pure and nanoparticle-decorated graphene nanosheets (Figure 20D) have also been utilized as labels for improving the sensitivity of an electrochemical immunoassay.^{110,116} In graphene-based sandwich assay platforms, the graphene itself not only promotes electron transfer, but also increases the loading of the capture antibody, thus increasing the detection sensitivity with a detection limit as low as 0.1 ng/mL.¹¹⁷ In addition to carbon-based nanomaterials, it has been demonstrated that gold nanoparticles may both offer a friendly environment to immobilize protein molecules and facilitate electron transfer between protein molecules and the underlying electrode.^{95,118}

As shown in Table 3, the higher enzyme carry efficiency and electron transfer efficiency of these nanomaterials provide them with higher catalytic and electronic communication efficiency, resulting in signal amplification up to hundreds-fold compared with traditional enzyme-based electrochemical sandwich assays.^{7,13,92,98a} These proposed nanomaterial-based electrochemical sandwich immunoassays show potential applications in clinical screening of cancer biomarkers and point-of-care diagnostics.

Table 3. Electrochemical Sandwich Assay Based on Nanomaterials

strategy	protein	nanomaterial	detection limit	linear area	ref
I	PSA	carbon nanotubes	4 pg/mL	0.4–40 ng/mL	7
	PSA	magnetic beads	0.5 pg/mL	1–40 ng/mL	104
	α -fetoprotein	silica NPs	0.01 ng/mL	0.05–3 ng/mL	105c
II	cytochrome c	SWNTs	1.0×10^{-5} M	0.03–0.7 mmol/L	119
	PSA	SWNTs	0.25 ng/mL	0–1 ng/mL	91b
	thrombin	SWNT-FET	10 nM	0–100 nM	107
I and II	α -fetoprotein	graphene sheets and carbon NPs	0.02 ng/mL	0.05–6 ng/mL	108
	PSA	carbon nanotubes	4 pg/mL	0.4–40 ng/mL	7

3.5. Other Sandwich Assays

3.5.1. Giant Magnetoresistive (GMR) Sandwich Assay.

In traditional fluorescent- or colorimetric-signal-based sandwich assays, the inherent opacity and autofluorescence of the surrounding matrix interfere with the readout, which becomes a major limiting factor in many opaque biological samples, notably blood. However, most of the surrounding biological matrix is intrinsic nonmagnetic, which would therefore enhance the sensitivity of magnetic-nanotag-sensing-based sandwich assay. Unlike fluorescent labels, magnetic nanotags (MNTs) can be sensitively detected by inexpensive GMR sensors such as spin-valve sensors.¹²⁰ As shown in Figure 21, Gaster et al.

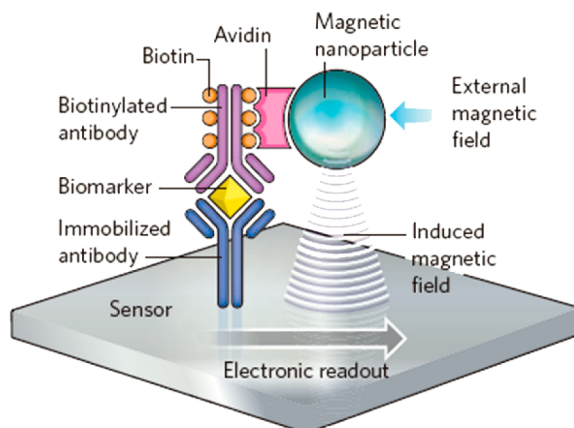


Figure 21. Mechanism of a magnetobiosensor. Reprinted with permission from ref 8. Copyright 2009 Nature Publishing Group.

utilized superparamagnetic nanoparticles as a nanotag to construct a sandwich assay, in which the target biomarker is sandwiched by immobilized antibody and biotinylated antibody, the avidin-linked magnetic nanoparticles bound to the biotinylated antibody.^{8,21,121} Under an external magnetic field, the nanoparticles magnetize, and their presence or absence can be detected in the form of electronic readout by the underlying GMR sensor. These GMR sandwich assays are capable of performing real-time multiplexed detection of protein tumor markers with concentrations down to the femtomolar level (10^{-15} M) in a variety of clinically relevant media with a linear dynamic range of over 6 orders of magnitude.¹²¹ The further development of giant magnetoresistive sandwich assay arrays with high sensitivity and specific multiplexed detection capability of protein tumor markers shows great promise in diverse applications such as medical diagnostics, therapy, clinical research, and basic science.

3.5.2. Localized Surface Plasmon Resonance (LSPR) Sandwich Assay. Localized surface plasmon resonance (LSPR) is a collection of electron charge oscillations usually occurring on the surface of metallic nanostructures (typically gold, silver, and platinum) and triggered by external electromagnetic radiation, mostly in the form of visible to infrared light (Figure 22A). As shown in Figure 22B, the sizes, shapes, and compositions of the metal nanoparticles can be systematically varied to produce materials with distinct light-scattering properties. The occurrence of LSPR results in an enhanced local electromagnetic field and strong light scattering, which result in the appearance of intense surface plasmon resonance absorption. As listed in Table 4, LSPR has been utilized in several different strategies to enhance the detection of protein.

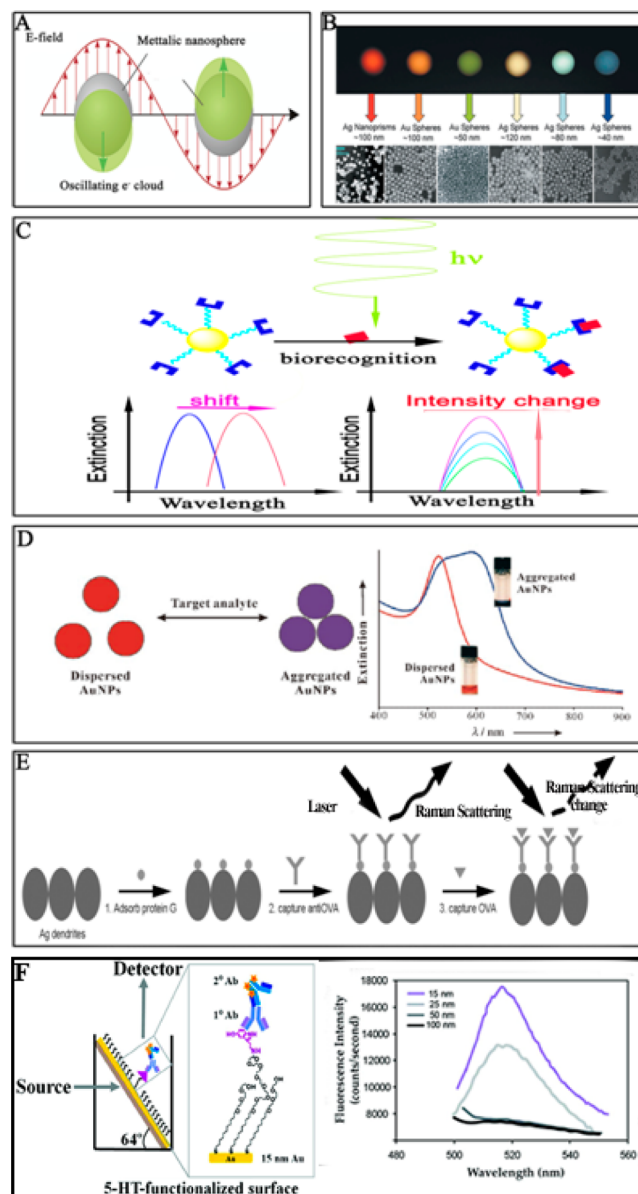


Figure 22. Schematic of the LSPR-based assay platform. (A) Plasmon oscillation for a sphere, showing the displacement of the conduction electron charge cloud relative to the nuclei. Reprinted from ref 131. Copyright 2002 American Chemical Society. (B) The sizes, shapes, and compositions of metal nanoparticles can be systematically varied to produce materials with distinct light-scattering properties. Reprinted from ref 57a. Copyright 2005 American Chemical Society. (C) Strategy I, plasmon resonance absorption band shift with biorecognition. (D) Strategy II, aggregation caused by immune complex formation and colorimetric assay. Reprinted with permission from ref 132. Copyright 2008 Wiley-VCH Verlag GmbH & Co. KGaA. (E) Strategy III, LSPR-enhanced Raman scattering. Reprinted from ref 9. Copyright 2011 American Chemical Society. (F) LSPR-enhanced fluorescence. Reprinted from ref 133. Copyright 2011 American Chemical Society.

First, the protein adsorption or antigen–antibody bioconjugation on the surface of metallic nanostructures changes the surrounding refractive index and finally leads to a shift or intensity change of the surface plasmon resonance absorption band, and this shift or intensity change is proportional to the concentration of the absorbate (Figure 22C).¹²² Second, biorecognition tailored reversible aggregation could introduce

Table 4. LSPR-Based Sandwich Protein Assay

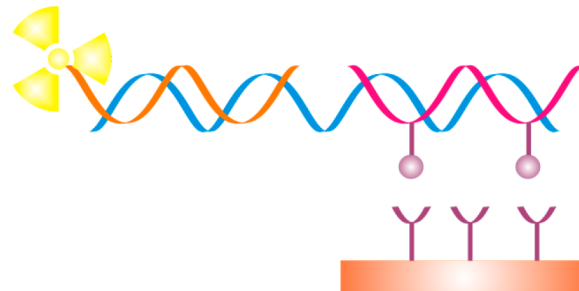
strategy	nanostructure	protein detected	detection limit	ref
I	Ag and Au NP assembled thin film	HSA	100 ng/mL	126
	ZnO–Au nanocomposite	rabbit IgG	0.15 μ g/mL	127
II	gold nanoparticles	antiprotein A	1 μ g/mL	128
	gold nanoparticles	PDGFs	15 nM	22
	gold nanorods	PDGFR	3.2 nM	23
III		h-IgG	60 ng/mL	
	silver NPs	lysozyme	5 μ g/mL	124
		catalase	50 ng/mL	
	silver NPs	BSA, catalase, pepsin	0.5 μ g/mL	129
	silver NPs	lysozyme, cytochrome c	0.2 μ g/mL	130
	silver dendrites	OVA	0.1 μ g/mL	9

a color change for colorimetric assay (Figure 22D).¹²³ Third, the enhanced local electromagnetic field allows the observation of an amplified spectroscopic response from target molecular species adsorbed at the planar surfaces of metallic nanostructures. These LSPR amplified signals have been utilized in several optical techniques, such as surface-enhanced Raman scattering (Figure 22E)^{123b,124} and surface-enhanced fluorescence (Figure 22F)¹²⁵ to detect protein. As shown in Figure 23, Yu et al. constructed a fluorescence sandwich LSPR assay based on the carboxymethyl dextran-matrix-modified CM5 sensor chip. In the detection process, the fluorophore (Alexa-Fluor 647) labeled rabbit antimouse antibody recognizes and binds to the mouse IgG covalently immobilized to the dextran matrix, forming a sandwich complex. The fluorescence response upon the injection of AF-RaM solutions has a detection limit of 500 aM (10^{-18} M), corresponding to a binding rate of 10 molecules mm^{-2} min^{-1} . The tunable LSPR and feasible surface biomodification properties of noble metal have shown great potential for applications in clinic biomedical diagnostic of biomarkers.

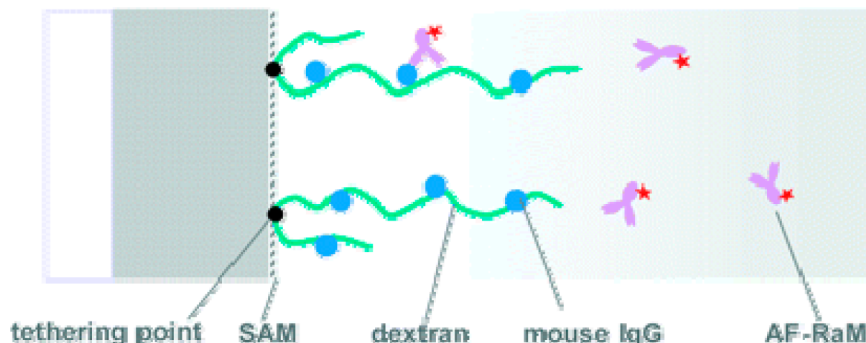
4. SANDWICH ASSAY FOR NUCLEIC ACIDS DETECTION

The sandwich assay plays an important role in the detection of oligonucleotides. Typically, in such sandwich assays, the capture probe specifically hybridizes with one region of a target oligonucleotide sequence and the signal probe (labeled with a fluorescent, enzymatic, electroactive signaling moiety) hybridizes with the other region on the target. These three components form a capture probe–target oligonucleotide–signal probe “sandwich” format. Like sandwich assays for proteins, the sandwich assays for nucleic acids do not require that the target oligonucleotides be fluorescently, enzymatically, or otherwise labeled. On the other hand, the capture and signal probes have minimal interaction in the absence of target, which ensures relatively low background signals, a high signal change upon target binding, and favorable detection limits.

As early as the 1970s, some researchers at Cold Spring Harbor Laboratory employed “sandwich hybridization” to map viral RNA transcripts.¹³⁴ They immobilized a capture probe which is used to hybridize one part of the target RNA on the filter. After the RNA target binding, the signal probe labeled with the radioactive ^{32}P (or ^{125}I , ^3H , or ^{35}S) hybridizes with the other part of the target RNA. Using a similar format (Scheme 1), a series of sandwich assays were successfully employed to detect DNA and RNA and were suitable for the direct detection in crude biological samples.¹³⁵

Scheme 1. Sandwich Assay for Nucleic Acids Based on Radioactive Detection

Although the sandwich assay based on radiolabels is sensitive enough, some limitations such as stability, safety, and detection system problems have stimulated the development of nonradioactive sandwich assay to fulfill the routine detection and diagnosis.¹³⁶ The techniques of DNA and RNA synthesis and chemical modification brought new opportunities to create a new type of nonradioactive sandwich assay. Through these, the signal probe can be labeled with fluorophore, a redox molecule, enzyme, etc. In recent years, many kinds of nucleic acid sandwich assays have been produced, including fluorescence sandwich assay, electrochemical sandwich assay, colorimetric sandwich assay, and nonlabel sandwich assays based on surface

**Figure 23.** Schematic of the fluorescence sandwich LSPR assay in a dextran matrix. Reprinted from ref 125a. Copyright 2004 American Chemical Society.

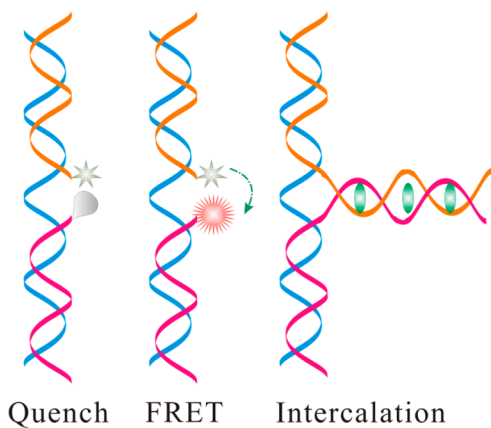
plasma resonance (SPR), the quartz crystal microbalance (QCM), and the microcantilever.

4.1. Fluorescence Nucleic Acid Sandwich Assay

4.1.1. Organic Dyes as Fluorophores. Organic dye has been widely and successfully used in biodetection and bioimaging because it is easy to synthesize and attach to biomolecules. For example, DNA (or RNA) modified with organic dye is well commercialized and can be synthesized on a relatively large scale. Also, scientists can readily attach it at the 3' (or 5') terminus of the DNA (or RNA) and any internal position of the DNA (or RNA). This continued progress greatly benefits the design of the sandwich assay for nucleic acids.

Usually, in a homogeneous system, there are two strategies to employ organic dye as the fluorophore in nucleic acid sandwich assay. One strategy is with labeled DNA recognition probes (Scheme 2, left and middle), and the other strategy is the label-

Scheme 2. Sandwich Assay for Nucleic Acids Based on Quenching (Left), FRET (Middle), and an Intercalation Dye (Right)



free method (Scheme 2, right). As we can see, two DNA (or RNA) probes with minimum preassociation are modified with a fluorophore and a quencher, respectively. At the initial state, the two probes are separated well from each other because there is no target in the detection system and the fluorescence is strong. Upon the target binding, the two probes hybridize with

different parts of the target, which makes the fluorophore approach the quencher and thus decrease the signal.

However, a limitation of the sandwich format mentioned above is that it is a “singal-off” assay. The nature of the signal-off assay makes it impossible for the signal change to be over 100%.¹³⁷ Motivated by this, sandwich assays based on the FRET (fluorescence resonance energy transfer) principle have been greatly developed and widely used (Scheme 2, middle). In this system, the fluorophore/quencher pairs in the signal-off sandwich assay are replaced by donor/acceptor pairs. The donor fluorophore in its excited state may transfer energy to the acceptor fluorophore. As a result, the fluorescence of the donor decreases and the fluorescence of the acceptor increases. As such, it is possible in principle that the signal increase is above 100%.

Labeling with organic fluorescent dye requires extra chemical synthesis and purification steps, which could introduce high cost and may be problematic in some remote areas. To overcome this, researchers from Columbia University developed a label-free DNA sandwich assay. Malachite green was used to produce a fluorescence signal, and after it bound with its aptamer, the fluorescence increased greatly. They separated the aptamer into two strands and added recognition arms to each strand. In the presence of the target, the two recognition strands hybridize with the target and the two strands reassociate, which allows the binding of malachite green and an increase in the fluorescence intensity (Figure 24).¹³⁸

When talking about organic dye, we should never ignore conjugated polymers. Conjugated polymers are excellent light-harvesting “antennae” owing to their high extinction coefficient,¹³⁹ so the energy collected by the polymer can be efficiently transferred to an adjacent acceptor because of the efficient energy migration along the polymer chains. As an example, Fan and his colleagues elegantly developed a magnetically assisted DNA sandwich assay with conjugated polymer amplification (Figure 25). It can detect the DNA target specifically and sensitively and identify single-base-mismatch DNA very well.¹³⁹ More importantly, it can be used in complex samples such as human serum. Some other works using conjugated polymers further demonstrated that they have an excellent light-harvesting property.^{82e,140}

4.1.2. Nanomaterials as Fluorophores. Despite the advantages of organic-dye-based assays, one intrinsic limitation of organic dyes is their poor photostability, which is very

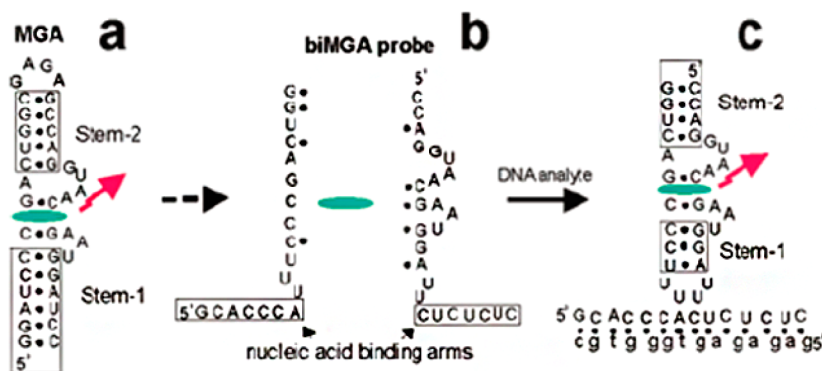


Figure 24. (a) Complex of malachite green with its aptamer. (b) The aptamer is split into two fragments, and each fragment is attached to a recognition probe. (c) In the presence of target, the target hybridizes with the two recognition probes and forms a sandwich format, which brings the two fragments into close proximity to bind their target, malachite green, and thus increase the signal. Reprinted from ref 138. Copyright 2005 American Chemical Society.

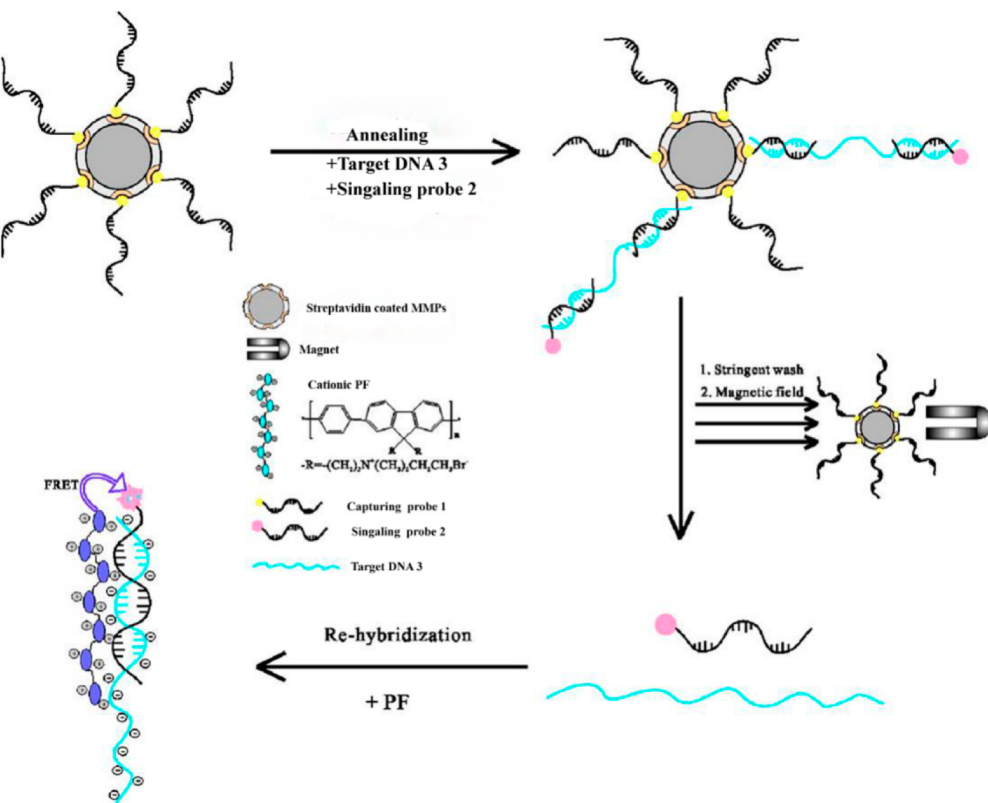


Figure 25. Magnetically assisted DNA sandwich assay proposed by Fan's group. In the presence of target DNA, the capture probe which is immobilized on the magnetic bead and the signal probe form a sandwich format with the target. After the washing and separation steps, the conjugated polymer shown binds to the signal probe and produces an amplified signal. Reprinted with permission from ref 139. Copyright 2005 Oxford University Press.

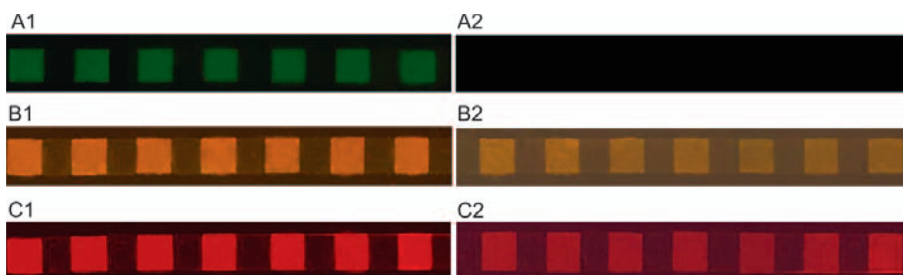


Figure 26. Comparison of the photostability of an organic dye (FITC) and quantum dots showing that quantum dots are more stable than FITC under photoirradiation. (A1) Fluorescence image of a microarray using avidin–FITC probes. (B1, C1) Fluorescence images of microarrays using two avidin-modified quantum dots with different emissions. (A2, B2, C2) Corresponding fluorescence images after 30 min of photoirradiation. Reprinted with permission from ref 72b. Copyright 2008 Tsinghua Press and Springer-Verlag.

important for a detection method. That is, the organic dyes will be destroyed by light exposure (this phenomenon is called photobleaching). Some advanced materials with high photostability need to be developed to overcome this limitation.

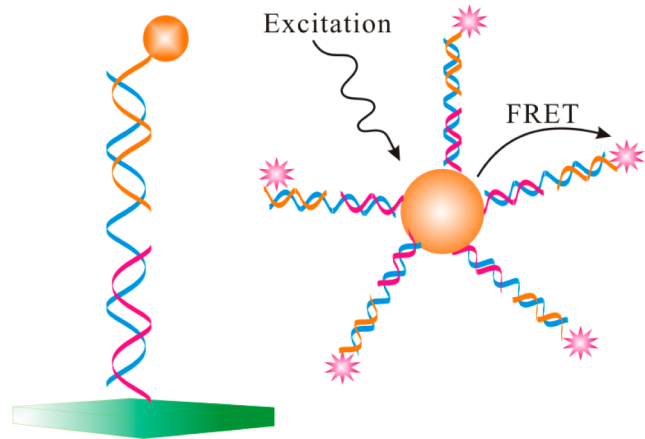
In recent years, with the development of nanotechnology, nanomaterial as a promising star has been developed greatly and applied widely in biosensing and bioimaging. Among the numerous nanomaterials, there are some such as quantum dots and dye-doped nanoparticles which have excellent optical properties.

Quantum dots are considered as the most promising fluorescent materials because of their several natural advantages, such as size-tunable emission, broad photoexcitation, narrow and symmetric emission spectra, strong fluorescence, and high photostability.^{59b,141} We can see clearly that quantum

dots have much higher photostability than traditional organic dyes (here, FITC; Figure 26).^{72b} The fluorescence signal from FITC almost disappeared after 30 min of irradiation with blue light, while fluorescence signals from two quantum dots decreased by a much smaller percentage. Even after irradiation for 4 h, the signals from quantum dots were still there and visible.

The application of quantum dots has attracted extensive interest in the biosensing field. Obviously, there are many DNA sandwich assays based on quantum dots. Usually, the strategies of these assays are almost the same as those of the sandwich assays based on organic dyes (Scheme 3), but with the advantages of quantum dots, the new assays have achieved much better sensitivity and stability. Wang and his colleagues attached two different DNA probes to two quantum dots with

Scheme 3. DNA Sandwich Assay Using Quantum Dots as the Signal Output (Left) or Using Quantum Dots as the Probe Carrier and Donor Dye in a FRET-Based Assay (Right)



discernible emission wavelengths, and these two probes can hybridize with different parts of the target DNA. After binding with the target, they form a sandwiched nanoassembly (Figure 27). They claimed that this method is capable of detecting

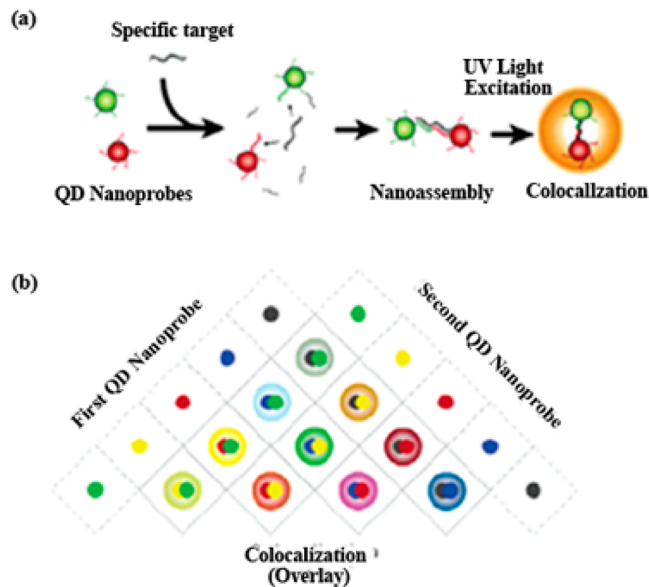


Figure 27. (a) Two capture probes are immobilized on two quantum dots with different emissions. After introduction of the target into the system, the two capture probes can hybridize with different regions of the target DNA and form a sandwiched nanoassembly which is detected as a blend color. (b) Multiplexed detection platform using different color combinations. Reprinted from ref 142. Copyright 2005 American Chemical Society.

DNA hybridization at the single-molecule/particle level and therefore ideal for analyzing low-abundance targets.¹⁴² Scientists in Korea developed a bead-based DNA sandwich assay with quantum dots as the signal producer (Figure 28). This method was successfully used to detect the *Bacillus* *spoOA* gene.¹⁴³

Quantum dots are also used as donors in FRET assays (Scheme 3, right).¹⁴⁴ Chan et al. developed a quantum-dot-encoded microbead for multiplexed genetic detection of nonamplified DNA samples. Specifically, they investigated the

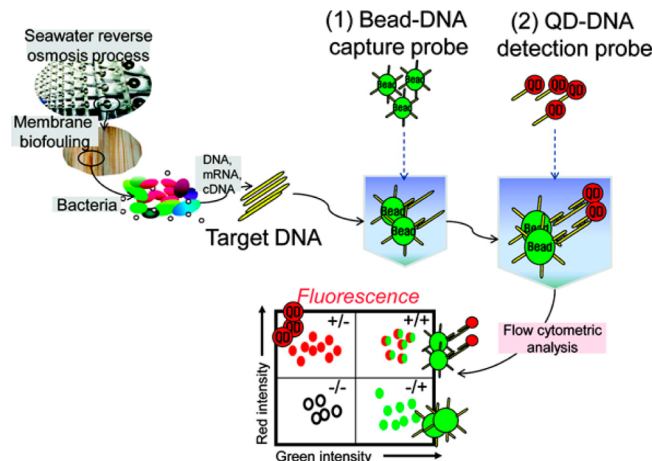
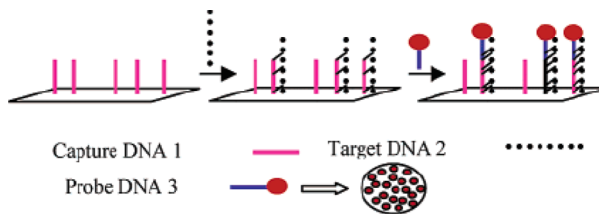


Figure 28. As shown, DNA capture probes are immobilized on beads ($5.6\ \mu\text{m}$ in diameter and with intact green fluorescence) and detection probes are immobilized on quantum dots. In the presence of target DNA from *Bacillus* sp. which is isolated from seawater, the sandwich complex forms and is detected by a flow cytometer. Reprinted from ref 143. Copyright 2010 American Chemical Society.

effect of the capture probe, reporter probe, and target DNA sequence lengths on the hybridization kinetics and efficiency. A 0.02 fmol detection limit was achieved, and they found out that the best sensor performance is with a short probe (15–18 nt) and short DNA targets (36 bp).¹⁴⁵ Krull and his colleagues created a multiplexed solid-phase assay using quantum dots as donors in FRET.^{145b}

In addition to the quantum dots, dye-doped nanoparticles have been greatly investigated in DNA sandwich assay recently. Tan and his co-workers pointed out two difficulties that limit the sensitivity of the fluorophore-based assay.¹⁴⁶ One is a DNA probe can only be labeled with one or a few fluorophores, which makes the signal too weak to detect in the very low concentration of target. The other is the photobleaching problem of fluorophores makes the assay irreproducible for ultratrace detection. To overcome these limitations of fluorophores and achieve high sensitivity, they developed a new sandwich assay based on dye-doped silica nanoparticles (Scheme 4). One particle entraps a large number of

Scheme 4. Sandwich Assay Based on Dye-Doped Nanoparticles^a



^aReprinted from ref 146. Copyright 2003 American Chemical Society.

fluorophores, which makes it highly fluorescent. Also, the dye-doped nanoparticle is highly photostable because of the silica matrix shielding effect. On the basis of these advantages, they achieve a detection limit of 0.8 fM. A group of scientists from Oak Ridge National Laboratory developed dye-doped core–shell silica nanoparticles and employed them to improve the sensitivity and photostability in DNA sandwich assay.¹⁴⁷ These particles are stable in both aqueous solutions and organic

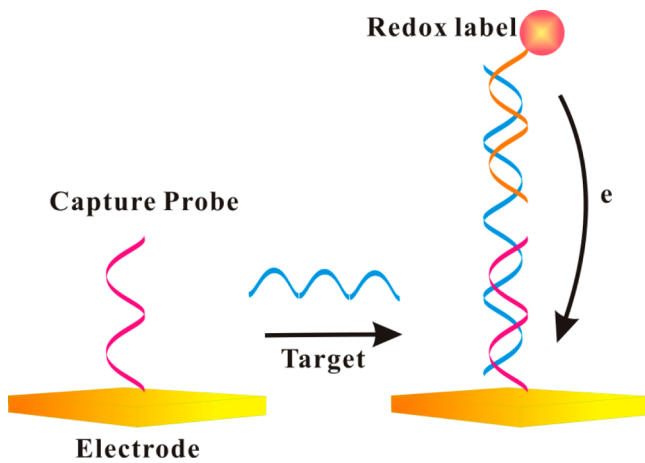
solvents and are successfully employed in the microarray system. However, there are still some problems with the application of quantum dots. For example, the water solubility of quantum dots needs to be improved for better biocompatibility. The stability of the biomolecule–quantum dot conjugates is still not high enough. Additionally, the cost of the quantum dots' synthesis is still high, which hinders practical applications on a large scale. Nontoxic quantum dots are needed too because the leak of heavy metal ions may inhibit the enzyme when coupled to many other detection systems.

Liposome is usually used as a substance carrier without fluorescence, but fluorophores or other signaling molecules can easily be loaded into the liposome, and this makes it a reporter particle.¹⁴⁸ Some studies indicated that one liposome can contain up to 105 fluorescent molecules so that it can produce much higher fluorescence than a single fluorophore.¹⁴⁹ For example, carboxyfluorescein-filled liposomes were used as reporter probes to detect viable *Cryptosporidium parvum* by testing RNA with nucleic-acid-sequence-based amplification.^{148a}

4.2. Electrochemical Nucleic Acid Sandwich Assay

Among a variety of signal transduction techniques, electrochemical signal transduction is widely recognized as the most promising one with its unique characteristics (simple, portable, and inexpensive), so not surprisingly, the DNA sandwich assays are expanded from fluorescence assays to electrochemical assays. Usually, an electrochemical sandwich assay is constructed by electrode-surface-confined capture probes and signal probes that freely exist in the detection solution and are modified with electrochemical (or redox) labels. The target binding brings the signal probes proximal to the electrode, thus producing a detectable electrochemical signal (Scheme 5).

Scheme 5. Scheme of the Electrochemical Nucleic Acid Sandwich Assay



4.2.1. Application of Redox Labels. The application of redox labels is the most direct way to produce an electrochemical signal. Nature has given a unique character (redox property) to some molecules that can transfer electrons to or from the electrode surface. Usually, we can see the wide application of ferrocene,¹⁵⁰ methylene blue,^{137,151} hexaammineruthenium(III) chloride ($[\text{Ru}(\text{NH}_3)_6]^{3+}$, Ru-Hex),^{151d,152} and Prussian blue.¹⁵³

Because of its excellent electrochemical properties (reversible oxidation/reduction, convenient redox potential) and commer-

cial availability (it is easy to conjugate ferrocene to oligonucleotides), ferrocene is widely used in electrochemical DNA detection. A group of scientists from Motorola, Inc. have designed a platform of electronic detection of nucleic acids through a sandwich assay.¹⁵⁴ In this assay they used a mixed self-assembled monolayer (SAM), which includes thiol-labeled DNA capture probes, polyglycol-terminated alkanethiols, and phenylacetylene molecules. Obviously, the DNA capture probe is used to hybridize the unlabeled target DNA, and the overhang portion of the target can bind to the ferrocene-modified signaling probe (Figure 29A). In this system, they creatively used polyglycol-terminated alkanethiols as insulator molecules and phenylacetylene as the molecular wire (Figure 29A). Through the hybridization, the ferrocene-labeled signaling probes are in close proximity to the SAM to produce a faradic current (Figure 29B), whereas the signal probes in solution cannot produce any signal. This makes this method a “washing”-free method and minimizes the electrochemical signal from the nonspecific adsorbed signaling probes on the surface. On the basis of this advantage, and using this creative platform, they successfully detected the amplicons of PCR products and demonstrated single-nucleotide polymorphism discrimination.

Usually, an electrochemical-sandwich-type assay needs three components (capture probe, target oligonucleotide, and signaling probe) to produce an electrochemical response. To simplify the sandwich assay and make it reagentless, Grinstaff and his colleagues developed a “two-piece” electrochemical sandwich assay.^{150c} They ingeniously linked the capture probe and ferrocene-labeled signaling probe together through a flexible poly(ethylene glycol) (PEG) spacer. This ABA triblock was immobilized on the electrode surface, and one only needs to add the target into the detection system to get the electrochemical response due to the conformational change of the ABA triblock (Figure 30). This design represents an important improvement to decrease the detection steps, which is potentially useful for some practical applications and to commercialize the electrochemical sandwich assay.

To improve the detection sensitivity of the ferrocene-based sandwich assay, Zhou and his colleagues attached gold nanoparticles capped with ferrocene to amplify the electrochemical signal upon the target binding.^{150a,b} One target binding brings a large number of ferrocenes and thus produces much more signal than the sandwich assay mentioned before (Figure 31). On the basis of this amplification, they obtained a detection limit of 2 pM. Some researchers from Xiamen University transferred the ferrocene-based sandwich assay onto the ultramicroelectrode and combined it with low-current voltammetry, which can detect trace electroactive species.^{150d} A detection limit of 100 fM was obtained.

Methylene blue is another redox label with a favorable redox potential and excellent stability. The Plaxco group has employed methylene blue to build a series of DNA- or aptamer-based sensors for sensitive and selective detection of nucleic acids, proteins, small molecules, and metal ions.^{151a,155} The use of methylene blue makes these sensors really stable when employed in complex matrixes such as serum and even whole blood, and these sensors can be regenerated easily and reused many times. They also detected DNA using a sandwich format with a methylene blue-labeled signaling probe.^{155b} The detection limit of this sandwich assay is 100 pM.

Working very well in complex matrixes is an obvious advantage compared with ferrocene. Ferapontova et al. found

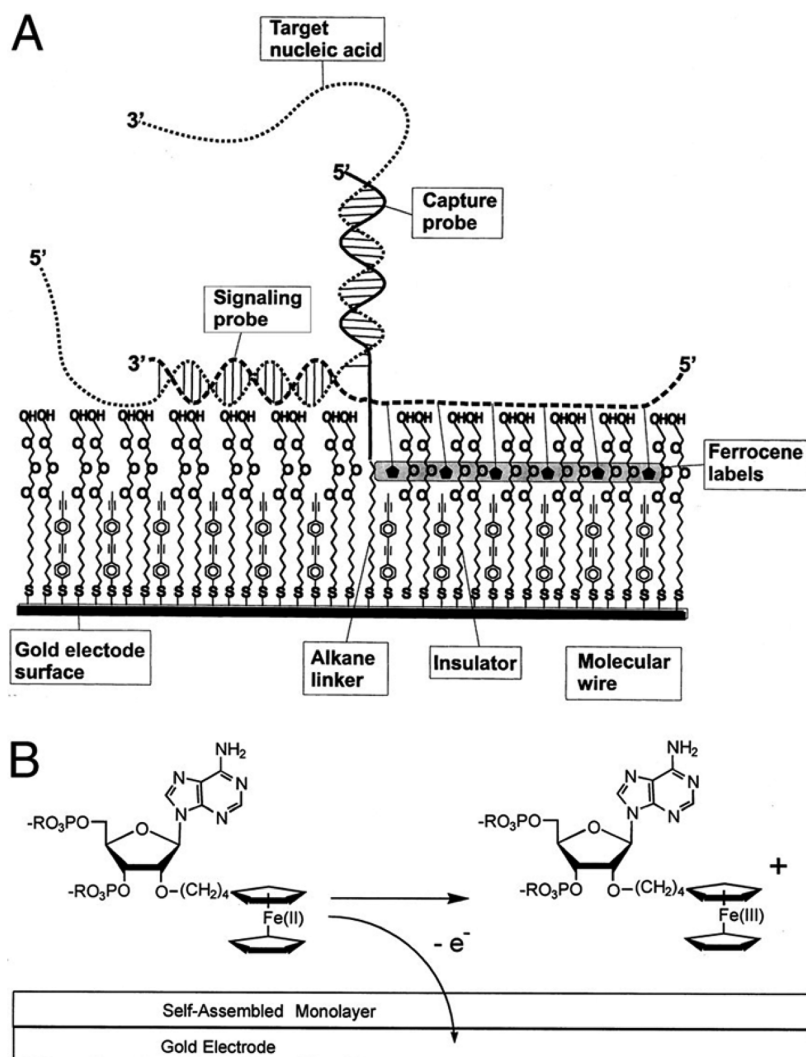


Figure 29. (A) Scheme of the electronic DNA sandwich assay. (B) Electrochemical oxidation of ferrocene-modified adenine and electron transfer to the electrode, which is detected by an electrochemical instrument. Reprinted with permission from ref 154a. Copyright 2001 Elsevier.

that a ferrocene-labeled RNA-aptamer-based sensor is inhibited in serum, but works well in serum-free buffer solutions (Figure 32).¹⁵⁶ They indicated that the adsorption of serum proteins at the positively charged electrode surface slows the electron transfer of ferrocene. White et al. systematically studied the differences between the sensors fabricated with methylene blue and ferrocene.^{151b} They demonstrated that methylene blue-based sensors have better solution-phase storage stability, electrochemical stability, and signal verity (Figure 33).

The application of ferrocene or methylene blue in sandwich assay requires chemical conjugation with the DNA signaling probes. To avoid the chemical synthesis step, some scientists employ some positively charged redox cations such as $[\text{Ru}(\text{NH}_3)_6]^{3+}$ (Ruhex) which can electrostatically associate with nucleotide phosphate residues of the DNA probe,^{152b,c} and the binding of Ruhex to DNA is completely through electrostatic interaction without any duplex intercalation. On this basis, the redox charge of Ruhex is directly used to indicate the amounts of DNA localized at the electrode surfaces.^{152b} A previous study demonstrated that Ruhex does not adsorb on the 6-mercapto-1-hexanol (MCH) self-assembled monolayer.^{152c} In many sensor designs, MCH serves as a spacer that modulates the surface density of DNA probes and a

passivation layer that effectively prevents nonspecific adsorption. Using Ruhex as the redox indicator, Chunhai Fan and his colleagues created a DNA sandwich assay based on gold nanoparticle amplification.^{151d,152a} Cleverly, they loaded hundreds of DNA probes onto gold nanoparticles as signal probes which can adsorb thousands of Ruhex ions (Figure 34). As a result, one hybridization event brings signal from more than 10^3 redox events. They achieved femtomolar sensitivity through the gold nanoparticle amplification. Another key point that represents a significant improvement is they finely controlled the density of capture probes to obtain an optimized hybridization efficiency.

4.2.2. Application of Enzyme-Based Amplification. As

As we all know, a redox label can only transfer one or a few electrons to or from the electrode surface. The limitation of the number of electrons transferred directly affects the sensitivity of the DNA sandwich assay. High sensitivity is usually demanded because in some real problems the DNA levels are really low, such as pathogen DNA detection and cancer or infectious disease DNA detection. To fulfill this demand, enzyme-linked DNA sandwich assay has attracted extensive attention as a method of signal amplification. During each catalytic reaction on the electrode, thousands of electrons are transferred to the

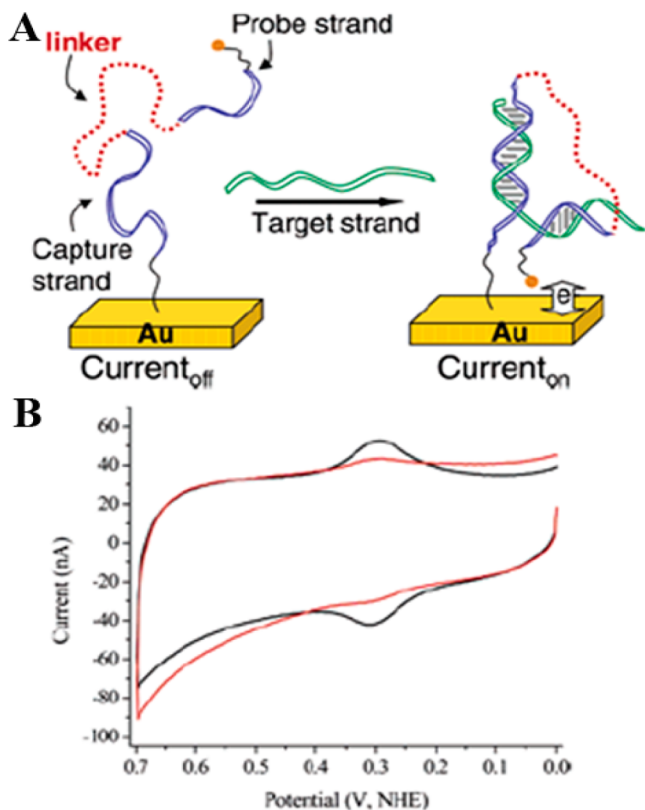


Figure 30. (A) The capture probe and signal probe (ferrocene-labeled) are connected through a soft linker which forms the ABA triblock. After the hybridization with the target, the conformational change forces the ferrocene into close proximity of the electrode surface to produce an electrochemical signal. (B) Typical electrochemical signals of cyclic voltammetry before (red) and after (black) addition of the target. Reprinted from ref 150c. Copyright 2004 American Chemical Society.

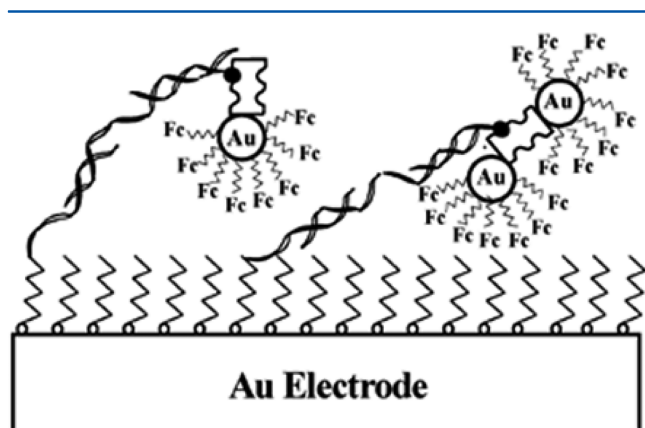


Figure 31. The signal of the electrochemical DNA sandwich assay is amplified by gold nanoparticles conjugated with ferrocene. Reprinted from ref 150a. Copyright 2003 American Chemical Society.

electrode. In the enzyme amplification system, enzymes such as HRP,¹⁵⁷ alkaline phosphatase (ALP),^{102a,158} and glucose oxidase¹⁵⁹ are used as a substitute for the redox label.

HRP is widely used to amplify the relatively weak signals and generate strong signals in a short time span. For example, Heller et al. developed an enzyme-amplified amperometric sandwich assay for DNA and RNA.^{157a} We should clarify that HRP itself does not directly exchange electrons with the

electrode because its redox site is embedded in insulating peptide backbones,¹⁵⁷ⁱ so in this assay, they employed a redox polymer (a water-soluble copolymer of acrylamide and vinylimidazole, complexed with osmium bis(4,4'-dimethyl-2,2'-bipyridine) chloride (PAA-PVI-Os; Figure 35) which can electronically “wire” the HRP reaction center upon contact and catalyze the electroreduction of H_2O_2 to water. They achieved a detection limit of 550 pM and have successfully employed the system in complex matrixes such as goat serum, which should contribute to the resistance of the polyacrylamide-based gels to nonspecific proteins or nucleic acids. After this, they made an effort to perform this sandwich DNA assay with a mass-manufacturable carbon electrode screen-printed on polyester sheets^{157b} (Figures 36 and 37) (just like the glucose meter people usually use) and achieved a 200 pM detection limit in a 5 μL droplet (which contains 5 fmol of target).

Interestingly, by using a 10 μm diameter microelectrode rather than a 3.6 mm diameter carbon electrode, Heller and his colleagues further improved the detection limit of this sandwich DNA assay by 10^4 -fold.^{157c} The detection limit of the microelectrode system is 0.5 fM, as few as 3000 copies in a 10 μL droplet, because a thicker film of the redox polymer and an increased loading of capture probes have increased the collection efficiency of electron vacancies originating in electron-reduced H_2O_2 .

The HRP-based sandwich assay mentioned above requires an additional reagent, H_2O_2 , which would be inconvenient in some real applications. To avoid this, the same group replaced the HRP with bilirubin oxidase (BOD), which effectively catalyzes the ambient O_2 to water at neutral pH (Figures 38 and 39).^{157d} In this system, like the HRP-based sandwich assay, ~3000 copies of *Shigella* DNA can be selectively detected.

Unlike the employment of a redox polymer as the molecular wire to transfer the electrons of HRP, a small redox molecule, TMB (3,3',5,5'-tetramethylbenzidine), has been widely employed as an electron shuttle that can diffuse in and out of the redox site of macromolecules, thus coupling the catalytic reduction of H_2O_2 with the redox reaction of TMB at the electrode surface.^{157e-g,i} On this basis, clearly and systematically, Fan et al. have developed a sandwich-type electrochemical sensor for sequence-specific DNA detection (the detection limit is 1 pM even in a complicated biological fluid such as human serum) (Figure 40).^{157e} This sensor was used for the detection of a PCR amplicon from the genomic DNA of *Escherichia coli* K12 (the detection limit is 60 fg, which is equal to 10 copies). The nonspecific adsorption of signaling proteins such as HRP is a serious problem in the enzyme-based DNA sandwich assay, bringing a high background signal and thus limiting the final detection sensitivity of the assay. They also found that the mixed SAM incorporating thiolated oligonucleotides and oligo(ethylene glycol)-terminated thiols is highly protein resistant and effectively repels nonspecific adsorption. The function of this system can be extended to single-nucleotide polymorphism (SNP) detection.^{157e,g} The employment of the sandwich format and the mixed SAM with high nonspecific resistance leads to a high differentiation ability of SNPs. The use of a 16-electrode sensor array also provides a multiplex platform for simultaneous detection of different SNPs. In addition, Joseph Wang and his colleagues also developed a new SAM (a mixture of thiolated DNA capture probe, mercaptohexanol, and dithiothreitol) which provides great improvement in the signal to noise ratio. Coupling the

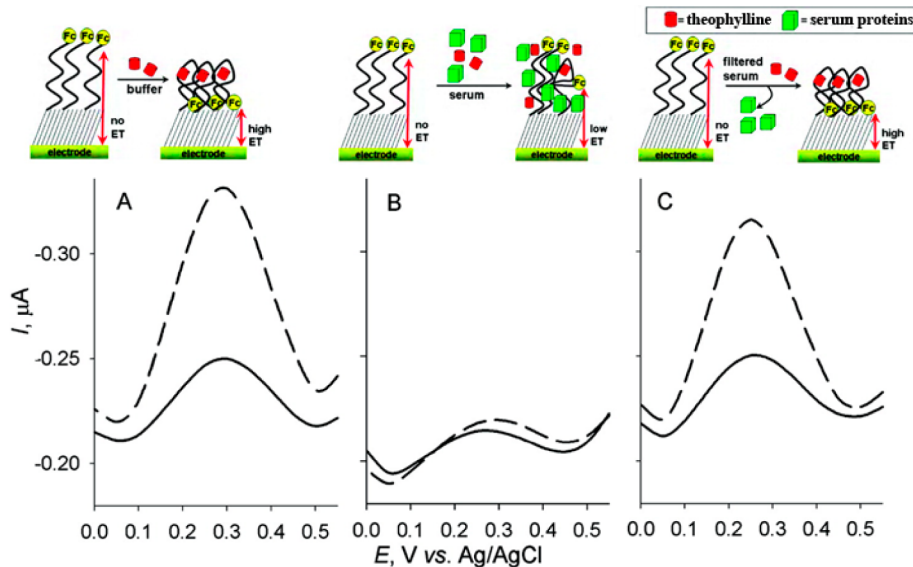


Figure 32. Electrochemical signal determined by differential pulse voltammetry (DPV) of the biosensor based on an RNA aptamer before (solid line) and after (dashed line) addition of the target. Experiments were conducted in buffer (A), serum (B), and filtered serum (C). Reprinted from ref 156. Copyright 2009 American Chemical Society.

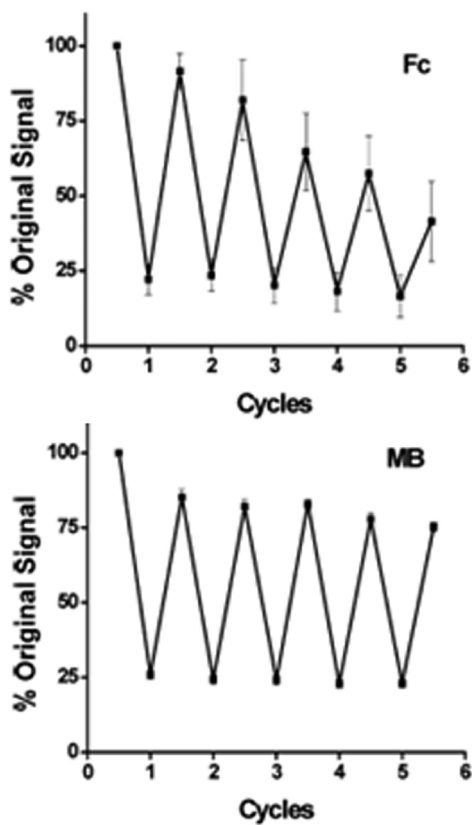


Figure 33. Electrochemical sensors based on ferrocene (Fc; top) show relatively poor stability when repeatedly challenged in blood serum, but the sensors based on methylene blue (MB; bottom) maintain at least 85% of the original signal because of their stability. Reprinted from ref 151b. Copyright 2009 American Chemical Society.

new SAM to the HRP-based DNA sandwich assay, as few as 40 zmol (4 μL of sample) of target can be detected.¹⁶⁰

Besides the improvement of the mixed self-assembled monolayer, DNA immobilization is also an important factor influencing the sensor's performance. In the traditional DNA

sandwich assay, single-stranded DNA is usually used as the capture probe and immobilized on the electrode surface followed by passivation with an alkanethiol (e.g., mercaptohexanol), which can occupy the free space on the surface to repel nonspecific adsorption, but the orientation and the distribution of DNA probes on the solid surface are difficult to control. Fan and his colleagues noted that this heterogeneous surface reduces the accessibility of the target to the probes. For the first time, they creatively developed a platform based on a 3D-nanostructured DNA probe.¹⁶¹ Their pioneering work is shown in Figure 41. A tetrahedron structure containing a capture probe at one vertex and three thiol groups at the other vertices is designed and immobilized on the gold electrode surface. This uniform and highly arrayed immobilization of probes ensured improved sensitivity compared to traditional immobilization based on single-stranded DNA considering the entanglement between the probes and the localized aggregation of probes.¹⁶² Even without the passivation with mercaptohexanol, the sensor based on tetrahedron probes can be used to detect the target because of the upright orientation of this kind of probe, which brings a high hybridization efficiency, while the sensor based on single-stranded DNA probes cannot produce a detectable signal without passivation because the flat orientation induced a poor hybridization efficiency. Furthermore, the resistance to non-specific proteins of the tetrahedron probes is much better than that of the passivation layer of mercaptohexanol. We should point out that this design could work well in all enzyme-based sandwich assays for nucleic acids.

Besides the contribution of HRP in the enzyme-linked sandwich assay, alkaline phosphatase (ALP) has been widely used in the sandwich assay.¹⁵⁸ ALP catalyzes a substrate such as *p*-APP, *p*-nitrophenyl phosphate, or phenyl phosphate with no electrochemical activity to a redox substrate that can be readily detected by the electrochemical method (Figure 42).^{157c} Kwak and his co-workers have developed a sensitive and selective DNA sandwich assay using an electrocatalytic ferrocenyl-tethered dendrimer.^{158a} In their system, the ferrocenyl-tethered poly(amidoamine) dendrimer (Fc-D) has two functions: one is as an electrocatalyst to enhance the electrochemical signal, and

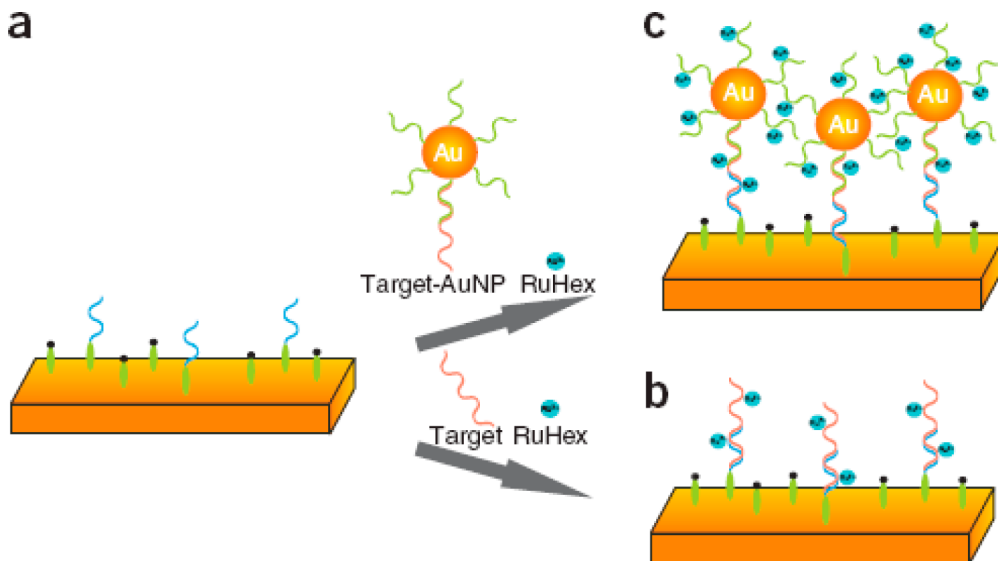


Figure 34. Capture probes are immobilized on a gold electrode via a Au–S bond, and MCHs are used as the spacer and passivation layer (a). Gold nanoparticles loaded with hundreds of DNA probes can adsorb thousands of Ruhex ions and bring an amplified signal (c). In comparison, DNA detection probes without nanoparticle amplification can only adsorb limited Ruhex ions, which results in a relatively small signal (b). Reprinted with permission from ref 151d. Copyright 2007 Nature Publishing Group.

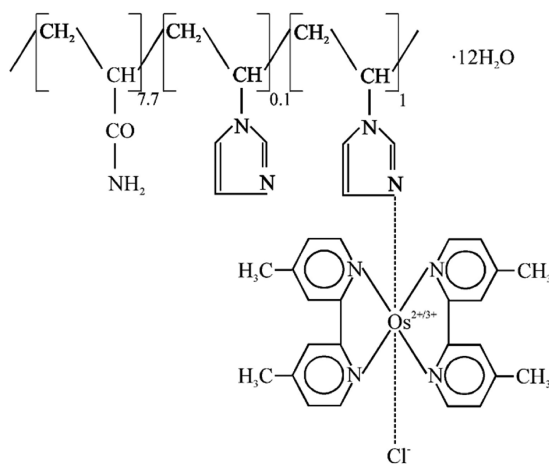


Figure 35. Structure of the polymer which is used by Heller and his colleagues. Shown is a hydrazine-treated copolymer of poly(acrylamide) and poly(*N*-vinylimidazole) complexed with $[\text{Os}(4,4'\text{-dimethyl-2,2'\text{-bipyridine}})_2\text{Cl}]^{1+/2+}$. Reprinted from ref 157a. Copyright 2002 American Chemical Society.

the other is as a building block to immobilize the DNA capture probe. After introduction of the target and signal probe, the sandwich-type assay forms and the ALP is attached on the

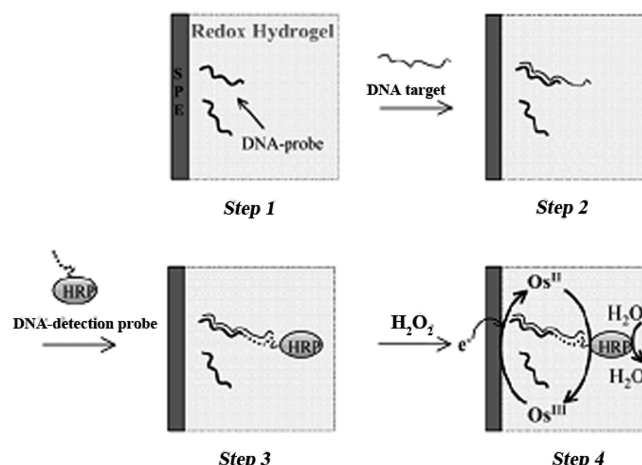


Figure 37. Steps of the sandwich assay based on screen-printed electrodes. In step 1, the redox polymer and capture probe are immobilized on the electrode surface through electrodeposition. In step 2, the capture probe hybridizes with the target. In step 3, the signal probe labeled with HRP hybridizes with the target. In step 4, the redox polymer contacts the center of HRP, which can catalyze the electroreduction of H_2O_2 . Reprinted from ref 157b. Copyright 2002 American Chemical Society.

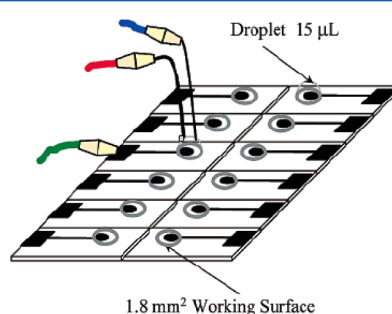
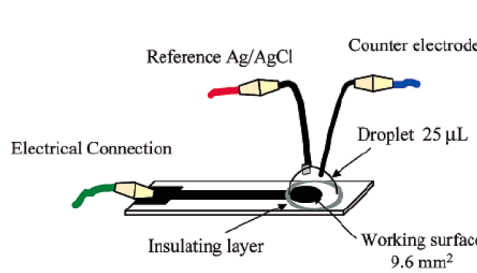


Figure 36. Scheme of an array based on screen-printed electrodes. Reprinted from ref 157b. Copyright 2002 American Chemical Society.

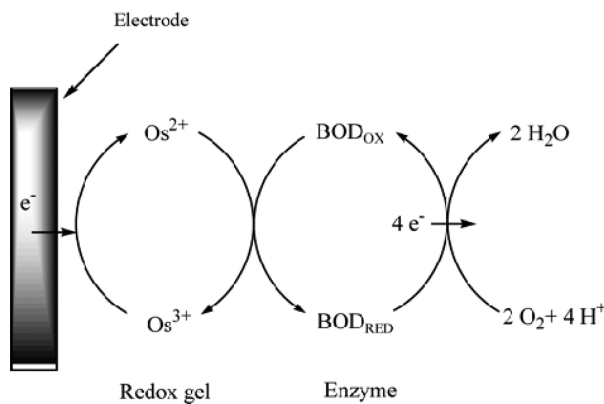


Figure 38. Principle of the electrocatalysis reaction of BOD. Reprinted from ref 157d. Copyright 2004 American Chemical Society.

signal probe through the biotin–avidin interaction. Then the redox product (*p*-aminophenol) is produced from the ALP enzymatic reaction. The *p*-aminophenol diffuses into the Fc-D layer and then is electrocatalytically oxidized by the Fc-D. This enzyme catalysis and Fc-D catalysis lead to a detection limit of 20 fM.

To further improve the sensitivity of ALP-based sandwich assay, Joseph Wang et al. have loaded the ALP on carbon nanotubes using a 1-ethyl-3-(3-(dimethylamino)propyl)-carbodiimide linker (Figure 43),¹⁹ and they estimated that about 9600 enzymes were immobilized per carbon nanotube. Then they compared the amplified enzyme system with the original enzyme system and found that the original enzyme system did not respond to 10 pg/mL target, while the amplified enzyme system can detect such a low concentration. A detection limit of 1 fg/mL (54 aM) was achieved in this amplified system.

The performance of the ALP-based sandwich assay is also improved by using the capture probe design.^{158c–e} For example, a hairpin probe was used to improve the sensitivity and selectivity of ALP-based sandwich assay.^{158c} The results showed that the signal to background ratio was 21 with 200 nM target using the hairpin capture probe, while a ratio of 8 was obtained by using a linear capture probe, and the hairpin probe system has better mismatch differentiation ability than the linear probe system. Lin and his colleagues designed an electrochemical branched DNA sandwich assay for PCR-free detection RNA.^{158d} A DNA amplifier with high loading of ALP was used to amplify the signal, and one hybridization event could bring ~1600 ALP enzymes.

Very similar to the HRP-based sandwich assay developed by Heller, glucose oxidase and a cationic redox polymer–osmium–bipyridine complex were employed to build the DNA sandwich assay (Figure 44).^{159c} Instead of electrodeposition of the polymer on the electrode surface, after forming the sandwich-type hybridization and introducing the glucose oxidase, they applied a technique of redox polymer overcoating through layer by layer electrostatic self-assembly, which can bring the glucose oxidase into electrical contact with the redox polymer and form an electrocatalytic bilayer for the oxidation of glucose. Thus, femtomolar DNA can be readily detected through this strategy.

Other than the employment of the redox polymer, the catalytic reaction of glucose oxidase can also be converted into an in situ enzyme-catalyzed deposition of cupric hexacyanoferate (CuHCF) nanoparticles in the presence of glucose, cupric ions, and ferricyanide. The electrochemical signal of the deposited CuHCF nanoparticles can be used as the signal readout.^{159d} Furthermore, glucose oxidase-based DNA sandwich assay can be accomplished by the electrochemiluminescence (ECL) signal of luminol with the in situ generated H_2O_2 .^{159b}

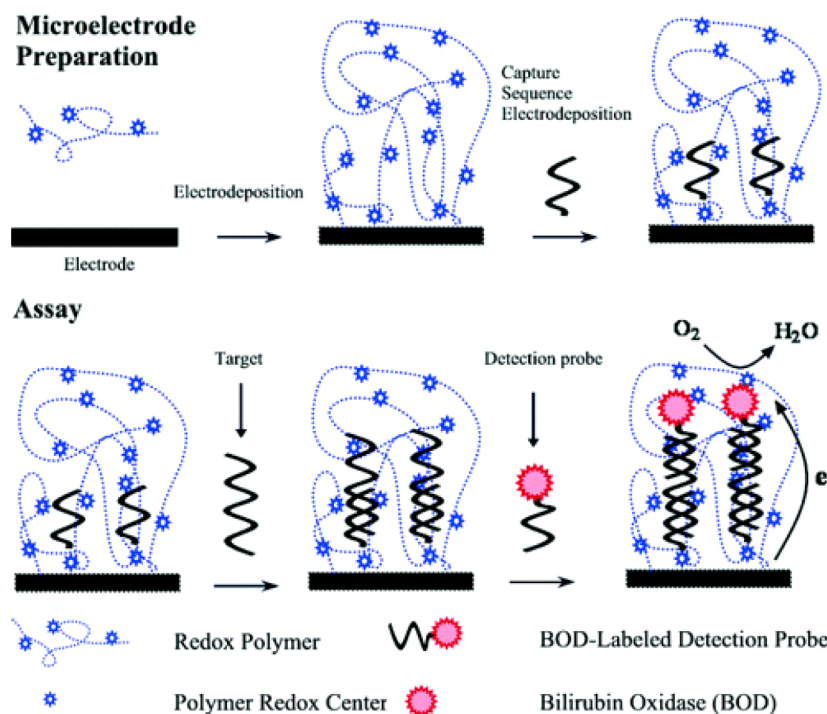


Figure 39. Scheme of the DNA sandwich assay based on BOD. Reprinted from ref 157d. Copyright 2004 American Chemical Society.

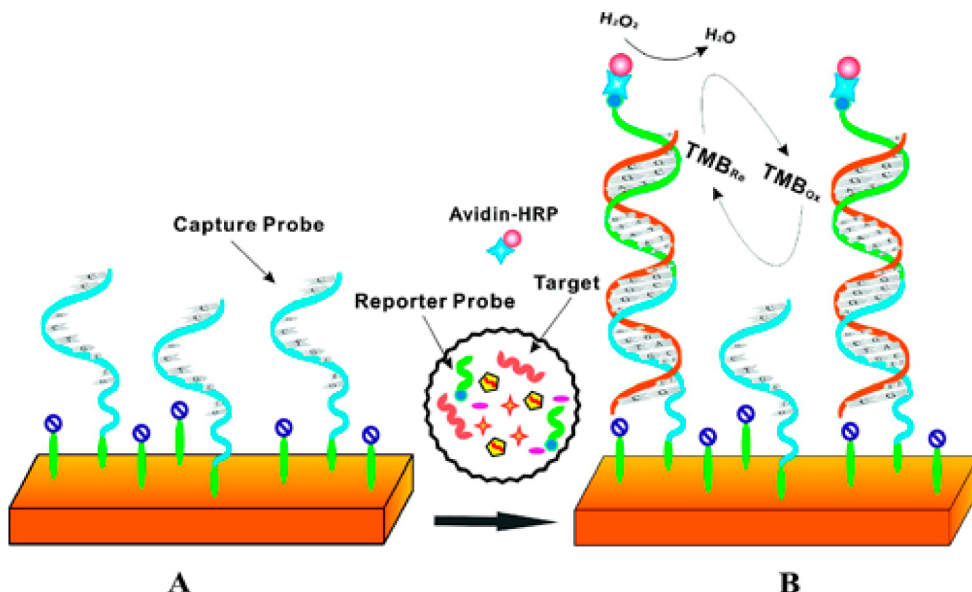


Figure 40. DNA sandwich assay based on HRP. In this system, TMB serves as an electron shuttle and assists the electroreduction of H_2O_2 . At the same time, the mixed monolayer has a high resistance property to nonspecific adsorption, which can greatly improve the performance of the sandwich assay. Reprinted from ref 157e. Copyright 2008 American Chemical Society.

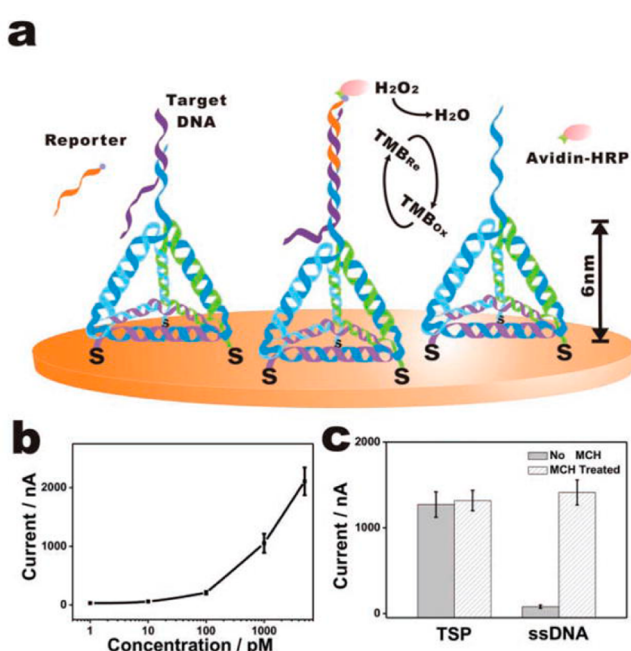


Figure 41. (a) Scheme of the DNA sandwich assay based on tetrahedron probes. The probes are immobilized on an electrode surface through three thiol groups and orientated upright. (b) As low as 1 pM target can be detected using the sandwich assay based on tetrahedron probes. (c) The sensor based on tetrahedron probes produces a comparable and detectable signal with or without a passivation layer of mercaptohexanol, but the sensor based on single-stranded DNA probes can be used for detection only with a passivation layer. Reprinted with permission from ref 161. Copyright 2010 Wiley-VCH Verlag GmbH & Co.

4.2.3. Application of Nanomaterials. Redox label and enzyme-linked DNA sandwich assays have been successful and widely used recently, but they have limitations in terms of sensitivity and stability, respectively. For example, redox-labeled signal probes are chemically stable enough, but usually produce

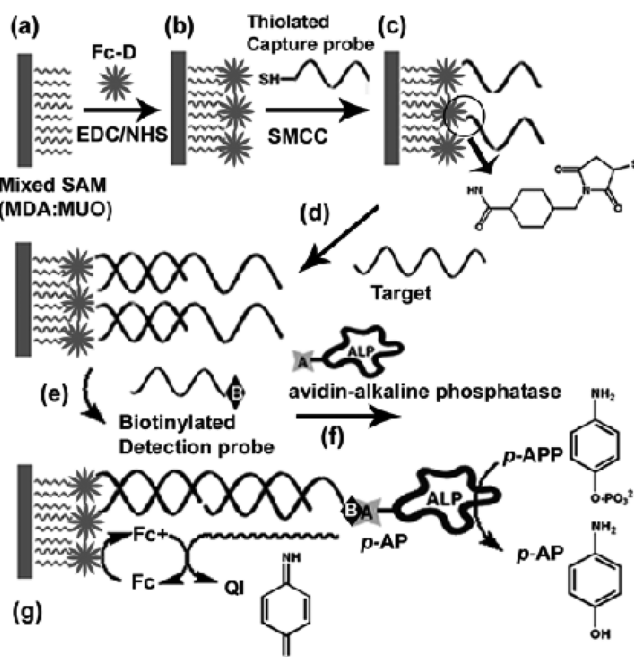


Figure 42. ALP-linked DNA sandwich assay based on Fc-D. Reprinted from ref 158a. Copyright 2003 American Chemical Society.

a relatively small signal, which is associated with poor sensitivity. Enzyme-based sandwich assay is ultrasensitive, but the intrinsic stability of the enzyme is relatively poor and the enzyme is expensive. With the development of nanotechnology, scientists can easily synthesize all kinds of nanoparticles and finely control the size, properties, and chemical conjugation of the nanoparticles. This brings a new opportunity for a stable, sensitive DNA sandwich assay. As we can see, DNA sandwich assays based on gold nanoparticles have attracted great attention in recent years. Electrochemical detection of Au^{3+} dissolved from gold nanoparticles,¹⁶³ gold-nanoparticle-based silver stain,^{163,164} and gold-nanoparticle-based electrochemilu-

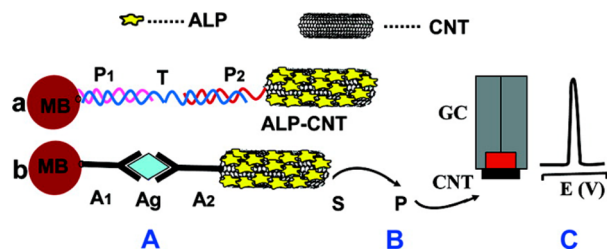


Figure 43. ALPs are loaded onto the carbon nanotube which is attached to the signal probes, and through sandwich hybridization, DNA or antigen is sensitively detected by the electrochemical method. Reprinted from ref 19. Copyright 2004 American Chemical Society.

minescence¹⁶⁵ has been widely used to build sensitive and selective DNA sandwich assays.

Brossier and his colleagues have developed a DNA sandwich assay based on gold nanoparticle amplification.^{163a} After dissolution of the gold nanoparticles in an acidic solution, Au³⁺ ions are released from the gold nanoparticles and directly quantified by electrochemical detection (here, anodic stripping voltammetry). We can imagine that thousands of Au³⁺ ions can be released from one gold nanoparticle, and one hybridization event which introduces one gold nanoparticle into the assay would bring the electrochemical signal from thousands of Au³⁺. Through this amplification, DNA target (human cytomegalovirus DNA sequence) as low as 5 pM can be detected.

Mirkin et al. have developed a DNA sandwich assay to close microelectrode gaps for electrical detection of DNA.^{163c,164a} In their system, targets bind with capture probes located between two fixed microelectrodes and signal probes attached to gold nanoparticles. Therefore, gold nanoparticles fill the gap between the microelectrodes. By enhancing the conductivity with silver stain, the conductivity change can be detected to quantify the DNA targets (Figure 45). DNA targets as low as

500 fM with a point mutation selectivity factor of about 100000:1 have been detected by controlling the salt concentration of the washing buffer.

An ultrasensitive DNA sandwich assay based on silver nanoparticle aggregates has been developed.^{164b} At first, signal probes and connector probes (polyA) are immobilized on silver nanoparticles. Then these nanoparticles hybridize with silver nanoparticles anchored with polyT, and after that, silver nanoparticle aggregates form. These nanoparticle aggregates are 10 times larger than a single nanoparticle and are employed to amplify the signal by differential pulse voltammetry. Thus, the sensitivity is enhanced by 1000-fold, and a 5 aM (~120 molecules in a 40 μ L volume) detection limit is achieved.

Cui and his colleagues synthesized luminol-coated gold nanoparticles by direct reduction of chloroauric acid (HAuCl₄) by luminol, and thus, a number of luminol molecules were attached to the gold nanoparticles.^{165b} At the same time, luminol molecules can stabilize the gold nanoparticles. The luminol-coated gold nanoparticles loaded with signal DNA probes are employed in sandwich assays. Other than that, they used a gold nanoparticle self-assembled electrode to enhance the electroluminescence intensity. As a result, an ultrasensitive assay has been developed and very low detection limit (190 aM) achieved.

4.3. Colorimetric Nucleic Acid Sandwich Assay

The sandwich assays based on fluorescence and electrochemistry are successful and have been widely used in hospitals and research laboratories, but for field detection and daily monitoring, requirements such as lowest power supply, miniaturization, low cost, and easy of use and reading would be difficult to fulfill by instrument-based detection. Therefore, colorimetric sandwich assays have attracted great interest because everyone can read the color change with the naked eye, just like pregnancy test sticks. In recent years, nano-

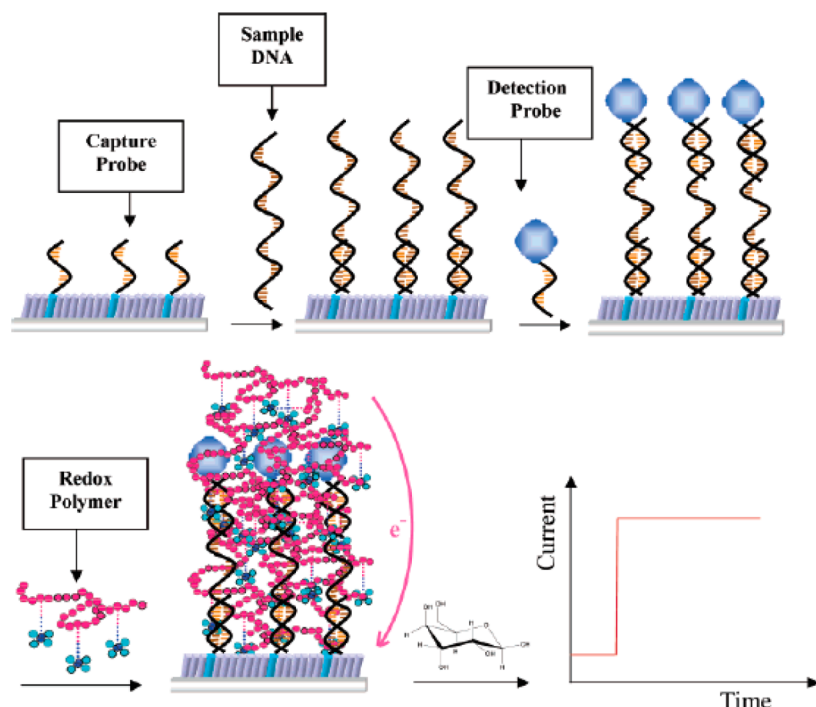


Figure 44. Scheme of the DNA sandwich assay based on glucose oxidase and a cationic redox polymer proposed by Gao and his colleagues. Reprinted from ref 159c. Copyright 2004 American Chemical Society.

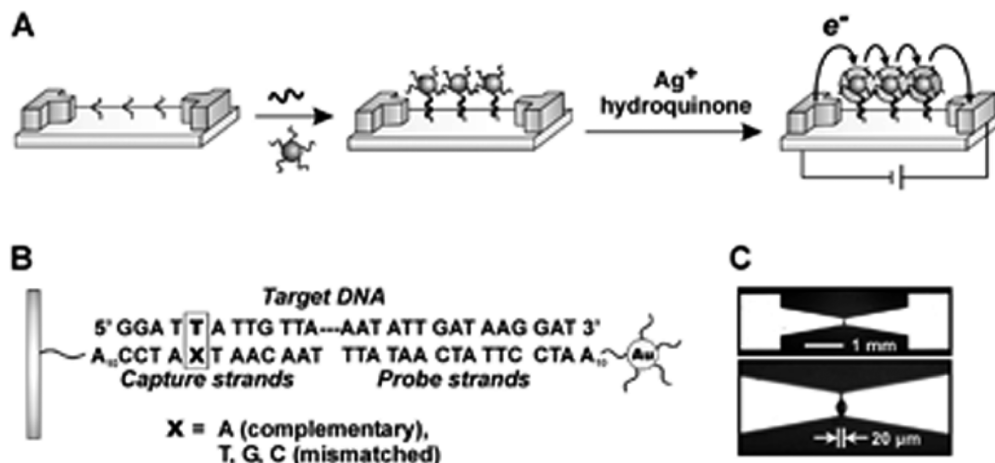


Figure 45. (A) After the sandwich-type hybridization, nanoparticles can fill the gap of two fixed microelectrodes, and through this, the DNA target is easily detected by conductivity. (B) Sequence information on the capture probe, target, and signal probe. (C) Image of the microelectrodes. Reprinted with permission from ref 164a. Copyright 2002 The American Association for the Advancement of Science.

particle-, traditional enzyme-, and DNAzyme-based colorimetric sandwich assays have been extensively investigated and employed in *in vitro* and *in vivo* detection.

4.3.1. Colorimetric Assay Based on Gold Nanoparticles. The color change of gold nanoparticles stems from the interparticle plasmon coupling during Au NP aggregation (red to purple or blue) or redispersion of a AuNP aggregate (purple to red),^{57a,166} so gold nanoparticle dispersion or aggregation upon target binding is widely used to build the colorimetric assay.¹⁶⁷ The first DNA sandwich assay based on the color change of gold nanoparticles was invented by the Mirkin group.^{167a,168} Unlike the fluorophore- or enzyme-labeled sandwich assay, the signal for hybridization is governed by the color change of gold nanoparticles, which is related to the interparticle distance (Figure 46). When the interparticle

took almost the whole night to get this color change because of the slow kinetics of hybridization. This slow kinetics can be improved dramatically by heating the solution at 50 °C for 5 min or freezing it in a bath of dry ice and isopropyl alcohol and then thawing it at room temperature. Through the denaturation of the hybridized aggregates, they found that the melting curve for the nanoparticle system is much sharper than that for the pure solution system without nanoparticles. On the basis of this mechanism, this sandwich assay can also differentiate mismatched targets.

To alleviate the secondary structure of the target, Gao and co-workers immobilized nonionic morpholino oligos on the gold nanoparticles and detected the target at extremely low salt concentration because of the salt-independent hybridization of this kind of probe with targets.¹⁶⁹ The advantage of using extremely low salt is destabilization of the secondary structure of the targets and improvement of the hybridization efficiency.

To improve the sensitivity of the gold-nanoparticle-based sandwich assay, the Mirkin group further developed a scanometric DNA sandwich array (Figure 47).^{167b} They immobilized the 3'-thiol-modified DNA probes on a surface of float glass microscope slides. After hybridization with the targets and reporter-probe-loaded gold nanoparticles, the high density of the hybridized nanoparticles made the slides appear light pink above a 1 nM target concentration, but at lower concentration of target ($\leq 100 \text{ pM}$), one cannot see the color of the gold nanoparticles on the slide because of their low density. To improve this, they amplified the signal through deposition of silver metal on the surface of the gold nanoparticles by reducing the silver ions by hydroquinone. Improvement of 2 orders of magnitude was achieved over the conventional fluorophore-based sandwich assay. Like the gold-nanoparticle-based colorimetric system they developed before, the silver amplification system inherently changed the melting profile of the targets, which permits the excellent differentiation of single-nucleotide mismatch. Pang et al. successfully employed this gold nanoparticle and silver stain system to detect different genotypes of hepatitis B and C virus in the serum sample from infected patients.¹⁷⁰

Because of the easy way (just using the unaided eye) to read the results, the colorimetric DNA sandwich assay has been widely used as a readout of DNA amplification. For example, a sensitive DNA detection that combines isothermal amplifica-

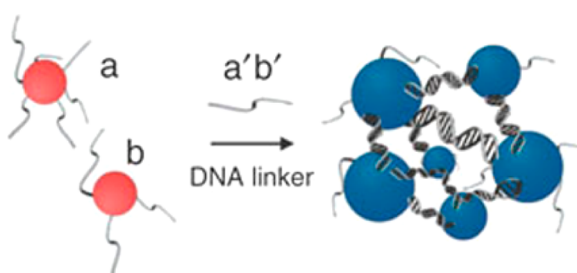


Figure 46. DNA capture probes are immobilized on the surface of gold nanoparticles, and after hybridization with the target, the gold nanoparticles aggregate and the color turns blue. Reprinted with permission from ref 168. Copyright 2003 Nature Publishing Group.

distance is greater than the average particle diameter, the nanoparticles are red, while when the interparticle distance is less than the average particle diameter, the nanoparticles appear blue or purple. On the basis of this interesting phenomenon, the Mirkin group developed a DNA sandwich assay which is sensitive, selective, and instrument-free. They immobilized the 28-base capture probes labeled with thiol on the gold nanoparticles (13 nm) through the gold–sulfur bond. The first 13 nucleotides of the 28-base capture probe serve as a flexible spacer, and the last 15 nucleotides serve as the recognition part. After introduction of the target, the color of the solution changed from red to purple, but unfortunately, it

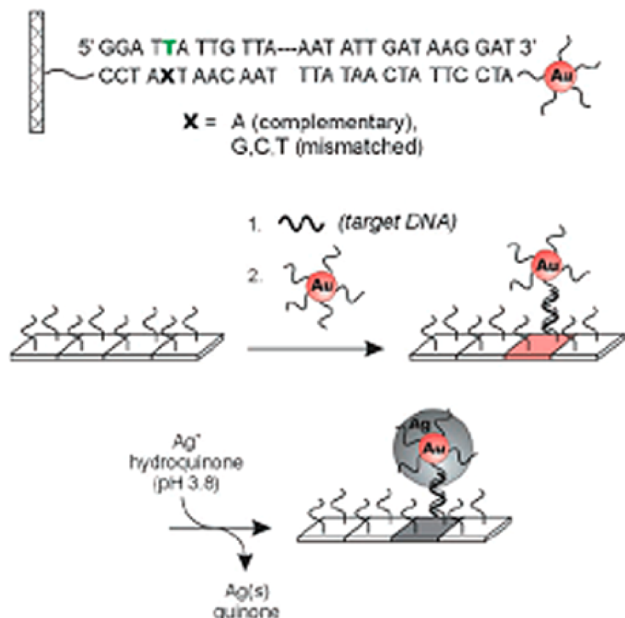


Figure 47. Scanometric DNA sandwich assay based on gold nanoparticles and silver stain. Reprinted with permission from ref 167b. Copyright 2000 The American Association for the Advancement of Science.

tion with a readout based on colorimetric DNA sandwich assay was developed.¹⁷¹ Through the isothermal amplification, the interrogated DNA sequences were exponentially amplified, and general DNA reporters which can bridge two nanoparticles loaded with DNA were produced. This method is sensitive enough to detect DNA at concentrations as low as 100 fM within 10 min.

The colorimetric DNA sandwich assay was also employed as the readout of the nicking endonuclease amplification system¹⁷² and rolling circle amplification system.¹⁷³

4.3.2. Colorimetric Assay Based on Traditional Enzymes. Like the enzyme-linked immunoassay, traditional enzymes such as HRP are widely used in colorimetric DNA sandwich assay because of the easy-to-read color change upon target binding.¹⁷⁴ Appella and Zhang developed a colorimetric DNA sandwich assay using HRP to catalyze the substrates.¹⁷⁵ In their system, they employed peptide nucleic acid (PNA) as the capture probe and signal probe because of its complete resistance to degradation by enzymes and increased specificity for complementary DNA. Importantly, they modified the PNA using cyclopentane, which can improve the detection sensitivity and the discrimination of single-base mismatch. By doing so, 10 zmol of DNA could be sensitively detected and two cell lines of anthrax could be clearly distinguished through the color change visible to the naked eye (Figure 48).

To employ the DNA as a probe and combine biotechnology and nanotechnology, Fan and his colleagues created an enzyme-based multicomponent optical nanoprobe for sequence-specific detection of DNA hybridization¹⁷⁶ (Figure 49), which is really impressive. The high surface to volume ratio of gold nanoparticles provides the opportunity to attach multiple kinds of biomolecules at the surface of the gold nanoparticles. To construct a nanoprobe that integrates DNA recognition, signal amplification, and nonspecific blocking, they coimmobilized thiolated signal probes (for DNA recognition), HRP (for signal amplification), and bovine serum albumin

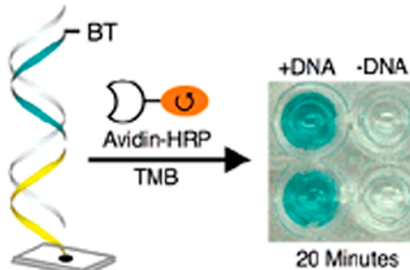


Figure 48. Colorimetric DNA sandwich assay based on the HRP catalytic reaction. As shown, the DNA probe (left, yellow) is immobilized on the surface and hybridizes with the target (left, gray) and biotin-modified signal probe (left, blue). After attachment of the HRP and the catalytic reaction, the solutions in the wells containing DNA target turn blue, but the other solutions without target remain colorless. Reprinted from ref 175. Copyright 2007 American Chemical Society.

(BSA; for nonspecific blocking) on the surface of the gold nanoparticles (15 nm in diameter). They immobilized capture probes on magnetic particles via biotin–avidin binding. After addition of the target to the detection system, the capture probe brought the target DNA and nanoprobe within proximity of the magnetic particles, which could be separated for subsequent optical detection. The nanoprobe can catalyze the oxidation of chromogenic reagent ABTS and bring a blue color. Only through the naked eye, 100 pM target can be distinguished from the color contrast. Using a microplate reader, 25 pM target can be easily detected. When challenged with a high concentration of noncomplementary DNA and complicated biological fluid such as serum, the nanoprobe-based sandwich assay performs very well.

To further improve the detection sensitivity of this nanoprobe-based sandwich assay, the same group creatively introduced a cross-link probe into the nanoprobe system, creating aggregates of the multicomponent nanoprobe (Figure 50).¹⁷⁷ Thus, upon target binding, a much higher signal change and detection sensitivity could be obtained. As expected, DNA target as low as \sim 1 fM can be easily detected.

Interestingly, it was recently found that Fe_3O_4 magnetic nanoparticles (MNPs) possess intrinsic HRP-like catalytic activity toward the reduction of H_2O_2 .³⁶ A nanocomplex of MNPs and carbon nanotubes that enhances the peroxidase-like activity of MNPs has been reported too¹⁷⁸ and was successfully used to detect H_2O_2 and glucose. Since the stability of MNPs and the nanocomplex is much higher than that of traditional enzymes, the nanoparticles and nanocomplex with peroxidase-like activity might be an excellent substitute for the traditional enzymes in the near future.

4.3.3. Colorimetric Assay Based on DNAzyme. As we all know, traditional enzymes are thermally unstable and difficult to engineer and modify. With the development of biochemistry, interestingly, researchers have found that some guanine-rich DNA sequences, including the human telomeric DNA sequence, have peroxidase activity after binding with hemin, this complex being called “DNAzyme”.¹⁷⁹ Taking the advantages of high stability, ease of use, and readiness for chemical conjugation, the DNAzyme is widely used in the biosensor and biodetection fields (including DNA detection, telomerase detection, and cancer biomarkers),¹⁸⁰ and DNAzyme might be a powerful competitor for the traditional enzyme because of these advantages.

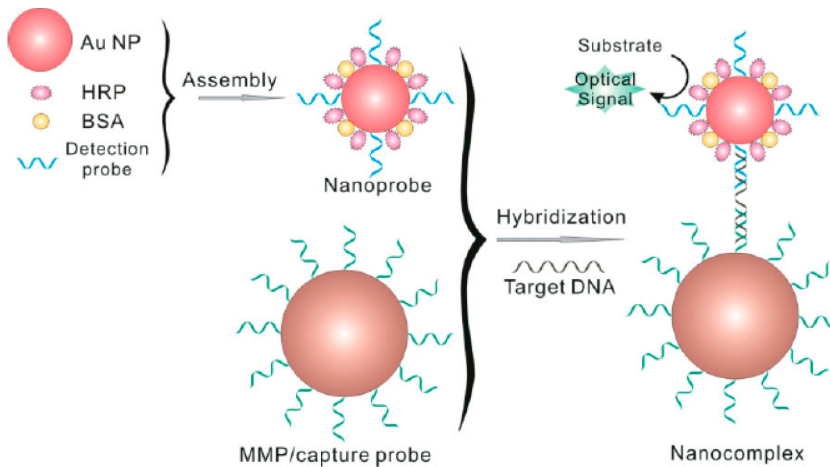


Figure 49. DNA sandwich assay based on the multicomponent nanoprobe. Reprinted with permission from ref 176. Copyright 2008 Wiley-VCH Verlag GmbH & Co.

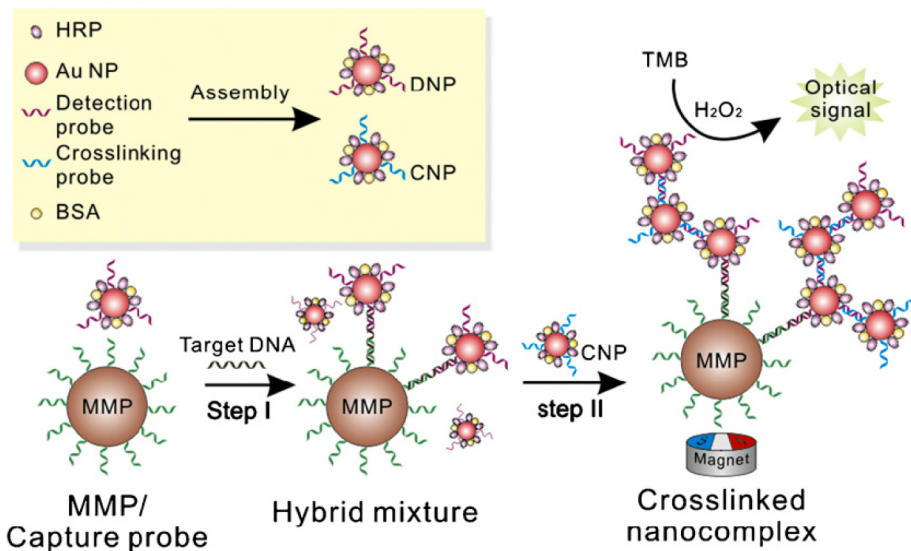


Figure 50. DNA sandwich assay based on the cross-linked nanocomplex (aggregated multicomponent nanoprobe). Reprinted with permission from ref 177. Copyright 2009 Elsevier.

Willner and his colleagues have engineered and split the DNAzyme into two fragments. In the presence of hemin, the two fragments can recombine together to catalyze H_2O_2 .¹⁸¹ This mechanism is the foundation of the DNAzyme-based colorimetric sandwich assay. In 2007, Wang et al. found that this complex (the recombination of two fragments and hemin) can also be employed in the H_2O_2 -ABTS system, where catalysis is associated with H_2O_2 -mediated oxidation of ABTS.¹⁸² After addition of target DNA which hybridizes the free nucleic acid parts of the two fragments, the catalysis activity is greatly enhanced (Figure 51). They employed this mechanism to detect the DNA target with a dynamic range from 0.01 to 0.3 μM . This G-quartet structure could be destroyed when the DNA target is above 1 μM as previously reported by Willner.

Similar to the research above, Kolpashchikov also split the DNAzyme into two halves and added target binding arms to each half via tris(ethylene glycol) linkers.¹⁸³ Without DNA target, the two halves disassociate from each other. After hybridizing with the target, the two halves assemble together to form a G-quartet structure to catalyze H_2O_2 and the

cosubstrate. This system can differentiate perfectly matched target and mismatched target very well.

The easiest way to split the DNAzyme is to split it into two equal parts (1:1), but Zhou et al. pointed out that if DNAzyme is split in this way, the two equal parts could easily form the G-quartet structure which has the peroxidase activity even in the absence of the target DNA and could produce a high background signal.¹⁸⁴ Therefore, as Willner did, they split the DNAzyme 3:1 (one fragment possesses three GGG repeats, and the other possesses one GGG repeat) to reduce the possibility of preassociation of fragments under the circumstance without target (Figure 52).

This split DNAzyme-based colorimetric sandwich assay is also successfully used to detect the DNA from *Salmonella* and *Mycobacterium*¹⁸⁵ and in SNP genotyping of actual human DNA samples.¹⁸⁶

4.4. Other Nucleic Acid Sandwich Assays

Besides the DNA sandwich assays based on fluorescence, electrochemistry, and color change mentioned above, there are some other techniques, such as use of a quartz crystal

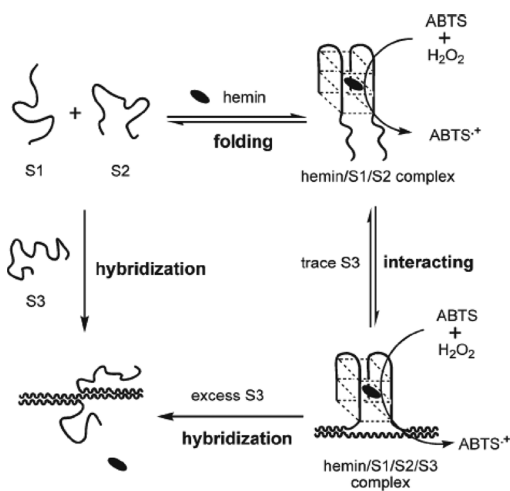
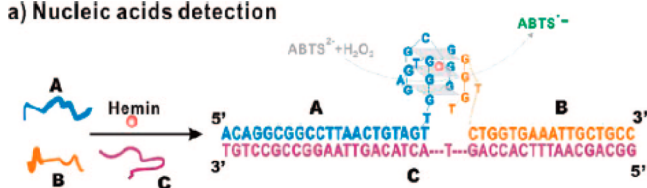


Figure 51. Two fragments of the split DNAzyme are attached to two free recognition arms that can hybridize with the target DNA. In the presence of a lower concentration of target, the catalytic ability of DNAzyme can be improved greatly, but a higher concentration of target could destroy the G-quartet structure and inhibit the catalytic ability. Reprinted with permission from ref 182. Copyright 2007 The Royal Society of Chemistry.

a) Nucleic acids detection



b) SNP detection

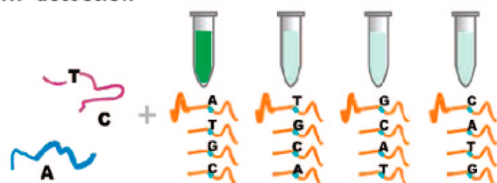


Figure 52. (a) Scheme of DNA detection based on the 3:1 split DNAzyme and (b) principle of single-nucleotide polymorphism detection using the split DNAzyme. Reprinted from ref 184. Copyright 2008 American Chemical Society.

microbalance (QCM), surface plasmon resonance (SPR), use of a microcantilever, and surface-enhanced Raman scattering (SERS), that play a very important role in the development of the sandwich assay. The combination of sandwich assay with these techniques has attracted extensive attention recently, and here we summarize some recent advances in these fields.

4.4.1. Sandwich Assay Based on the QCM. The QCM is a very sensitive mass detector which measures the changes of the resonance frequency of a piezoelectric crystal after binding of certain molecules. The targets it can detect include whole cells, proteins, nucleic acids, small molecules, and ions.¹⁸⁷ Usually, the sandwich assay requires the labeling of signal probes (such as fluorophore-labeled signal probes and redox-moiety-labeled signal probes). In principle, the use of the QCM does not require the labeling of molecules. For example, the QCM was used to monitor the DNA hybridization^{152c} and DNA sandwich-type structure formation without using any label¹⁸⁸ in real time. The surface with thiolated single-stranded DNA (SH-ssDNA) attached demonstrates a sharp decrease of

frequency in the presence of target DNA, which indicates the occurrence of hybridization, and the hybridization is really fast (minutes), but the surface with non-SH-ssDNA attached demonstrates no significant change in frequency (Figure S3).^{152c} Fawcett et al. monitored the stepwise sandwich

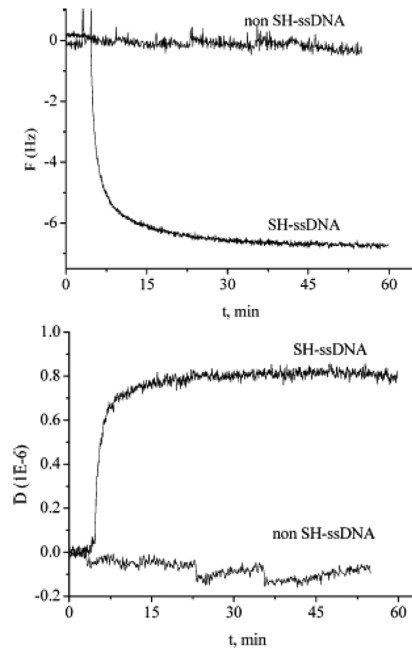


Figure 53. Comparison of the real-time hybridization process of SH-ssDNA and non-SH-ssDNA monolayers using the QCM. Reprinted from ref 152c. Copyright 2005 American Chemical Society.

hybridization of DNA using the QCM. They found that different orientations of the QCM chip could affect the length of the sandwich structure because of gravity's influence. Ten additions of the DNA sandwich structure were found when the active surface of the QCM chip was up and only seven additions when the active surface of the QCM chip was down (Figure S4).¹⁸⁸

To push the detection limit down, sandwich assay using gold nanoparticle amplification has been widely investigated. Li et al. compared the detection limit of the conventional non-amplification method and sandwich assay using gold nanoparticles (Figure 55).¹⁸⁹ They found an about 100-fold

Base-Strand: 5'- GGATTTATGTATGAAAAGGCCAC - 3'
(25-MER)

Strand-1: 3'- CCTAAAAATACATACTTTGCGGGGGTTACTCGTCGTCTCTAAATTACG - 5'
(50-MER)

Strand-2: 5'- CAATGAGCAGCACAGAGATAATGCGGATTTATGTATGAAAAGGCCAC - 3'
(50-MER)

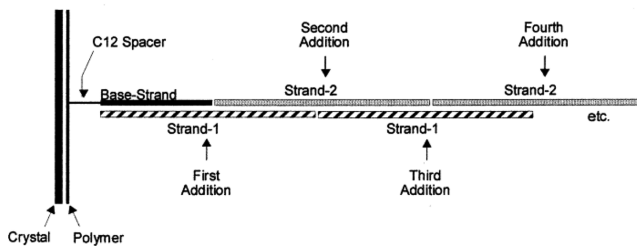


Figure 54. Stepwise sandwich hybridization. Reprinted from ref 188. Copyright 2004 American Chemical Society.

improvement, and the detection limit was pushed down to 32 pM.

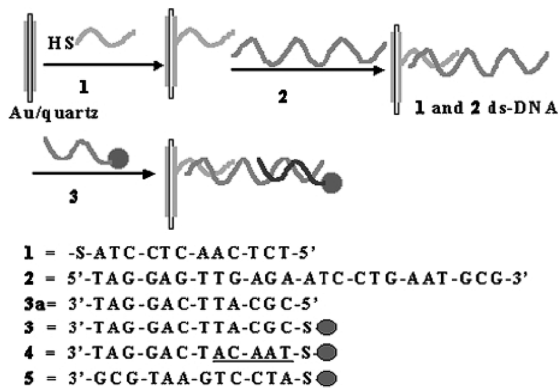


Figure 55. Scheme of the sandwich assay based on gold nanoparticle amplification and QCM detection. Reprinted with permission from ref 189. Copyright 2000 The Royal Society of Chemistry.

A similar method has been successfully employed to detect *E. coli* O157:H7, but this time Fe_3O_4 nanoparticles were used as the “mass enhancer” to amplify the frequency change. In their assay, 267 colony-forming units (CFU)/mL *E. coli* O157:H7 cells can be sensitively detected.¹⁹⁰

4.4.2. Sandwich Assay Based on SPR. SPR can also monitor the interaction of chemical and biological interactions in real time by measuring the changes in the refractive index occurring at the metal surface where the interaction of molecules takes place. Recently, we have seen the wide use of SPR in the detection of proteins and nucleic acids.¹⁹¹ The sandwich assays based on SPR mostly are focused on the gold nanoparticle amplification strategy. The group of Corn has developed SPR imaging technology and used SPR to image the gold nanoparticle amplification (Figure 56).¹⁹² The detection limit in this SPR assay is 10 fM. Through the use of PNA as a capture probe, Spoto and co-workers achieved a detection limit as low as 1 fM.¹⁹³

4.4.3. Sandwich Assay Based on the Microcantilever. The mechanism of the microcantilever is that intermolecular forces produced by adsorption of molecules (such as small molecules, nucleic acids, and proteins) cause the mechanical bending of the cantilever.¹⁹⁴ Like the QCM and SPR, the microcantilever directly translates molecular recognition into nanomechanics and does not require the labeling of targets. Gerber et al. investigated DNA hybridization using a silicon cantilever array (Figure 57).^{194a} They monitored the bending of each cantilever in real time by detecting changes in the optical beam deflection. In the opposite direction, the thermal dehybridization of double-stranded DNA on the microcantilever surface has been investigated by the Majumdar group.¹⁹⁵ Interestingly, Mckendry and co-workers have proved that the forces generated by an i-motif conformational change can perform micromechanical work on an array of silicon cantilevers.¹⁹⁶

Usually the detection limit of the assay based on direct hybridization using a cantilever system is about 10 nM as reported previously.^{194a,f} To develop a more sensitive assay, the Dravid group has employed DNA sandwich format hybridization and attached gold nanoparticles on signal probes (Figure 58).¹⁹⁷ The final signal was amplified by catalyzing the nucleation of silver on the surfaces of gold nanoparticles. By

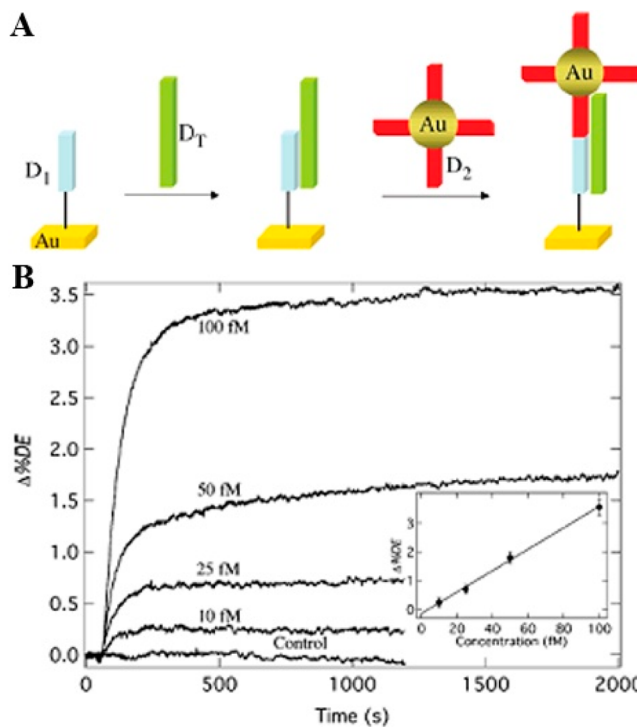


Figure 56. (A) Scheme of the sandwich assay based on gold nanoparticle amplification and SPR detection. (B) Real-time SPR signals with different concentrations of target DNA (ranging from 10 to 100 fM). Reprinted from ref 192. Copyright 2007 American Chemical Society.

doing so, they achieved a detection limit of 50 pM, and by stringent washing, this method can discriminate a single-base-pair-mismatched DNA strand.

4.4.4. Sandwich Assay Based on SERS. Because of the weak signals, Raman scattering has been largely limited in the biosensor field, but the situation changed greatly after the discovery of SERS. That is, the Raman signal can be enhanced greatly when molecules adsorb onto or near a roughened noble metal surface. This phenomenon revolutionized the application of SERS in the biosensor field.¹⁹⁸

By labeling the nanoparticles with signaling DNA probes and Raman dyes, Mirkin et al. have developed a DNA sandwich assay using SERS as the readout, which is used as a multiplex detection platform (Figure 59).¹⁹⁹ After the formation of sandwich hybridization, gold nanoparticles were attached onto each DNA target and then immediately treated with Ag enhancement solution, leading to strong Raman signals. They pointed out that without the Ag enhancement the gold nanoparticle spacings are too large to produce an SERS signal at a target concentration lower than 1 nM.

To build a multiplex platform, they selected six dyes as Raman labels in their system for the detection of (A) hepatitis A virus Vall7 polyprotein gene (HVA), (B) hepatitis B virus surface antigen gene (HBV), (C) human immunodeficiency virus (HIV), (D) Ebola virus (EV), (E) variola virus (smallpox, VV), and (F) *Bacillus anthracis* (BA) protective antigen gene. This method is sensitive enough to detect as low as 20 fM target and has an excellent ability to differentiate SNPs. Very similar to the strategy above, ZnO–Au nanocomposites were employed to enhance the Raman signal even without the Raman enhancer, Ag.²⁰⁰ A DNA sandwich assay using the formation of multilayer metal–molecule–metal junctions as the

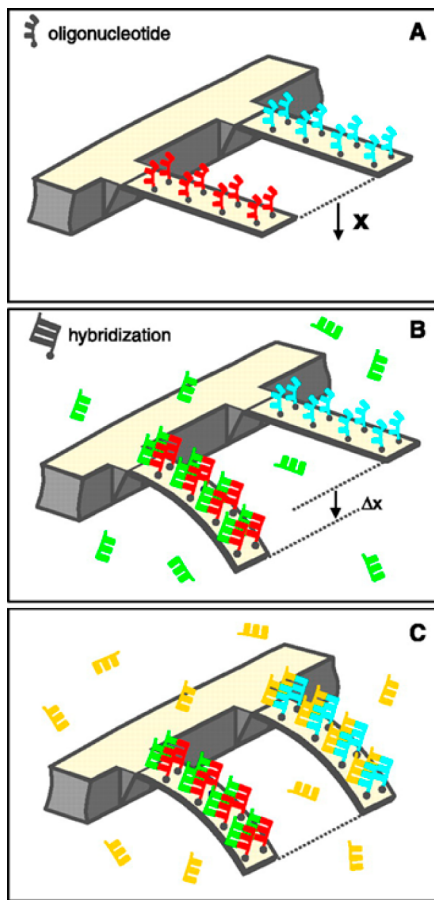


Figure 57. Scheme of the multidetection principle of a microcantilever. (A) Immobilization of two capture probes at different cantilevers. (B, C) Mechanical bending of the corresponding cantilever with its target. Reprinted with permission from ref 194a. Copyright 2000 The American Association for the Advancement of Science.

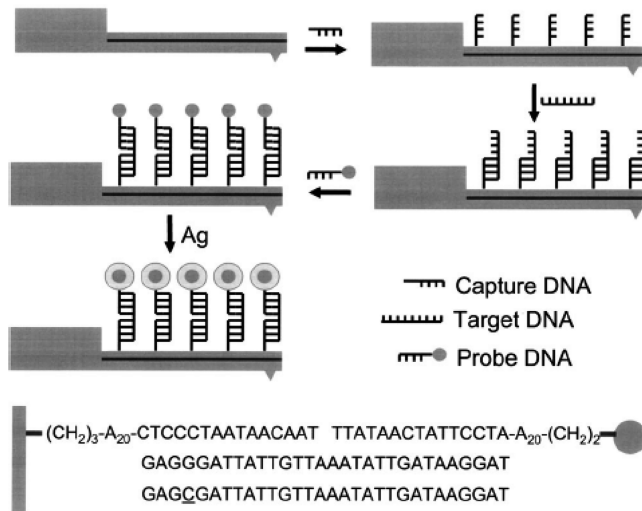


Figure 58. Scheme of the DNA sandwich assay based on nanoparticle amplification and microcantilever detection. Reprinted with permission from ref 197. Copyright 2003 American Institute of Physics.

Raman promoter was also reported to sensitively detect HIV-1 DNA.²⁰¹

Moskovits and Reich developed a DNA sandwich assay by nanoparticle assembly on a smooth surface.²⁰² They immobilized

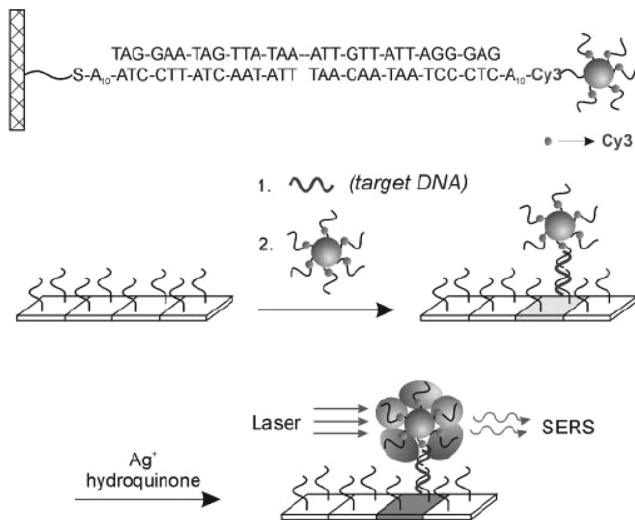


Figure 59. Scheme of the DNA sandwich assay based on gold nanoparticles and silver enhancement. Reprinted with permission from ref 199. Copyright 2002 The American Association for the Advancement of Science.

lized capture probes and Raman dye on a smooth Ag film which only brings very weak Raman signals. Through the sandwich hybridization with target and Ag nanoparticles conjugated with signal probes, they created “hot spots” to greatly enhance the Raman signals (Figure 60). The highly stable and reproducible Raman signal can be obtained at near signal particle level.

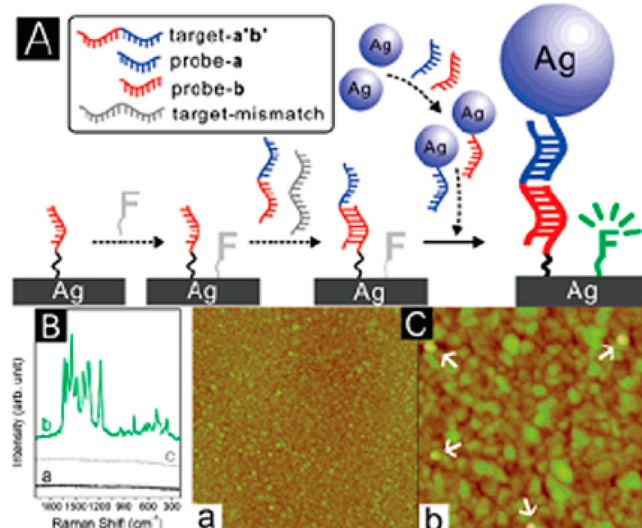
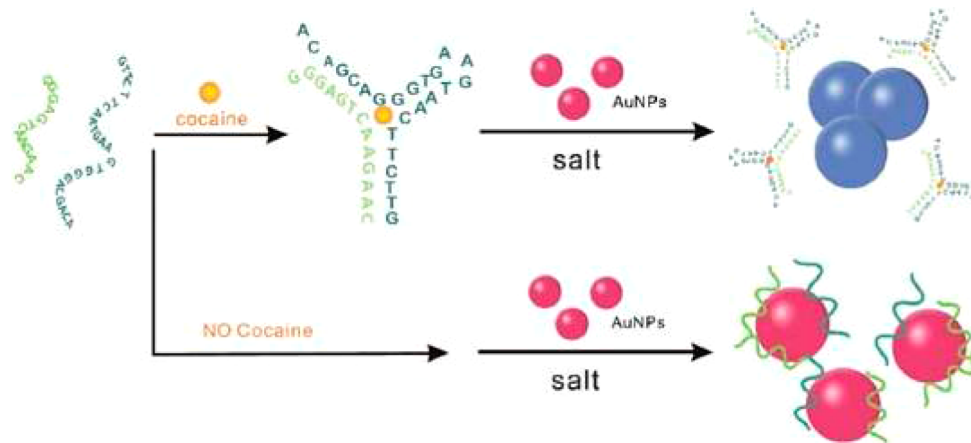


Figure 60. (A) Scheme of the DNA sandwich assay based on SERS. (B) SERS signals are obtained from the background (a), after hybridization with the target DNA and signal probe (b), and after hybridization with the noncomplementary target and signal probe (c). (C) AFM image obtained after hybridization with the target DNA and signal probe (a, $5 \times 5 \mu\text{m}$; b, $1 \times 1 \mu\text{m}$). Reprinted from ref 202. Copyright 2007 American Chemical Society.

Besides the systems based on the surface-attached DNA capture probes, some DNA sandwich assays in homogeneous solution have been developed too. For example, Song et al. have developed a multiplex DNA detection format based on silver nanoparticles. They immobilized different DNA probes and Raman dyes on the silver nanoparticles, and after addition

Scheme 6. Scheme of the Cocaine Sandwich Assay Based on the Split Aptamer Strategy^a

^aThe color change of the gold nanoparticles is used as the readout. Reprinted with permission from ref 209b. Copyright 2008 Wiley-VCH Verlag GmbH & Co.

of the target to the solution, the silver nanoparticles aggregated to enhance the Raman signal.²⁰³ Graham et al. developed a detection platform to discriminate SNP through rational control of the formation of nanostructures of dye-coded oligonucleotide–silver nanoparticle conjugates in a sandwich assay format.²⁰⁴ Gold nanoparticles conjugated with DNA probes are also used to enhance the Raman signal in the presence of target DNA.²⁰⁵

We should point out that these techniques are so sensitive to the changes of mass, refractive index, and nanomachines that nonspecific adsorptions may cause relatively big signal changes and thus increase the background signals. This situation may become more serious when these techniques are used in complex matrixes such as serum and blood considering the large amount of nonspecific proteins in these samples. Therefore, how to construct the surfaces with high resistance to nonspecific adsorptions is really important. Some methods mentioned in section 4.2.2 could be used to minimize nonspecific adsorption in these techniques.

5. SANDWICH ASSAY FOR SMALL-MOLECULE AND ION DETECTION

The sandwich assays for proteins and nucleic acids mentioned above have attracted tremendous attention because of their high sensitivity and specificity, ensuring their widespread use in clinic diagnostics and laboratory analysis, but for the detection of small molecules and ions, it is difficult to build sandwich assays because of the requirement that the target be exposed to two distinct epitopes (for example, it is difficult for a small molecule or metal ion to simultaneously bind to two antibodies). Even so, Self's group and others have developed some immunoassays for small molecules with ultrahigh specificity, and their works are summarized in another review paper.²⁰⁶ Notably, the Ueda group created an open sandwich assay by using the interchain interaction of the antibody variable region.²⁰⁷ In recent years, aptamers have been selected *in vitro* for their ability to bind specific targets (whole cells, proteins, small molecules, and ions).²⁰⁸ Compared to antibodies, aptamers are easy to select and synthesize and are more stable, which ensures them wide use in the biosensor field, but the problem of steric effects of the aptamer remains, inhibiting their use in sandwich assays for small molecules and ions. To

overcome this, Fan's group, Plaxco's group, and Willner's group pioneered the development of sandwich assays based on single aptamer sequences suitable for direct detection of small-molecule targets in blood or other complex matrixes.²⁰⁹

5.1. Sandwich Assay for Small Molecules

As early as 2000, Stojanovic's group found that removing some loop regions from a single aptamer of cocaine or ATP would split it into two fragments, and these two fragments can reassemble to form the aptamer–target binding complex.²¹⁰ On the basis of this interesting finding, Fan et al. cut the aptamer of cocaine (or ATP) into two pieces through rational design.^{209b} In the absence of the target, these two pieces are separated from each other and diffuse homogeneously in solution. Target binding pushes the equilibrium toward the folded aptamer–target complex (Scheme 6), which forms the sandwich assay format. These two states can be differentiated very well by unmodified gold nanoparticles. This is because the negatively charged single-stranded DNA can bind to gold nanoparticles and stabilize them against salt-induced aggregation. However, due to the relatively rigid structure, the folded aptamer–target complex does not have this kind of binding property to gold nanoparticles and cannot protect gold nanoparticles from salt-induced aggregation. Through this novel method, cocaine can be detected in 5 min, and the results can be read using just the unaided eye (Figure 61).

By using the same principle of split aptamers, the Willner group attached two different enzymes to the anticocaine aptamer fragments. In the presence of cocaine, the two enzyme-labeled fragments reassemble into the sandwich format, activating the biocatalytic cascade (Scheme 7).²¹¹

On the basis of the findings above, Zuo and Plaxco have developed and claimed an electrochemical sandwich assay for small molecules (Figure 62).^{209a} They immobilized one fragment on the electrode surface via a gold–sulfur bond and modified the other fragment with a redox label (methylene blue), which diffuses freely in solution. Target-binding-induced association of these two fragments increases the concentration of methylene blue at the electrode surface and therefore increases the current of voltammetry. Using this detection platform, as low as 1 μM cocaine (or ATP) can be readily detected even in whole blood, cell lysates, and other complex matrixes in minutes.

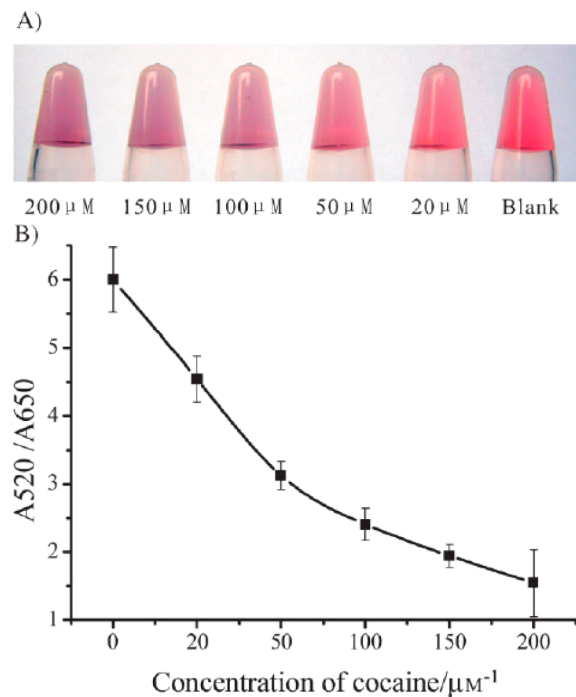
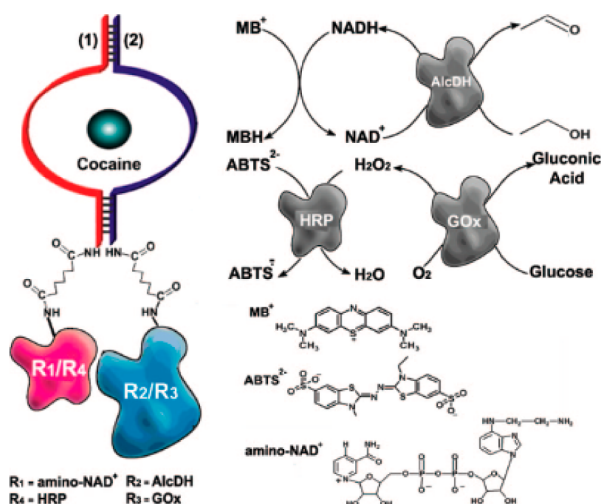


Figure 61. (A) Using the sandwich assay based on the split aptamer, different concentrations of cocaine can be differentiated by the naked eye. (B) Titration curve for cocaine detection (the ratio of UV/vis absorption at 520 nm to that at 650 nm versus the concentration of cocaine). Reprinted with permission from ref 209b. Copyright 2008 Wiley-VCH Verlag GmbH & Co.

Scheme 7. Cocaine Can Induce the Reassembly of Split Aptamers That Are Conjugated with Different Enzymes (or Cofactor/Enzyme Pairs)^a



^aThus, the coupled biocatalytic reaction is activated. Reprinted from ref 211. Copyright 2009 American Chemical Society.

Some other sandwich assays have also been extensively developed. For example, Pt nanoparticles, gold nanoparticles, semiconductor nanoparticles (NPs), conjugated polymers, enzymes, DNAzyme, and organic molecules are used as labels for the electrochemical, colorimetric, photoelectrochemical, or SPR detection of cocaine.^{209c–i,212}

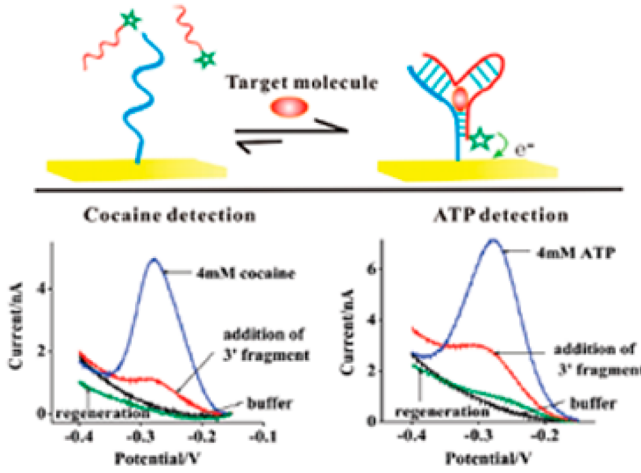
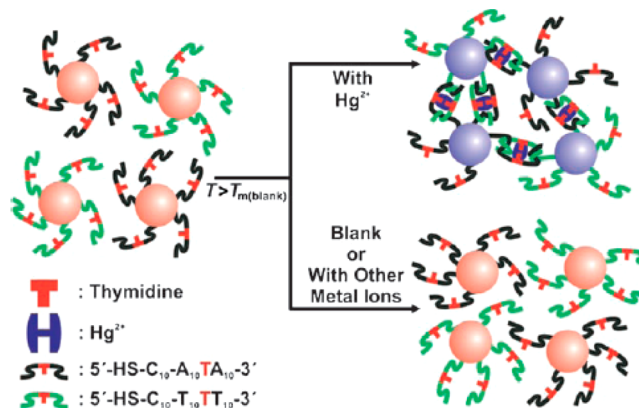


Figure 62. (Top) Scheme of electrochemical sandwich assays for cocaine and ATP. (Bottom) Upon target binding (cocaine or ATP), the current of square wave voltammetry (SWV) increases greatly. The sensors can be readily regenerated via a 30 s rinse with distilled water. Reprinted from ref 209a. Copyright 2009 American Chemical Society.

5.2. Sandwich Assay for Ions

The sandwich assay for ions benefits from the discovery of the interaction of ions and nucleic acids. The Mirkin group has employed the thymidine–Hg²⁺–thymidine interaction and rationally designed complementary DNA–gold nanoparticle conjugates with thymidine–thymidine mismatch (Scheme 8).²¹³ In this assay, they used two types of gold nanoparticle

Scheme 8. Sandwich Assay for Hg²⁺ Based on Thymidine–Hg²⁺–Thymidine Interaction^a



^aReprinted with permission from ref 213. Copyright 2007 Wiley-VCH Verlag GmbH & Co.

conjugates modified with probe A (5'-SH-C₁₀-A₁₀-T-A₁₀) and probe B (5'-SH-C₁₀-T₁₀-T-T₁₀). These two types of conjugates can form a stable aggregate at temperatures lower than the melting temperature (T_m), but disassociate reversibly at temperatures higher than the melting temperature (T_m) with a color change from blue to red. Because of the interaction of Hg²⁺ with thymidine, the presence of Hg²⁺ would increase the melting temperature (T_m). The increase of T_m is the foundation of this sandwich assay. As shown in Figure 58, when the temperature is higher than T_m (here, 47 °C), the gold nanoparticles disperse well in solution and the color is red. After addition of Hg²⁺, the gold nanoparticles aggregate and the

color changes to blue. Hg^{2+} can be identified easily from a series of metal ions by the color change (Figure 63).

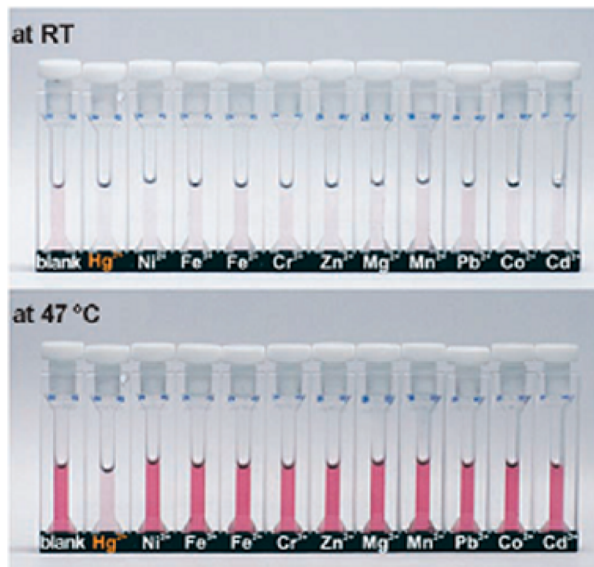


Figure 63. (Top) At room temperature, the color of all solutions containing various metal ions is blue. (Bottom) After the temperature is increased to $47\text{ }^{\circ}\text{C}$, the solution with Hg^{2+} remains blue and the other solutions turn red. Reprinted with permission from ref 213. Copyright 2007 Wiley-VCH Verlag GmbH & Co.

Through the combination of the principle above and the conventional scanometric detection of nucleic acids based on silver amplification, a sensitive scanometric for Hg^{2+} was developed.²¹⁴ As shown by the results, when the temperature is higher than T_m , the gold nanoparticle conjugates cannot bind to the capture probes attached on the surface. In the presence of Hg^{2+} , because of the thymidine– Hg^{2+} –thymidine interaction and the increase of T_m , the gold nanoparticle conjugates hybridize with the capture probes and bring amplified signals. As low as 10 nM (2 ppb) is readily detected using this assay.

The sandwich assays for Hg^{2+} developed by the Mirkin group require a relatively higher temperature. To develop a sandwich assay at room temperature, Fan et al. elegantly designed gold nanoparticles functionalized with thiolated thymine oligonucleotides (a mixture of T_6 and T_{10}) to detect Hg^{2+} .²¹⁵ The functionalized nanoparticles are highly stable even in solution with high ionic strength and present a red color. In the presence of Hg^{2+} , the distribution of the charges at the surfaces of the gold nanoparticles is changed upon Hg^{2+} binding, leading to instability of the gold nanoparticles in the solution with high ionic strength, and the color changes to blue. More interestingly, they integrated this sandwich assay in power-free PDMS microchannels, which can be used in high-throughput detection (Figure 64).

Besides the gold-nanoparticle-based colorimetric sandwich assay,^{213–216} some fluorescence and electrochemical sandwich assays for Hg^{2+} have been developed too. Zhou and his colleagues developed a label-free method to detect Hg^{2+} .^{216b} They employed thymine-rich Hg^{2+} aptamer and malachite green as the indicator. Only in the presence of Hg^{2+} , the ternary complex forms because of the thymine– Hg^{2+} –thymine interaction, and malachite green dye intercalates into the complex, which leads to an increase in the resonance scattering intensity.

Fan's group rationally designed a very sensitive sandwich assay for Hg^{2+} using gold nanoparticle amplification.²¹⁷ At first, they used thymine-rich, Hg^{2+} -specific probes as the capture probes, which include seven thymine bases at both ends and a mute spacer in the middle, and immobilized the probes on the gold electrode surface. In the presence of Hg^{2+} , the capture probes capture the Hg^{2+} and form a hairpin structure. At the same time, the Hg^{2+} captured on the surface can be readily detected through the electrochemical reduction signal of Hg^{2+} (Scheme 9A). The detection limit of this assay is 1 μM . To improve the sensitivity, they immobilized the thymine-rich capture probes and linker probes on gold nanoparticles, and the linker probes were hybridized with probes immobilized on the gold electrode (Scheme 9B). Thus, in the presence of Hg^{2+} , a large amount of Hg^{2+} ions were captured on the electrode

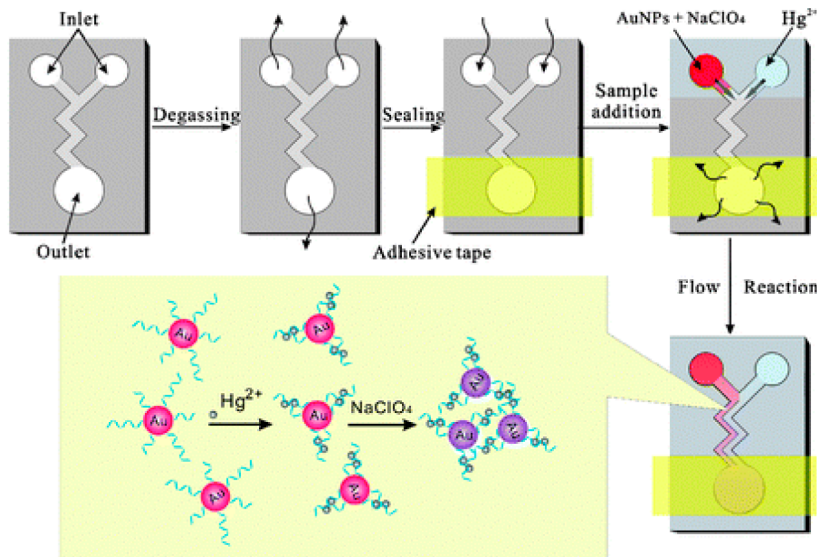
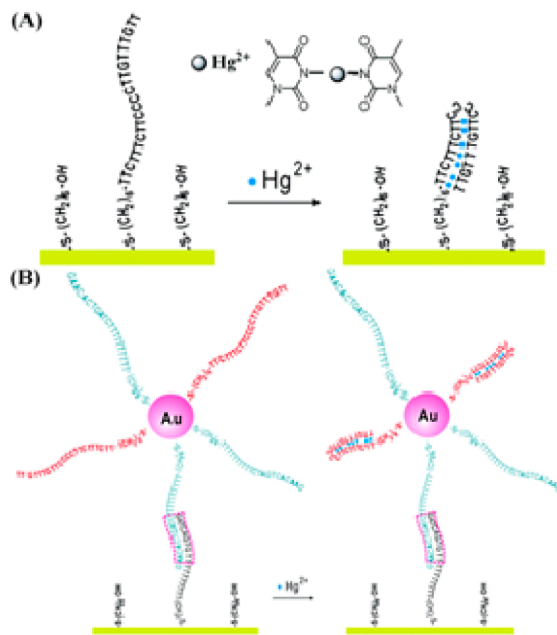


Figure 64. Sandwich assay for Hg^{2+} detection using gold nanoparticles and power-free microchannels. The direction of air transfer is demonstrated by the black arrows in each step. Reprinted with permission from ref 215. Copyright 2008 The Royal Society of Chemistry.

Scheme 9. Direct Detection of Hg^{2+} on the Electrode Surface and Amplified Detection of Hg^{2+} through Gold Nanoparticles^a



^aReprinted from ref 217. Copyright 2009 American Chemical Society.

surface, which leads to a large electrochemical signal. Through this amplification, they achieved a detection limit of 0.5 nM (3 orders of magnitude improvement). Similarly, Yu and his colleagues employed methylene blue as the electrochemical indicator and gold-nanoparticle-based amplification to detect Hg^{2+} , and a detection limit of 0.5 nM was achieved.²¹⁸

Most assays mentioned above are for Hg^{2+} detection because of the well-known principle of thymine- Hg^{2+} -thymine interaction, but with the development of aptamer technology, the aptamer of any metal ion could be selected in vitro. For example, there is an aptamer for K^+ , and Xu's group has developed a sandwich assay for K^+ by splitting it into two fragments (Scheme 10).²¹⁹ The G-rich sequence specific for K^+

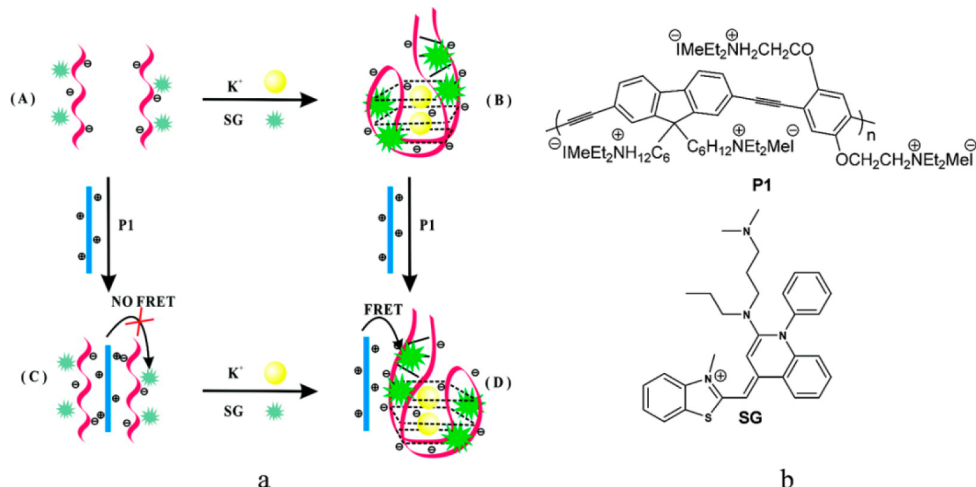
was used and split into two fragments. In the absence of K⁺, the two fragments are in a linear state, and in this state SYBR green 1 does not bind to the fragments. In the presence of K⁺, the two fragments recombine together and form a folded G-quadruplex, and in this state SYBR green 1 intercalates into the complex, which leads to a large increase of the fluorescence intensity. This signal increase can be further improved through FRET from positively charged conjugated polymer to SYBR green 1.

6. SANDWICH ASSAY FOR PATHOGENS AND CELLS

Usually, the detection of pathogens and cells depends on the detection of nucleic acids and proteins (or biomarkers) associated with the pathogens and cells. These detection methods, generally based on PCR and immunoassays, are well established with high sensitivity. However, methods for the direct detection of intact pathogens and cells would provide good opportunities for the development of cheap, rapid, and simple biosensors. Here we summarize the recent advances of direct detection of intact pathogens and cells based on the sandwich assay, and these assays play a very important role in human health and bioterrorism prevention.²²⁰

One example of a new development in this field is the work of Porter and colleagues, who have developed a direct, low-level assay for the detection of feline calicivirus (FCV), an analogue for the human calicivirus, which has been identified as a bioterrorism agent.²²¹ As shown in Figure 65, they immobilized the monoclonal antibody (mAb) specific for FCV on a gold-bound thiolate adlayer through succinimidyl ester chemistry. In the presence of FCV, the FCVs are captured by the mAb layer, and then gold nanoparticles conjugated with Raman reporters and mAb's are attached on the surface, which could produce an enhanced Raman signal. Using this method, 10^6 viruses can be readily detected. Nie et al. have employed color-coded nanoparticles and dual-color fluorescence coincidence for the real-time detection of single respiratory syncytial virus (RSV), which is responsible for respiratory tract illness in infants and young children.²²² Wild-type RSV, which has F and G proteins on the virus surface, can be detected because of the formation of a sandwich structure of the virus, green nanoparticles, and red nanoparticles. However, mutant virus which lacks G protein

Scheme 10. (a) Sandwich Assay for K⁺ Based on the Split Aptamer Strategy and Conjugated Polymer Amplification and (b) Chemical Structure of the Conjugated Polymer and SYBR Green 1^a



^aReprinted from ref 219. Copyright 2010 American Chemical Society.

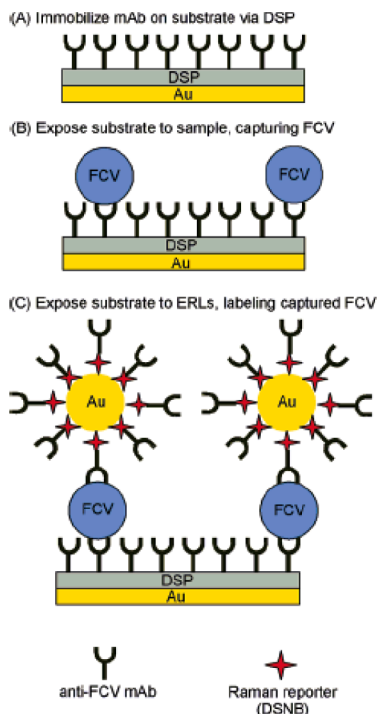


Figure 65. Direct sandwich assay for feline calicivirus using Raman spectroscopy. Reprinted from ref 221. Copyright 2005 American Chemical Society.

cannot be detected because it cannot bind with green nanoparticles, allowing for specific detection of this mutant form (Figure 66).

Influenza has attracted global concern because of its rapid pandemic threat. Wolff et al. have developed an avian influenza detection platform based on a fluorescent DNA barcode.²²³ The magnetic immunoprobes bearing the influenza type A nucleoprotein monoclonal antibodies and polystyrene microbead immunoprobes conjugated with the influenza type A matrix-protein monoclonal antibodies and fluorophore-tagged oligonucleotides form a sandwich complex structure in the presence of target avian influenza virus. After magnetic separation, the fluorophore-tagged oligonucleotides are released by heating the sandwich complex and detected. Because of the high loading of fluorophore-tagged oligonucleotides, one binding event can trigger signaling of thousands of fluorophores, which greatly amplifies the signal and improves the detection sensitivity (Figure 67). Driskell and co-workers conjugated influenza-specific antibodies to gold nanoparticles, and the aggregation of such conjugates induced by influenza viruses was detected by dynamic light scattering. This assay provides a detection limit of 100 TCID₅₀/mL, which is a 1–2 orders of magnitude improvement over that of commercial diagnostic kits.²²⁴

Schmidt and Iyer pointed out that the stability of recognition elements for point-of-care diagnostics is a major problem

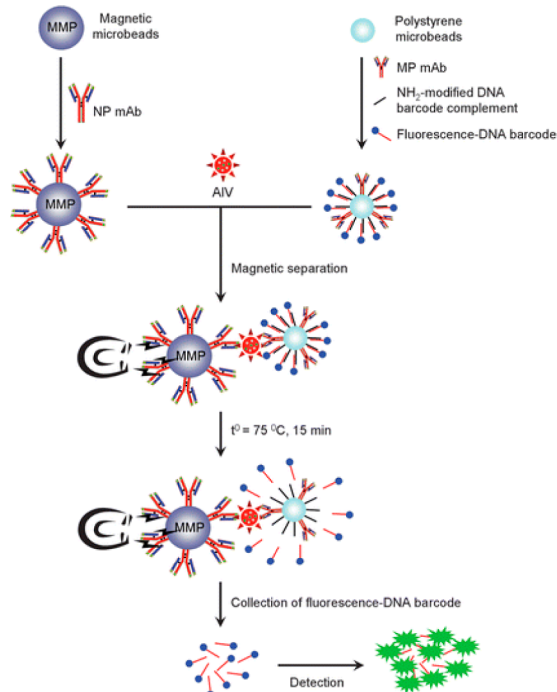


Figure 67. Sandwich assay for avian influenza virus based on the fluorophore–DNA barcode. Reprinted with permission from ref 223. Copyright 2010 The Royal Society of Chemistry.

because the recent H5N1 outbreaks have originated in remote areas of the world where refrigeration for reagents is always problematic.²²⁵ They synthesized viral neuraminidase-resistant S-sialosides and employed them as capture and reporter recognition elements (with high stability at ambient temperatures) for the rapid detection of two strains of influenza A viruses through a waveguide-based biosensor platform. The results demonstrated for the first time influenza detection using glycans as capture and reporter recognition elements simultaneously (Figure 68). An excellent discrimination of two specific strains (A/Sydney/26/95 (H3N2) and A/Beijing/262/95 (H1N1)) was also demonstrated.

Using cell-binding aptamers as recognition elements, Ramos cells (a kind of human Burkitt's lymphoma cell) were sensitively detected on the basis of sandwich-type assay. For example, Liu et al. have developed an aptamer–nanoparticle strip biosensor for the detection of Ramos cells.²²⁶ Through the cell SELEX (systematic evolution of ligands by exponential enrichment) process, the aptamers for Ramos cells with high binding affinity were selected and used to build the sandwich assay. As shown in Figure 69, TE02 aptamer was immobilized on the test zone on the strip and used to capture the Ramos cells. After the cells were captured, gold nanoparticles conjugated with TD05 aptamers were attached on the surface of the cells, and the capture aptamer–cell–gold nanoparticle sandwich structure formed, which is visualized as a red zone.

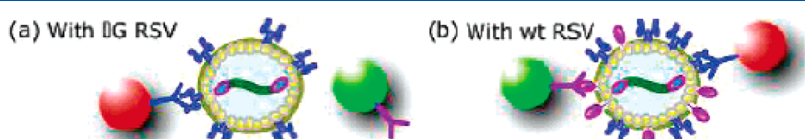


Figure 66. (a) Mutant RSV cannot bind to a green nanoparticle because of the lack of G protein. (b) Wild-type RSV can bind to red and green nanoparticles simultaneously to form a sandwich assay. Reprinted from ref 222. Copyright 2006 American Chemical Society.

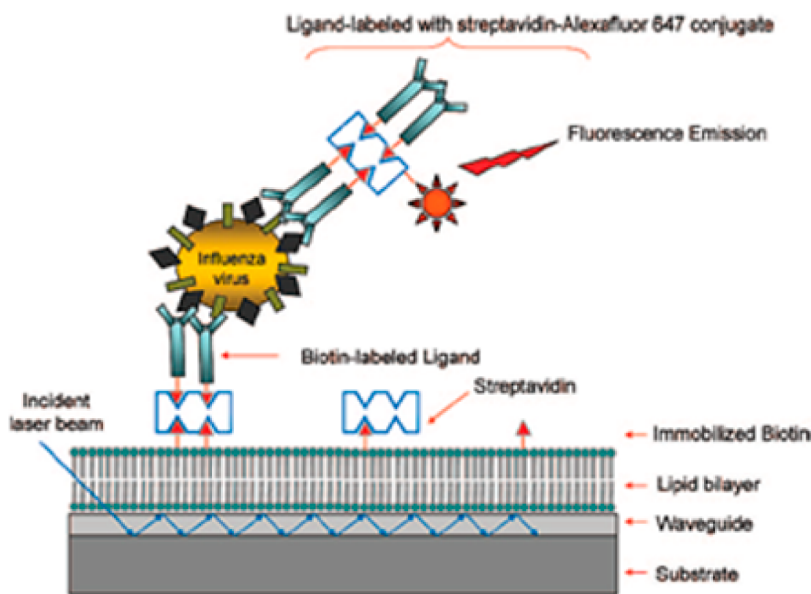


Figure 68. Sandwich assay for influenza virus based on a carbohydrate ligand and planar optical waveguide biosensor. Reprinted from ref 225. Copyright 2008 American Chemical Society.

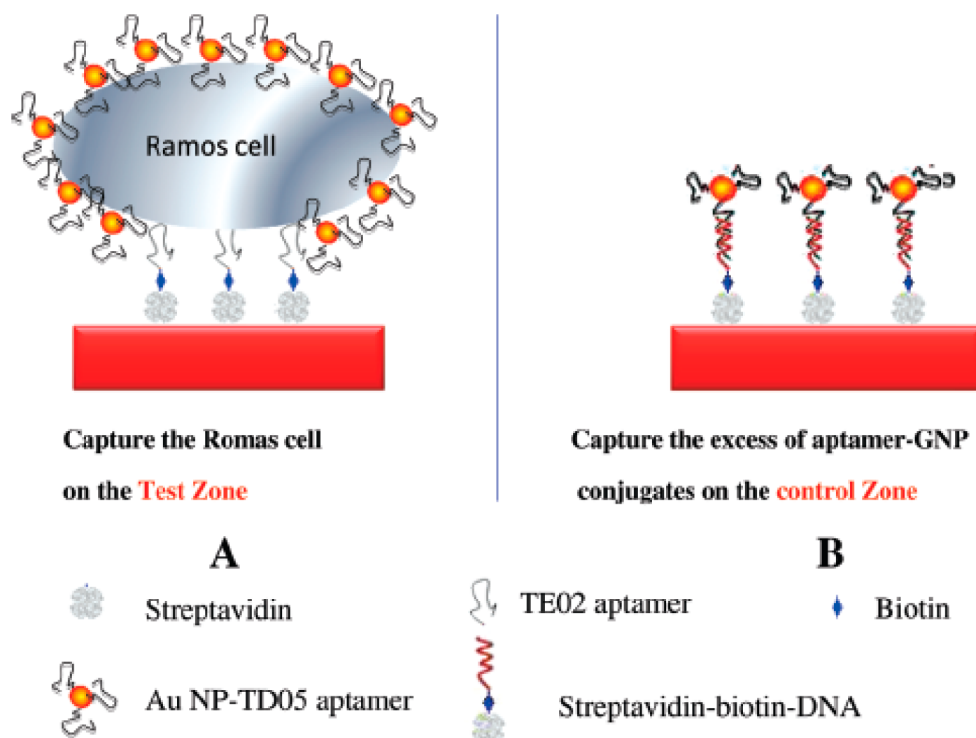


Figure 69. Schematic illustration of the sandwich assay for Ramos cells based on aptamers and gold nanoparticle visualization. Reprinted from ref 226. Copyright 2009 American Chemical Society.

The excess gold nanoparticles were captured by the DNA probes immobilized at the control zone of the strip. Zhang et al. also developed a sensitive electrochemical sandwich detection of Ramos cells using an extracellular supermolecular reticular DNA–quantum dot sheath.²²⁷

7. SUPERSANDWICH ASSAY

Usually in a sandwich assay, a target binds to only one signal probe (such as antibody in protein sandwich assay and DNA signal probe in DNA sandwich assay), which limits the total

signal gain and thus sensitivity. To overcome this, some techniques integrating multiple signal probes together to amplify the final signal have been developed and used in sandwich assay. This is the so-called “supersandwich” assay.

For protein detection, multiple HRP-modified antihuman IgG antibodies were immobilized on the surface of gold nanoparticles and used as the signal probe.²²⁸ Magnetic beads conjugated with capture probes were used to capture the human IgG, and then the gold nanoparticles with multiple antibodies were attached to form the sandwich assay. Due to

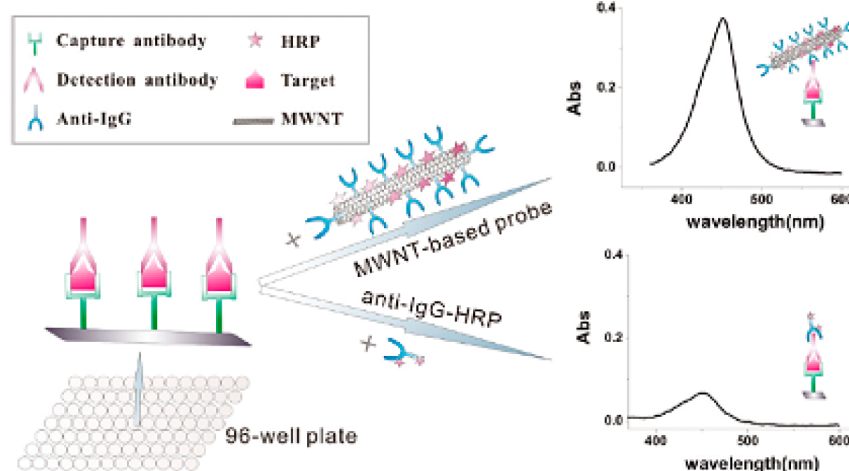
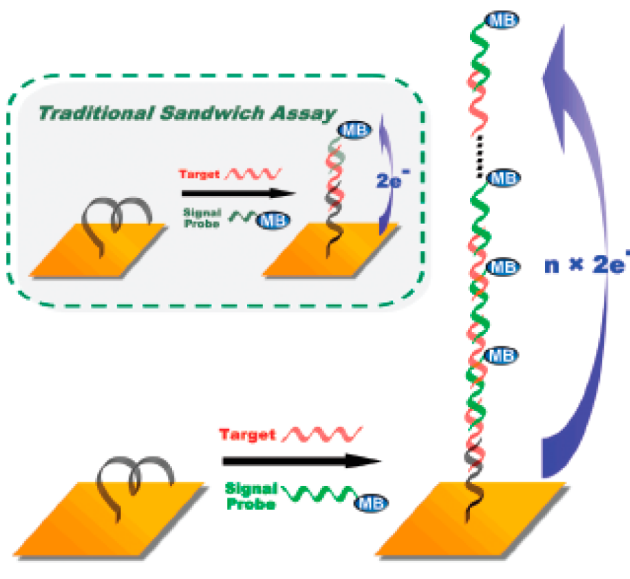


Figure 70. Scheme of the immunoassay based on supersandwich amplification. The nanotubes are used to carry multiple antibodies and HRP to amplify the final signal. Thus, a detection limit of 0.2 fg/mL (54 aM, about 32 molecules in 1 μ L of sample) is obtained. Reprinted from ref 105c. Copyright 2011 American Chemical Society.

the signal amplification of multiple HRP-labeled antibodies, the detection limit is \sim 50 times lower than that of the traditional sandwich assay, which has only one HRP-modified antibody for each target IgG. Carbon nanotubes are also used as a supporting material to carry a large number of enzymes and Pd nanoparticles.²²⁹ This carbon-nanotube-based complex can be used to detect α -1-fetoprotein with a detection limit of 33 fg/mL. Lin et al. have employed gold nanorods as nanocarriers for coimmobilization of HRP and detection antibodies, which can amplify the signal.²³⁰ Song et al. clearly demonstrated signal amplification based on carbon nanotubes that are labeled with antibodies and HRP (Figure 70).^{105c} The results showed that the sensitivity is improved 5000-fold compared to that of conventional ELISA, and the dynamic range is 10000 times wider too. Rusling and his colleagues have developed a carbon nanotube microwell array for sensitive detection of cancer biomarkers (prostate-specific antigen (PSA) and interleukin-6 (IL-6)).²³¹ In their method, silica nanoparticles containing $[\text{Ru}(\text{bpy})_3]^{2+}$ and secondary antibodies were used to amplify the signal. The detection limit for PSA was 1 pg/mL, and that for IL-6 was 0.25 pg/mL.

For nucleic acid detection, Xia, Zuo, Plaxco, and Heeger pioneered the supersandwich assay.^{155b} They pointed out that, in traditional sandwich assay, a DNA target hybridizes with a single copy of the signal probe. To improve the signal gain and detection sensitivity, they innovatively employed a modified signal probe containing a redox label—methylene blue—and a “sticky end”. In the presence of the target, the target hybridizes with the signal probe and the sticky end remains free to hybridize with another target. Finally, a supersandwich structure with multiple labels forms (Figure 71). This amplification leads to significantly improved detection limits (100 fM) relative to that of traditional sandwich assay (the detection limit is 100 pM). Chen and his colleagues noticed that the consumption of multiple targets in the supersandwich structure would limit the detection sensitivity, and they modified the method proposed by Plaxco’s group by using an auxiliary probe which can hybridize with two different regions of a signal probe and assemble into a long DNA structure.²³² Thus, only one target is needed to bring such a long DNA structure close to the electrode surface to produce amplified signal (Figure 72). A detection limit of 100 aM was achieved.



Supersandwich Assay

Figure 71. The supersandwich structure is employed in the DNA sandwich assay to amplify the signal and improve the detection sensitivity. Shown is the scheme of the traditional sandwich assay (inset) and supersandwich assay. Reprinted from ref 155b. Copyright 2010 American Chemical Society.

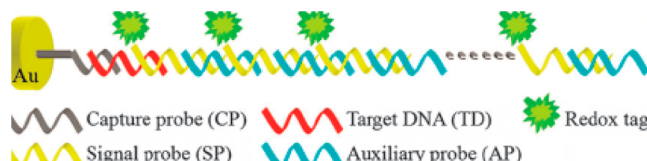


Figure 72. Example of the improved supersandwich assay. In this assay, auxiliary probes are used to form the supersandwich, which avoids the consumption of target. This can improve the detection sensitivity (100 aM). Reprinted with permission from ref 232. Copyright 2011 The Royal Society of Chemistry.

For metal ion detection, Xu and his colleagues have developed a sensitive and selective supersandwich assay for

Hg^{2+} .²³³ They immobilized capture probes (A_1) on a gold electrode via Au–S bonds. Then they employed two probes (A_2 and A_3) that are T-rich oligonucleotides at the 3' terminus and can partially hybridize with each other at the 5' terminus. Thus, on the electrode surface, a supersandwich structure forms upon Hg^{2+} binding because of the T– Hg^{2+} –T interaction (Figure 73). On the basis of this amplification, a detection limit of 0.5 nM was achieved.

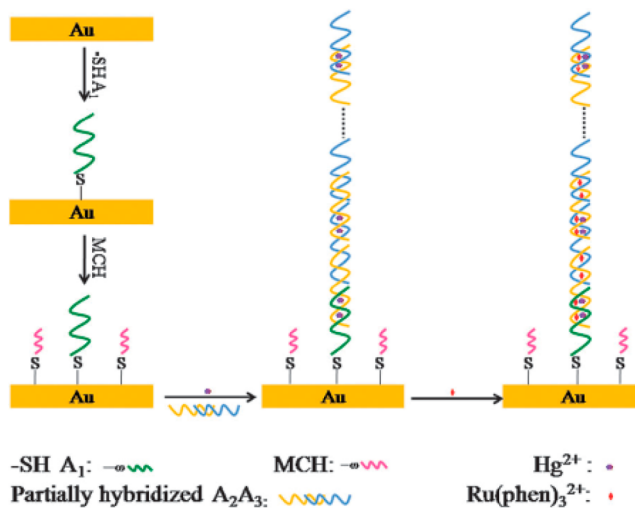


Figure 73. Scheme of the supersandwich assay for Hg^{2+} . Reprinted with permission from ref 233. Copyright 2011 The Royal Society of Chemistry.

8. PORTABLE DIAGNOSTIC DEVICES BASED ON THE SANDWICH ASSAY

Portable and disposable diagnostic devices are really important for home testing, point-of-care testing, and routine laboratory applications. In some developing countries or remote areas, such devices are equally important too because of the shortage of instruments and power sources. For example, lateral flow tests have been successfully developed and commercialized very

well for the detection of proteins, so here we focus on the recent development of portable devices for DNA detection.

Baeumner et al. have developed a simple and universal DNA test strip based on sandwich assay and lateral flow technology.²³⁴ In their system, a dye-entrapping liposome which bears generic oligonucleotides on its outer surface was used to indicate the presence of a specific target. The reporter probes can hybridize partially with the generic oligonucleotides on the liposome, and at the same time the reporter probes can also hybridize with the target. Then this complex was captured by a biotin-modified capture probe, pipetted onto a poly(ether sulfone) membrane, and allowed along the strip with a detection zone modified with streptavidin (Figure 74). In the presence of target, the complex will be captured at the detection zone via biotin–streptavidin binding, and the signal can be read using a portable reflectometer or the unaided eye. A detection limit of 1 nM was achieved using this device.

Wilson and his colleagues developed a nucleic acid lateral flow device based on sandwich assay and gold nanoparticles.²³⁵ This device was used to detect PCR products. To avoid using antibodies or streptavidin, they immobilized reporter oligonucleotides on the surface of gold nanoparticles and capture probes at the detection zone of plastic-backed nitrocellulose. The target can be captured by the capture probes along with the gold nanoparticle conjugates because of the formation of a sandwich format, which appears as a red zone on the strip. A similar system was used for visual detection of single-nucleotide polymorphism.²³⁶

Liu and his colleagues clearly demonstrated the structure of the lateral flow strip and the detection process of such devices based on sandwich assay and gold nanoparticles.²³⁷ As we can see (Figure 75), the main components of the strip include a sample pad which is saturated with buffer, a conjugation pad which adsorbs gold nanoparticles conjugated with signal DNA probes, a nitrocellulose membrane which is modified with capture probes at the test zone and control DNA at the control zone, and an adsorption pad. By using a laminator, the four components are assembled on a plastic back layer with 2 mm overlaps between each component to ensure the migration of the solution through the strip. During the assay, the sample solution containing the target DNA is pipetted onto the sample

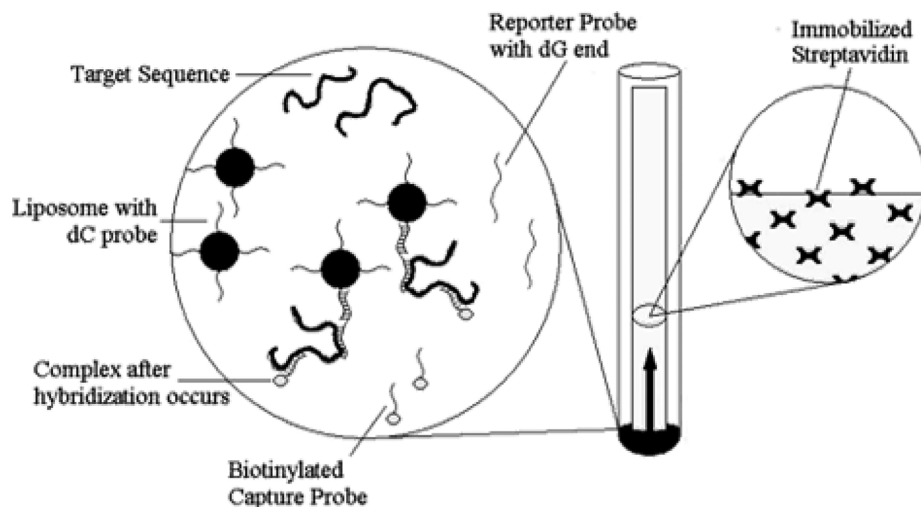


Figure 74. Principle of the DNA sandwich assay based on a liposome and the lateral flow test. Reprinted from ref 234. Copyright 2004 American Chemical Society.

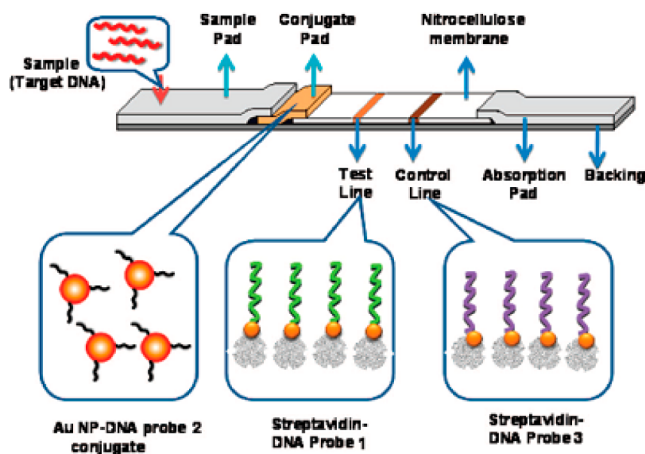


Figure 75. Detailed structure of the lateral flow device based on the DNA sandwich assay and gold nanoparticles. Reprinted from ref 237. Copyright 2009 American Chemical Society.

pad and migrates and passes the conjugation pad to hybridize with the signal probes on the gold nanoparticles and form a complex. The complex migrates forward along the strips and is captured by the capture probes at the test zone, which appears as a red band in the presence of target (in the absence of target no red band appears at the test zone). Then the additional gold nanoparticles conjugated with signal probes migrate forward to hybridize with the control probes at the control zone, and thus, another red band appears, which indicates the strip works well (Figure 76). A detection limit of 0.5 nM was achieved. To improve the sensitivity, they amplified the signal with immobilization of signal probes and HRP simultaneously on

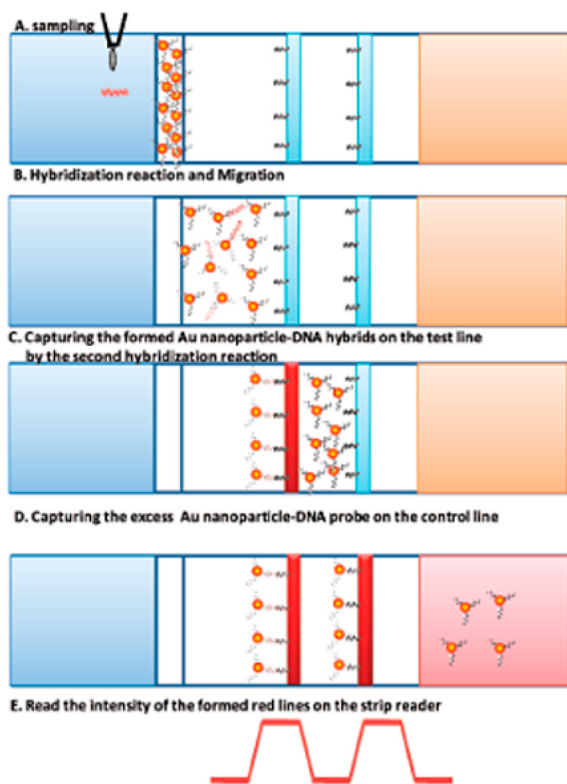


Figure 76. Detection principle of the DNA lateral flow device. Reprinted from ref 237. Copyright 2009 American Chemical Society.

gold nanoparticles, and a detection limit of 50 pM was achieved.

Besides the lateral flow strip, some other portable devices integrated with microfluidic and electronic technologies have been developed too.²³⁸ For example, a sequential injection analysis lab-on-valve system was used to detect nucleic acids on the basis of sandwich assay.^{238a} Within 20 min, the system can detect as low as 1 pM synthetic DNA. Most recently, an ovarian cancer biomarker (HE4) detection system was developed by integration of cell phone imaging with microchip ELISA.^{238b} The application of cell phone imaging eliminates the use of a large, expensive spectrometer for the results readout, and this interesting system can be used to detect HE4 in urine samples of patients.

9. CONCLUSIONS AND OUTLOOK

It is clear that sandwich assays are and will be widely used in clinic diagnostics, routine laboratory detection, food safety, environmental monitoring, and antiterrorism. The development of the sandwich assay benefits from the recent advancements of biotechnology, synthetic chemistry, nanotechnology, and electronics. On the basis of these advancements, some efforts have been extensively made to improve the performance of sandwich assay from all aspects. For example, aptamers are introduced into the sandwich assay which expand the targets of sandwich assay from protein and DNA (or RNA) to small molecules and ions. The applications of nanoparticles in sandwich assay significantly amplify the signal and push the detection limit down. In addition, some fluorescent nanoparticles such as quantum dots and dye-doped nanoparticles can produce a more stable and strong signal than traditional organic dyes. Some surface modifications have also been investigated to reduce nonspecific adsorption, which is a bottleneck of sandwich assay, and diverse signal transducers are widely used to read the signal of sandwich assay (such as a fluorometer, an electrochemical workstation, a QCM, SPR, and a microcantilever).

We are happy to see the achievements of the sandwich assay developed in recent decades, but we also note that there are still some problems that need to be solved in this fast-growing area. For example, the sandwich assay is not a reagent-free method (which means reagents usually need to be added by the users). If we could develop a reagent-free sandwich assay, that would simplify the detection and make it easier to use. The stability (thermal stability and long-time storage stability) of the complex of biomolecules and nanoparticles is still a problem. The surface passivation methods should be further developed to resist nonspecific adsorption. This relies on the further development of chemistry, physics, and biology and the cutting edge research of these fields.

AUTHOR INFORMATION

Corresponding Authors

*E-mail: xiafan@mail.hust.edu.cn.
*E-mail: zuoxiaolei@sinap.ac.cn.

Author Contributions

[†]J.S. and Y.L. contributed equally to this work.

Notes

The authors declare no competing financial interest.

Biographies



Juwen Shen received her Ph.D. in 2008 from the Shanghai Institute of Materia Medica, Chinese Academy of Sciences. Right now, she is working as an assistant professor in the Key Laboratory of Systems Biology, Shanghai Institutes for Biological Sciences, Chinese Academy of Sciences, Shanghai. Her research interests include biosensor design and optimization based on mathematic modeling and prediction of the interaction of biomolecules (protein–protein interaction, DNA–small-molecule interaction, aptamer–target interaction, etc.). Another important research direction focuses on epigenetic analysis.



Haoshuang Gu is currently a professor and director of the State Key Laboratory of Ferro- and Piezoelectric Materials and Devices of Hubei Province, Faculty of Physical and Electronic Sciences at Hubei University. He received his B.S. degree in physics from Hubei University in 1982 and his Ph.D. in electronic materials and devices from HUST in 1996. From 2000 to 2001, he worked at the National University of Singapore as a senior visiting scholar. His current research focuses on functional thin films, nanostructured sensors, and nanocapsules for targeted drug delivery.



Fan Xia is currently a professor at HUST. He received his B.S. degree (2003) from HUST and M.S. degree (2005) and Ph.D. degree (2008) from the Institute of Chemistry, Chinese Academy of Sciences (Prof. Lei Jiang's group). He then worked as a postdoctoral fellow in Prof. Alan J. Heeger and Prof. Kevin W. Plaxco's group at the University of California, Santa Barbara. He joined HUST as a professor in 2012. His scientific interest is focused on DNA- and protein-based biosensors, cancer cell detection, and bioinspired hybrid materials.



Yuebin Li earned his B.S. in physics from Hubei University in 2006, and then he obtained his Ph.D. in materials science and engineering from a joint program between HUST and the University of Texas at Arlington supported by the China Scholarship Council. After that, he visited Prof. Fan Xia's group at HUST as a research fellow from June 2011 to March 2012. He is currently a member of the Faculty of Physical and Electronic Sciences, Hubei University. His current research focuses on the fabrication and bioapplications of functional optical nanomaterials and nanodevices.



Xiaolei Zuo received his bachelor's and master's degrees from Central South University, and then he obtained his Ph.D. in 2008 from the

Chinese Academy of Sciences. After that, he moved to the University of California, Santa Barbara, as a postdoctoral researcher under the guidance of Prof. Kevin W. Plaxco. Right now, he is a professor in the Laboratory of Physical Biology, Shanghai Institute of Applied Physics. His current research focuses on the sensitive and selective detection of a spectrum of targets (including biomarkers for diseases, small molecules for human health and environmental safety, etc.).

ACKNOWLEDGMENTS

This research was supported by initiatory funding from HUST and the 100-Talent Project from the Chinese Academy of Sciences (to X.Z.) and Shanghai Pujiang Project with Grant 13PJ1410700 (to X.Z.). We acknowledge partial support from the National Natural Science Foundation of China (Grants 51303046, 51173038, and 11274127), National Basic Research Program of China (973 Program, Grant 2012CB932600), Natural Science Foundation of Hubei Province of China (Grant 2012FFB00301), and Specialized Research Fund for the Doctoral Program of Higher Education (Grant 20114208130001). We also acknowledge support from Zihang Xia, Wei Lin, and Zixi Xia and thank the HUST Analytical and Testing Center for allowing us to use its facilities.

ABBREVIATIONS

ABTS	2,2'-azinobis(3-ethylbenzthiazoline-6-sulfonic acid)
ALP, AP	alkaline phosphatase
ATP	adenosine triphosphate
BA	<i>Bacillus anthracis</i>
BOD	bilirubin oxidase
BSA	bovine serum albumin
CEA	carcinoembryonic antigen
CFU	colony-forming unit
CNT	carbon nanotube
CPs	conjugated polymers
CuHCF	cupric hexacyanoferrate
Cyt c	cytochrome c
DPV	differential pulse voltammetry
ECL	electrochemiluminescence
ELISA	enzyme-linked immunosorbent assay
Fc-D	ferrocenyl-tethered poly(amidoamine) dendrimer
FCV	feline calicivirus
FET	field effect transistor
FITC	fluorescein isothiocyanate
FRET	fluorescence resonance energy transfer
GMR	giant magnetoresistive
GO	graphene oxide
HAS	human serum albumin
HBsAg	hepatitis B surface antigen
HCG	human chorionic gonadotropin
h-IgG	human immunoglobulin G
HIV	human immunodeficiency virus
HRP	horseradish peroxidase
HVA	hepatitis A virus <i>Vall7</i> polyprotein gene
HVB	hepatitis B virus surface antigen gene
IGF-1	insulin-like growth factor 1
IgG	immunoglobulin G
IL-1 α	interleukin-1 α
IL-6	interleukin-6
ITO	indium–tin oxide
LH	luteinizing hormone
LSPR	localized surface plasmon resonance

mAb	monoclonal antibody
MB	methylene blue
MLB-PPV	poly[lithium 5-methoxy-2-(4-sulfobutoxy)-1,4-phenylenevinylene]
MCH	6-mercaptop-1-hexanol
MNTs	magnetic nanotags
MPC	microfluidic purification chip
MWCNT	multiwall carbon nanotube
NPs	nano particles
OPD	o-phenylenediamine
OVA	ovalbumin
p53	tumor protein 53
PCR	polymerase chain reaction
PDGF-BB	platelet-derived growth factor-BB
PEG	poly(ethylene glycol)
PNA	peptide nucleic acid
pNPP	p-nitrophenyl phosphate
PSA	prostate-specific antigen
QCM	quartz crystal microbalance
QDs	quantum dots
RSV	respiratory syncytial virus
SAM	self-assembled monolayer
SERS	surface-enhanced Raman scattering
SNP	single-nucleotide polymorphism
SPR	surface plasmon resonance
SWCNT	single-wall carbon nanotube
TMB	3,3',5,5'-tetramethylbenzidine
TNF	tumor necrosis factor
VV	variola virus

REFERENCES

- (a) Hochstrasser, M. *Nature* **2009**, *458*, 422. (b) Petsko, G. A.; Ringe, D. *Protein Structure and Function*; New Science Press Ltd.: London, 2004; pp 42–46.
- (a) Wisdom, G. B. *Clin. Chem.* **1976**, *22*, 1243. (b) Self, C. H.; Cook, D. B. *Curr. Opin. Biotechnol.* **1996**, *7*, 60.
- (a) Vasan, R. S. *Circulation* **2006**, *113*, 2335. (b) Molitoris, B. A.; Melnikov, V. Y.; Okusa, M. D.; Hirnmelfarb, J. *Nat. Clin. Pract. Nephrol.* **2008**, *4*, 154.
- Gochman, N.; Bowie, L. *J. Anal. Chem.* **1977**, *49*, 1183A.
- Piletska, E. V.; Piletsky, S. S.; Whitcombe, M. J.; Chianella, I.; Piletsky, S. A. *Anal. Chem.* **2012**, *84*, 2038.
- Grate, J. W.; Warner, M. G.; Ozanich, J. R. M.; Miller, K. D.; Colburn, H. A.; Dockendorff, B.; Antolick, K. C.; Anheier, N. C., Jr.; Lind, M. A.; Lou, J.; Marks, J. D.; Bruckner-Lea, C. J. *Analyst* **2009**, *134*, 987.
- Yu, X.; Munge, B.; Patel, V.; Jensen, G.; Bhirde, A.; Gong, J. D.; Kim, S. N.; Gillespie, J.; Gutkind, J. S.; Papadimitrakopoulos, F.; Rusling, J. F. *J. Am. Chem. Soc.* **2006**, *128*, 11199.
- Fishbein, I.; Levy, R. J. *Nature* **2009**, *461*, 890.
- He, L.; Rodda, T.; Haynes, C. L.; Deschaines, T.; Strother, T.; Diez-Gonzalez, F.; Labuza, T. P. *Anal. Chem.* **2011**, *83*, 1510.
- Basu, A.; Shrivastav, T. G.; Maitra, S. K. *J. Immunoassay Immunochem.* **2005**, *26*, 313.
- Wide, L.; Porath, J. *Biochim. Biophys. Acta, Gen. Subj.* **1966**, *130*, 257.
- Castigliego, L.; Li, X.; Armani, A.; Mazzi, M.; Guidi, A. *Int. Dairy J.* **2011**, *21*, 421.
- Jia, C.-P.; Zhong, X.-Q.; Hua, B.; Liu, M.-Y.; Jing, F.-X.; Lou, X.-H.; Yao, S.-H.; Xiang, J.-Q.; Jin, Q.-H.; Zhao, J.-L. *Biosens. Bioelectron.* **2009**, *24*, 2836.
- Ke, R.; Yang, W.; Xia, X.; Xu, Y.; Li, Q. *Anal. Biochem.* **2010**, *406*, 8.
- Hashida, S.; Nakagawa, K.; Yoshitake, S.; Imagawa, M.; Ishikawa, E.; Endo, Y.; Ohtaki, S.; Ichioka, Y.; Nakajima, K. *Anal. Lett.* **1983**, *16*, 31.

- (16) Islam, K. N.; Ihara, M.; Dong, J.; Kasagi, N.; Mori, T.; Ueda, H. *Anal. Chem.* **2011**, *83*, 1008.
- (17) Hayes, M. A.; Petkus, M. M.; Garcia, A. A.; Taylor, T.; Mahanti, P. *Analyst* **2009**, *134*, 533.
- (18) Mukundan, H.; Xie, H.; Price, D.; Kubicek-Sutherland, J. Z.; Grace, W. K.; Anderson, A. S.; Martinez, J. S.; Hartman, N.; Swanson, B. I. *Anal. Chem.* **2009**, *82*, 136.
- (19) Wang, J.; Liu, G.; Jan, M. R. *J. Am. Chem. Soc.* **2004**, *126*, 3010.
- (20) Zhang, Y.-L.; Huang, Y.; Jiang, J.-H.; Shen, G.-L.; Yu, R.-Q. *J. Am. Chem. Soc.* **2007**, *129*, 15448.
- (21) Osterfeld, S. J.; Yu, H.; Gaster, R. S.; Caramuta, S.; Xu, L.; Han, S.-J.; Hall, D. A.; Wilson, R. J.; Sun, S.; White, R. L.; Davis, R. W.; Pourmand, N.; Wang, S. X. *Proc. Natl. Acad. Sci. U.S.A.* **2008**, *105*, 20637.
- (22) Huang, C.-C.; Huang, Y.-F.; Cao, Z.; Tan, W.; Chang, H.-T. *Anal. Chem.* **2005**, *77*, 5735.
- (23) Wang, C.; Chen, Y.; Wang, T.; Ma, Z.; Su, Z. *Chem. Mater.* **2007**, *19*, 5809.
- (24) Glick, S. *Nature* **2011**, *474*, 580.
- (25) Kimball, J. W. Radioimmunoassay (RIA). Kimball's Biology Pages, 2007. <http://users.rcn.com/jkimball.ma.ultranet/BiologyPages/R/Radioimmunoassay.html> (accessed on March 9, 2011).
- (26) Miles, L. E. M.; Hales, C. N. *Biochem. J.* **1968**, *108*, 611.
- (27) (a) Stanley J, G. *Semin. Nucl. Med.* **1975**, *5*, 125. (b) Józefowski, S.; Czernies, M.; Sobota, A.; Kwiatkowska, K. *Anal. Biochem.* **2011**, *413*, 185. (c) Barbato, O.; Sousa, N. M.; Debenedetti, A.; Canali, C.; Todini, L.; Beckers, J. F. *Theriogenology* **2009**, *72*, 993. (d) Holtom, P. E.; Wasuntarawat, C.; Moss, S. H.; Aspley, S.; Needham, P. L.; Bennett, G. W. *J. Neurosci. Methods* **2000**, *100*, 151. (e) Avir, K. *Semin. Nucl. Med.* **1975**, *5*, 183. (f) Ikeda, K.; Stenflo, J. *Thromb. Res.* **1985**, *39*, 297. (g) Wu, G. *Assays with GPCRs*; John Wiley & Sons, Inc.: Hoboken, NJ, 2010; pp 265–288.
- (28) Soini, E.; Hemmila, I. *Clin. Chem.* **1979**, *25*, 353.
- (29) Engvall, E.; Perlmann, P. *Immunochemistry* **1971**, *8*, 871.
- (30) (a) BK, V. W.; AH, S. *FEBS Lett.* **1971**, *15*, 232. (b) Adachi, H.; Fukuda, T.; Funahashi, S.; Kurahori, T.; Ishikawa, E. *Vox Sang.* **1978**, *35*, 219. (c) Uotila, M.; Ruoslahti, E.; Engvall, E. *J. Immunol. Methods* **1981**, *42*, 11. (d) Masayoshi, I.; Shinji, Y.; Eiji, I.; Yoshiro, N.; Ichiro, U.; Reizo, K.; Sciji, T.; Nobuhiko, N.; Hiroshi, O. *Clin. Chim. Acta* **1982**, *121*, 277.
- (31) (a) Imagawa, M.; Hashida, S.; Ishikawa, E.; Mori, H.; Nakai, C.; Ichioka, Y.; Nakajima, K. *Anal. Lett.* **1983**, *16*, 1509. (b) Inoue, S.; Hashida, S.; Ishikawa, E.; Mori, T.; Imura, H.; Ogawa, H.; Ichioka, T.; Nakajima, K. *Anal. Lett.* **1986**, *19*, 845. (c) Tomita, H.; Ogawa, M.; Kamijo, T.; Mori, O.; Ishikawa, E.; Mohri, Z.-i.; Murakami, Y. *Acta Endocrinol.* **1989**, *121*, 513.
- (32) (a) Walker, J. M.; Rapley, R. *Molecular Biomethods Handbook*; Humana Press Inc.: Totowa, NJ, 2008; pp 657–682. (b) Hamaguchi, Y.; Kato, K.; Fukui, H.; Shirakawa, I.; Okawa, S.; Ishikawa, E.; Kobayashi, K.; Katunuma, N. *Eur. J. Biochem.* **1976**, *71*, 459.
- (33) Cleland, W. W.; Hengge, A. C. *Chem. Rev.* **2006**, *106*, 3252.
- (34) Ko, Y.-c.; Mukaida, N.; Panyutich, A.; Voitenok, N. N.; Matsushima, K.; Kawai, T.; Kasahara, T. *J. Immunol. Methods* **1992**, *149*, 227.
- (35) Laing, S.; Hernandez-Santana, A.; Sassmannshausen, J. r.; Asquith, D. L.; McInnes, I. B.; Faulds, K.; Graham, D. *Anal. Chem.* **2010**, *83*, 297.
- (36) Daniilidou, M.; Tsolaki, M.; Giannakouros, T.; Nikolakaki, E. *J. Neuroimmunol.* **2011**, *238*, 67.
- (37) (a) Vandermeeren, M.; Mercken, M.; Vanmechelen, E.; Six, J.; Van de Voorde, A.; Martin, J.-J.; Cras, P. *J. Neurochem.* **1993**, *61*, 1828. (b) Surojanametakul, V.; Doi, H.; Shibata, H.; Mizumura, T.; Takahashi, T.; Varanyanond, W.; Wannapinpong, S.; Shoji, M.; Ito, T.; Tamura, H. *J. Agric. Food Chem.* **2011**, *59*, 2131. (c) Mercken, M.; Vandermeeren, M.; Lübbke, U.; Six, J.; Boons, J.; Vanmechelen, E.; Van De Voorde, A.; Gheuens, J. *J. Neurochem.* **1992**, *58*, 548. (d) Frey, A.; Mecklein, B.; Externest, D.; Schmidt, M. A. *J. Immunol. Methods* **2000**, *233*, 47. (e) El Mouedden, M.; Vandermeeren, M.; Meert, T.; Mercken, M. *J. Neurosci. Methods* **2005**, *145*, 97.
- (38) Wang, J.; Cao, Y.; Xu, Y.; Li, G. *Biosens. Bioelectron.* **2009**, *25*, 532.
- (39) Abuknesha, R.; Jegannathan, F.; DeGroot, R.; Wildeboer, D.; Price, R. *Anal. Bioanal. Chem.* **2010**, *396*, 2547.
- (40) (a) Liu, X.; Eichenberger, M.; Fujioka, Y.; Dong, J.; Ueda, H. *Anal. Sci.* **2012**, *28*, 861. (b) Ihara, M.; Suzuki, T.; Kobayashi, N.; Goto, J.; Ueda, H. *Anal. Chem.* **2009**, *81*, 8298.
- (41) Ambrosi, A.; Airo, F.; Merkoci, A. *Anal. Chem.* **2010**, *82*, 1151.
- (42) (a) Ambrosi, A.; Airò, F.; Merkoçi, A. *Anal. Chem.* **2009**, *82*, 1151. (b) Ambrosi, A.; Castañeda, M. T.; Killard, A. J.; Smyth, M. R.; Alegría, S.; Merkoçi, A. *Anal. Chem.* **2007**, *79*, 5232. (c) Liu, M.; Jia, C.; Huang, Y.; Lou, X.; Yao, S.; Jin, Q.; Zhao, J.; Xiang, J. *Analyst* **2010**, *135*, 327.
- (43) Cao, X.; Ye, Y.; Liu, S. *Anal. Biochem.* **2011**, *417*, 1.
- (44) Tang, S.; Hewlett, I. *J. Infect. Dis.* **2010**, *201*, S59.
- (45) Dixit, C. K.; Vashist, S. K.; O'Neill, F. T.; O'Reilly, B.; MacCraith, B. D.; O'Kennedy, R. *Anal. Chem.* **2010**, *82*, 7049.
- (46) (a) Gao, L.; Zhuang, J.; Nie, L.; Zhang, J.; Zhang, Y.; Gu, N.; Wang, T.; Feng, J.; Yang, D.; Perrett, S.; Yan, X. *Nat. Nano* **2007**, *2*, 577. (b) Song, Y.; Wang, X.; Zhao, C.; Qu, K.; Ren, J.; Qu, X. *Chem.—Eur. J.* **2010**, *16*, 3617. (c) Dai, Z.; Liu, S.; Bao, J.; Ju, H. *Chem.—Eur. J.* **2009**, *15*, 4321. (d) Chen, W.; Chen, J.; Liu, A. L.; Wang, L. M.; Li, G. W.; Lin, X. H. *ChemCatChem* **2011**, *3*, 1151.
- (47) Fan, J.; Yin, J.-J.; Ning, B.; Wu, X.; Hu, Y.; Ferrari, M.; Anderson, G. J.; Wei, J.; Zhao, Y.; Nie, G. *Biomaterials* **2011**, *32*, 1611.
- (48) He, W.; Liu, Y.; Yuan, J.; Yin, J.-J.; Wu, X.; Hu, X.; Zhang, K.; Liu, J.; Chen, C.; Ji, Y.; Guo, Y. *Biomaterials* **2011**, *32*, 1139.
- (49) (a) Wang, E.; Wei, H. *Anal. Chem.* **2008**, *80*, 2250. (b) Yang, V. C.; Yu, F. Q.; Huang, Y. Z.; Cole, A. J. *Biomaterials* **2009**, *30*, 4716.
- (c) Gao, D.; Gao, L. Z.; Wu, J. M.; Lyle, S.; Zehr, K.; Cao, L. L. *J. Phys. Chem. C* **2008**, *112*, 17357. (d) Liu, S.; Lu, F.; Xing, R.; Zhu, J.-J. *Chem.—Eur. J.* **2011**, *17*, 620. (e) Yihang, W.; et al. *Nanotechnology* **2011**, *22*, 225703. (f) Chang, Q.; Deng, K.; Zhu, L.; Jiang, G.; Yu, C.; Tang, H. *Microchim. Acta* **2009**, *165*, 299.
- (50) (a) Asati, A.; Santra, S.; Kaittanis, C.; Nath, S.; Perez, J. M. *Angew. Chem., Int. Ed.* **2009**, *48*, 2308. (b) Ornatska, M.; Sharpe, E.; Andreescu, D.; Andreescu, S. *Anal. Chem.* **2011**, *83*, 4273.
- (51) Song, Y.; Qu, K.; Zhao, C.; Ren, J.; Qu, X. *Adv. Mater.* **2010**, *22*, 2206.
- (52) Zhang, Z.; Wang, Z.; Wang, X.; Yang, X. *Sens. Actuators, B* **2010**, *147*, 428.
- (53) Ma, M.; Zhang, Y.; Gu, N. *Colloids Surf., A* **2011**, *373*, 6.
- (54) Barbara, K. P.; et al. *Nanotechnology* **2010**, *21*, 035102.
- (55) Chaudhari, K. N.; Chaudhari, N. K.; Yu, J.-S. *Catal. Sci. Technol.* **2012**, *2*, 119.
- (56) (a) Coons, A. H.; Creech, H. J.; Jones, R. N. *Proc. Soc. Exp. Biol. Med.* **1941**, *47*, 200. (b) AH, C.; MH, K. *J. Exp. Med.* **1950**, *91*, 1.
- (57) (a) Rosi, N. L.; Mirkin, C. A. *Chem. Rev.* **2005**, *105*, 1547. (b) Ho, H.-A.; Najari, A.; Leclerc, M. *Acc. Chem. Res.* **2008**, *41*, 168.
- (58) Raj, J.; Herzog, G.; Manning, M.; Volcke, C.; MacCraith, B. D.; Ballantyne, S.; Thompson, M.; Arrigan, D. W. M. *Biosens. Bioelectron.* **2009**, *24*, 2654.
- (59) (a) Zhu, X.; Chen, L.; Shen, P.; Jia, J.; Zhang, D.; Yang, L. *J. Agric. Food Chem.* **2011**, *59*, 2184. (b) Chan, W. C. W.; Nie, S. *Science* **1998**, *281*, 2016.
- (60) (a) Traina, C. A.; Bakus, Ii, R. C.; Bazan, G. C. *J. Am. Chem. Soc.* **2011**, *133*, 12600. (b) Thomas, S. W.; Joly, G. D.; Swager, T. M. *Chem. Rev.* **2007**, *107*, 1339.
- (61) (a) Nutiu, R.; Li, Y. *Chem.—Eur. J.* **2004**, *10*, 1868. (b) Nutiu, R.; Li, Y. *Methods* **2005**, *37*, 16. (c) Cao, Z.; Suljak, S. W.; Tan, W. *Curr. Proteomics* **2005**, *2*, 31.
- (62) (a) Wang, X.; Ren, L.; Tu, Q.; Wang, J.; Zhang, Y.; Li, M.; Liu, R.; Wang, J. *Biosens. Bioelectron.* **2011**, *26*, 3353. (b) Yan, J.; Estévez, M. C.; Smith, J. E.; Wang, K.; He, X.; Wang, L.; Tan, W. *Nano Today* **2007**, *2*, 44.
- (63) Hun, X.; Zhang, Z. *Biosens. Bioelectron.* **2007**, *22*, 2743.
- (64) Wang, J. Y.; Wang, X. Q.; Ren, L.; Wang, Q.; Li, L.; Liu, W. M.; Wan, Z. F.; Yang, L. Y.; Sun, P.; Ren, L. L.; Li, M. L.; Wu, H.; Wang, J. F.; Zhang, L. *Anal. Chem.* **2009**, *81*, 6210.

- (65) Gruber, H. J.; Hahn, C. D.; Kada, G.; Riener, C. K.; Harms, G. S.; Ahrer, W.; Dax, T. G.; Knaus, H.-G. *Bioconjugate Chem.* **2000**, *11*, 696.
- (66) Bünzli, J.-C. *G. Chem. Rev.* **2010**, *110*, 2729.
- (67) (a) Giepmans, B. N. G.; Adams, S. R.; Ellisman, M. H.; Tsien, R. Y. *Science* **2006**, *312*, 217. (b) Haugland, R. P.; Spence, M. T. Z.; Johnson, I. D. *The Handbook: A Guide to Fluorescent Probes and Labeling Technologies; Molecular Probes*: Eugene, OR, 2005; pp 35–105.
- (68) Hage, D. S. *Anal. Chem.* **1999**, *71*, 294.
- (69) Ozanich, R. M.; Bruckner-Lea, C. J.; Warner, M. G.; Miller, K.; Antolick, K. C.; Marks, J. D.; Lou, J.; Grate, J. W. *Anal. Chem.* **2009**, *81*, 5783.
- (70) Reed, M. A.; Stern, E.; Vacic, A.; Rajan, N. K.; Criscione, J. M.; Park, J.; Ilic, B. R.; Mooney, D. J.; Fahmy, T. M. *Nat. Nanotechnol.* **2010**, *5*, 138.
- (71) (a) Huhtinen, P.; Kivelä, M.; Kuronen, O.; Hagren, V.; Takalo, H.; Tenhu, H.; Lövgren, T.; Härmä, H. *Anal. Chem.* **2005**, *77*, 2643. (b) Wang, L.; Yang, C.; Tan, W. *Nano Lett.* **2004**, *5*, 37. (c) Knopp, D.; Tang, D.; Niessner, R. *Anal. Chim. Acta* **2009**, *647*, 14. (d) Wang, L.; Zhao, W.; O'Donoghue, M. B.; Tan, W. *Bioconjugate Chem.* **2007**, *18*, 297.
- (72) (a) Michalet, X.; Pinaud, F. F.; Bentolila, L. A.; Tsay, J. M.; Doose, S.; Li, J. J.; Sundaresan, G.; Wu, A. M.; Gambhir, S. S.; Weiss, S. *Science* **2005**, *307*, 538. (b) Yan, J.; Hu, M.; Li, D.; He, Y.; Zhao, R.; Jiang, X.; Song, S.; Wang, L.; Fan, C. *Nano Res.* **2008**, *1*, 490. (c) Hu, M.; Yan, J.; He, Y.; Lu, H.; Weng, L.; Song, S.; Fan, C.; Wang, L. *ACS Nano* **2009**, *4*, 488.
- (73) (a) Hilderbrand, S. A.; Shao, F.; Salthouse, C.; Mahmood, U.; Weissleder, R. *Chem. Commun.* **2009**, 4188. (b) Feng, J.; Shan, G.; Maquieira, A.; Koivunen, M. E.; Guo, B.; Hammock, B. D.; Kennedy, I. M. *Anal. Chem.* **2003**, *75*, 5282.
- (74) (a) Bailey, R. E.; Nie, S. J. *Am. Chem. Soc.* **2003**, *125*, 7100. (b) Regulacio, M. D.; Han, M.-Y. *Acc. Chem. Res.* **2010**, *43*, 621.
- (75) Gu, B.; Xu, C.; Yang, C.; Liu, S.; Wang, M. *Biosens. Bioelectron.* **2011**, *26*, 2720.
- (76) (a) Mukundan, H.; Xie, H.; Anderson, A. S.; Grace, W. K.; Shively, J. E.; Swanson, B. I. *Bioconjugate Chem.* **2009**, *20*, 222. (b) Mukundan, H.; Anderson, A. S.; Grace, W. K.; Grace, K. M.; Hartman, N.; Martinez, J. S.; Swanson, B. I. *Sensors* **2009**, *9*, 5783. (c) Martinez, J. S.; Grace, W. K.; Grace, K. M.; Hartman, N.; Swanson, B. I. *J. Mater. Chem.* **2005**, *15*, 4639.
- (77) (a) Larson, D. R.; Zipfel, W. R.; Williams, R. M.; Clark, S. W.; Bruchez, M. P.; Wise, F. W.; Webb, W. W. *Science* **2003**, *300*, 1434. (b) Wuister, S. F.; Swart, I.; van Driel, F.; Hickey, S. G.; de Mello Donegá, C. *Nano Lett.* **2003**, *3*, 503.
- (78) Hoshino, A.; Fujioka, K.; Oku, T.; Suga, M.; Sasaki, Y. F.; Ohta, T.; Yasuhara, M.; Suzuki, K.; Yamamoto, K. *Nano Lett.* **2004**, *4*, 2163.
- (79) Dubertret, B.; Skourides, P.; Norris, D. J.; Noireaux, V.; Brivanlou, A. H.; Libchaber, A. *Science* **2002**, *298*, 1759.
- (80) (a) Álvarez-Díaz, A. n.; Salinas-Castillo, A.; Camprubí-Robles, M. a.; Costa-Fernández, J. M.; Pereiro, R.; Mallavia, R.; Sanz-Medel, A. *Anal. Chem.* **2011**, *83*, 2712. (b) Wang, S.; Hong, J. W.; Bazan, G. C. *Org. Lett.* **2005**, *7*, 1907.
- (81) (a) Burroughes, J. H.; Bradley, D. D. C.; Brown, A. R.; Marks, R. N.; Mackay, K.; Friend, R. H.; Burns, P. L.; Holmes, A. B. *Nature* **1990**, *347*, 539. (b) Zhang, C. *J. Appl. Phys.* **1993**, *73*, 5177. (c) Braun, D. *Appl. Phys. Lett.* **1991**, *58*, 1982. (d) Pei, Q.; Yu, G.; Zhang, C.; Yang, Y.; Heeger, A. J. *Science* **1995**, *269*, 1086. (e) Gao, J. *Appl. Phys. Lett.* **1997**, *71*, 1293. (f) Cao, Y. *Appl. Phys. Lett.* **1996**, *68*, 3218. (g) Günes, S.; Neugebauer, H.; Sariciftci, N. S. *Chem. Rev.* **2007**, *107*, 1324.
- (82) (a) McQuade, D. T.; Pullen, A. E.; Swager, T. M. *Chem. Rev.* **2000**, *100*, 2537. (b) Klingstedt, T.; Nilsson, K. P. R. *Biochim. Biophys. Acta, Gen. Subj.* **2011**, *1810*, 286. (c) He, F.; Tang, Y.; Yu, M.; Feng, F.; An, L.; Sun, H.; Wang, S.; Li, Y.; Zhu, D.; Bazan, G. C. *J. Am. Chem. Soc.* **2006**, *128*, 6764. (d) Wang, S.; Gaylord, B. S.; Bazan, G. C. *J. Am. Chem. Soc.* **2004**, *126*, 5446. (e) Gaylord, B. S.; Heeger, A. J.; Bazan, G. C. *J. Am. Chem. Soc.* **2003**, *125*, 896. (f) Wang, S.; Bazan, G. C. *Chem.* **2004**, *2508*. (g) Wang, S.; Bazan, G. C. *Adv. Mater.* **2003**, *15*, 1425.
- (83) (a) Wang, Y.; Pu, K.-Y.; Liu, B. *Langmuir* **2010**, *26*, 10025. (b) Fan, C.; Plaxco, K. W.; Heeger, A. J. *J. Am. Chem. Soc.* **2002**, *124*, 5642. (c) Ho, H.-A.; Leclerc, M. *J. Am. Chem. Soc.* **2004**, *126*, 1384.
- (84) (a) Fan, L.-J.; Zhang, Y.; Murphy, C. B.; Angell, S. E.; Parker, M. F. L.; Flynn, B. R.; Jones, W. E., Jr. *Coord. Chem. Rev.* **2009**, *293*, 410. (b) Chen, L.; McBranch, D. W.; Wang, H.-L.; Helgeson, R.; Wudl, F.; Whitten, D. G. *Proc. Natl. Acad. Sci. U.S.A.* **1999**, *96*, 12287.
- (85) (a) Swager, T. M. *Acc. Chem. Res.* **1998**, *31*, 201. (b) Wang, H. L.; O'Connell, M. J.; Chan, C. K.; Li, W. G.; Hicks, R. K.; Doorn, S. K. *Polymer* **2007**, *48*, 7582. (c) Zhang, Y.; Liu, B.; Cao, Y. *Chem.—Asian J.* **2008**, *3*, 739.
- (86) (a) Thayumanavan, S.; Ambade, A. V.; Sandanaraj, B. S.; Klaikherd, A. *Polym. Int.* **2007**, *56*, 474. (b) Herland, A.; Inganas, O. *Macromol. Rapid Commun.* **2007**, *28*, 1703. (c) Wang, S.; Feng, F. D.; He, F.; An, L. L.; Li, Y. H.; Zhu, D. B. *Adv. Mater.* **2008**, *20*, 2959. (d) Li, D.; Song, S.; Fan, C. *Acc. Chem. Res.* **2010**, *43*, 631.
- (87) Wang, Y.; Liu, B. *Langmuir* **2009**, *25*, 12787.
- (88) Liu, B.; Bazan, G. C. *Chem. Mater.* **2004**, *16*, 4467.
- (89) Zhou, Q.; Swager, T. M. *J. Am. Chem. Soc.* **1995**, *117*, 12593.
- (90) Willner, I.; Willner, B. *Trends Biotechnol.* **2001**, *19*, 222.
- (91) (a) Vestergaard, M. d.; Kerman, K.; Tamiya, E. *Sensors* **2007**, *7*, 3442. (b) Okuno, J.; Maehashi, K.; Kerman, K.; Takamura, Y.; Matsumoto, K.; Tamiya, E. *Biosens. Bioelectron.* **2007**, *22*, 2377.
- (92) Wang, J. *Analyst* **2005**, *130*, 421.
- (93) Badia, A.; Carlini, R.; Fernandez, A.; Battaglini, F.; Mikkelsen, S. R.; English, A. M. *J. Am. Chem. Soc.* **1993**, *115*, 7053.
- (94) Akanda, M. R.; Aziz, M. A.; Jo, K.; Tamilavan, V.; Hyun, M. H.; Kim, S.; Yang, H. *Anal. Chem.* **2011**, *83*, 3926.
- (95) Xiao, Y.; Patolsky, F.; Katz, E.; Hainfeld, J. F.; Willner, I. *Science* **2003**, *299*, 1877.
- (96) Wei, M.-Y.; Wen, S.-D.; Yang, X.-Q.; Guo, L.-H. *Biosens. Bioelectron.* **2009**, *24*, 2909.
- (97) Willner, I.; Katz, E. *Angew. Chem., Int. Ed.* **2000**, *39*, 1180.
- (98) (a) Xiao, Y.; Lubin, A. A.; Heeger, A. J.; Plaxco, K. W. *Angew. Chem., Int. Ed.* **2005**, *44*, 5456. (b) Xiao, Y.; Piorek, B. D.; Plaxco, K. W.; Heeger, A. J. *J. Am. Chem. Soc.* **2005**, *127*, 17990.
- (99) Das, J.; Jo, K.; Lee, J. W.; Yang, H. *Anal. Chem.* **2007**, *79*, 2790.
- (100) Pei, H.; Wan, Y.; Li, J.; Hu, H.; Su, Y.; Huang, Q.; Fan, C. *Chem. Commun.* **2011**, *47*, 6254.
- (101) Jia, C. P.; Liu, M. Y.; Jin, Q. H.; Lou, X. H.; Yao, S. H.; Xiang, J. Q.; Zhao, J. L. *Talanta* **2010**, *81*, 1625.
- (102) (a) Wang, J.; Liu, G.; Jan, M. R. *J. Am. Chem. Soc.* **2004**, *126*, 3010. (b) Malhotra, R.; Patel, V.; Vaqué, J. P.; Gutkind, J. S.; Rusling, J. F. *Anal. Chem.* **2010**, *82*, 3118. (c) Chikkaveeraiah, B. V.; Bhirde, A.; Malhotra, R.; Patel, V.; Gutkind, J. S.; Rusling, J. F. *Anal. Chem.* **2009**, *81*, 9129. (d) Gooding, J. J.; Wibowo, R.; Liu, J.; Yang, W.; Losic, D.; Orbons, S.; Mearns, F. J.; Shapter, J. G.; Hibbert, D. B. *J. Am. Chem. Soc.* **2003**, *125*, 9006. (e) Zhang, Q.; Zhao, B.; Yan, J.; Song, S.; Min, R.; Fan, C. *Anal. Chem.* **2011**, 9191.
- (103) Du, D.; Wang, L.; Shao, Y.; Wang, J.; Engelhard, M. H.; Lin, Y. *Anal. Chem.* **2011**, *83*, 746.
- (104) Rusling, J. F.; Mani, V.; Chikkaveeraiah, B. V.; Patel, V.; Gutkind, J. S. *ACS Nano* **2009**, *3*, 585.
- (105) (a) Tang, D.; Su, B.; Tang, J.; Ren, J.; Chen, G. *Anal. Chem.* **2010**, *82*, 1527. (b) Yang, M.; Li, H.; Javadi, A.; Gong, S. *Biomaterials* **2010**, *31*, 3281. (c) Wu, Y.; Chen, C.; Liu, S. *Anal. Chem.* **2009**, *81*, 1600.
- (106) Jiang, W.; Yuan, R.; Chai, Y.-Q.; Yin, B. *Anal. Biochem.* **2010**, *407*, 65.
- (107) So, H.-M.; Won, K.; Kim, Y. H.; Kim, B.-K.; Ryu, B. H.; Na, P. S.; Kim, H.; Lee, J.-O. *J. Am. Chem. Soc.* **2005**, *127*, 11906.
- (108) Du, D.; Zou, Z.; Shin, Y.; Wang, J.; Wu, H.; Engelhard, M. H.; Liu, J.; Aksay, I. A.; Lin, Y. *Anal. Chem.* **2010**, *82*, 2989.
- (109) Huang, J.; Liu, Y.; You, T. *Anal. Methods* **2010**, *2*, 202.
- (110) Yang, M.; Javadi, A.; Li, H.; Gong, S. *Biosens. Bioelectron.* **2010**, *26*, 560.
- (111) Balasubramanian, K.; Burghard, M. *Small* **2005**, *1*, 180.

- (112) (a) Pumera, M.; Sánchez, S.; Ichinose, I.; Tang, J. *Sens. Actuators, B* **2007**, *123*, 1195. (b) Musameh, M.; Wang, J.; Merkoci, A.; Lin, Y. *Electrochim. Commun.* **2002**, *4*, 743.
- (113) (a) Wang, J.; Musameh, M.; Lin, Y. *J. Am. Chem. Soc.* **2003**, *125*, 2408. (b) Wang, J.; Musameh, M. *Anal. Chem.* **2003**, *75*, 2075.
- (114) (a) Xiang, C.; Zou, Y.; Sun, L. X.; Xu, F. *Talanta* **2007**, *74*, 206. (b) Liu, Z.; Shen, Z.; Zhu, T.; Hou, S.; Ying, L.; Shi, Z.; Gu, Z. *Langmuir* **2000**, *16*, 3569.
- (115) (a) Gooding, J. J.; Chou, A.; Eggers, P. K.; Paddon-Row, M. N. *J. Phys. Chem. C* **2009**, *113*, 3203. (b) Yu, X.; Kim, S. N.; Papadimitrakopoulos, F.; Rusling, J. F. *Mol. Biosyst.* **2005**, *1*, 70.
- (116) Yang, Y.-C.; Dong, S.-W.; Shen, T.; Jian, C.-X.; Chang, H.-J.; Li, Y.; Zhou, J.-X. *Electrochim. Acta* **2011**, *56*, 6021.
- (117) Xie, Y.; Chen, A.; Du, D.; Lin, Y. *Anal. Chim. Acta* **2011**, *699*, 44.
- (118) Feng, J.-J.; Zhao, G.; Xu, J.-J.; Chen, H.-Y. *Anal. Biochem.* **2005**, *342*, 280.
- (119) Wang, J.; Li, M.; Shi, Z.; Li, N.; Gu, Z. *Anal. Chem.* **2002**, *74*, 1993.
- (120) Mak, A. C.; Osterfeld, S. J.; Yu, H.; Wang, S. X.; Davis, R. W.; Jejelowo, O. A.; Pourmand, N. *Biosens. Bioelectron.* **2010**, *25*, 1635.
- (121) Gaster, R. S.; Hall, D. A.; Nielsen, C. H.; Osterfeld, S. J.; Yu, H.; Mach, K. E.; Wilson, R. J.; Murmann, B.; Liao, J. C.; Gambhir, S. S.; Wang, S. X. *Nat. Med.* **2009**, *15*, 1327.
- (122) (a) Englebienne, P. *Analyst* **1998**, *123*, 1599. (b) Yamamichi, J.; Ojima, T.; Yurugi, K.; Iida, M.; Imamura, T.; Ashihara, E.; Kimura, S.; Maekawa, T. *Nanomed. Nanotechnol. Biol. Med.* **2011**, *7*, 889. (c) Mayer, K. M.; Lee, S.; Liao, H.; Rostro, B. C.; Fuentes, A.; Scully, P. T.; Nehl, C. L.; Hafner, J. H. *ACS Nano* **2008**, *2*, 687.
- (123) (a) Nam, J.-M.; Park, S.-J.; Mirkin, C. A. *J. Am. Chem. Soc.* **2002**, *124*, 3820. (b) Han, X. X.; Kitahama, Y.; Tanaka, Y.; Guo, J.; Xu, W. Q.; Zhao, B.; Ozaki, Y. *Anal. Chem.* **2008**, *80*, 6567.
- (124) Han, X. X.; Kitahama, Y.; Itoh, T.; Wang, C. X.; Zhao, B.; Ozaki, Y. *Anal. Chem.* **2009**, *81*, 3350.
- (125) (a) Yu, F.; Persson, B.; Löfås, S.; Knoll, W. *J. Am. Chem. Soc.* **2004**, *126*, 8902. (b) Aroca, R.; Kovacs, G. J.; Jennings, C. A.; Loutray, R. O.; Vincett, P. S. *Langmuir* **1988**, *4*, 518.
- (126) Frederix, F.; Friedt, J.-M.; Choi, K.-H.; Laureyn, W.; Campitelli, A.; Mondelaers, D.; Maes, G.; Borghs, G. *Anal. Chem.* **2003**, *75*, 6894.
- (127) Wang, L.; Sun, Y.; Wang, J.; Wang, J.; Yu, A.; Zhang, H.; Song, D. *J. Colloid Interface Sci.* **2010**, *351*, 392.
- (128) Thanh, N. T. K.; Rosenzweig, Z. *Anal. Chem.* **2002**, *74*, 1624.
- (129) Kahraman, M.; Sur, I. I.; Culha, M. *Anal. Chem.* **2010**, *82*, 7596.
- (130) Yang, X.; Gu, C.; Qian, F.; Li, Y.; Zhang, J. *Z. Anal. Chem.* **2011**, *83*, 5888.
- (131) Kelly, K. L.; Coronado, E.; Zhao, L. L.; Schatz, G. C. *J. Phys. Chem. B* **2002**, *107*, 668.
- (132) Zhao, W.; Brook, M. A.; Li, Y. *ChemBioChem* **2008**, *9*, 2363.
- (133) Vaish, A.; Liao, W.-S.; Shuster, M. J.; Hinds, J. M.; Weiss, P. S.; Andrews, A. M. *Anal. Chem.* **2011**, *83*, 7451.
- (134) Dunn, A. R.; Hassell, J. A. *Cell* **1977**, *12*, 23.
- (135) (a) Jalava, T.; Kallio, A.; Leinonen, A. W.; Ranki, M. *Mol. Cell. Probes* **1990**, *4*, 341. (b) Parkkinen, S.; Mantyjarvi, R.; Syrjanen, K.; Syvanen, A. C.; Ranki, M. *Mol. Cell. Probes* **1989**, *3*, 1. (c) Syvanen, A. C.; Laaksonen, M.; Soderlund, H. *Nucleic Acids Res.* **1986**, *14*, 5037. (d) Polksy-Cynkin, R.; Parsons, G. H.; Allerdt, L.; Landes, G.; Davis, G.; Rashtchian, A. *Clin. Chem.* **1985**, *31*, 1438. (e) Ranki, M.; Palva, A.; Virtanen, M.; Laaksonen, M.; Soderlund, H. *Gene* **1983**, *21*, 77. (f) Virtanen, M.; Syvanen, A. C.; Oram, J.; Soderlund, H.; Ranki, M. *J. Clin. Microbiol.* **1984**, *20*, 1083. (g) Langdale, J. A.; Malcolm, A. D. *Gene* **1985**, *36*, 201.
- (136) (a) Langer, P. R.; Waldrop, A. A.; Ward, D. C. *Proc. Natl. Acad. Sci. U.S.A.* **1981**, *78*, 6633. (b) Forster, A. C.; McInnes, J. L.; Skingle, D. C.; Symons, R. H. *Nucleic Acids Res.* **1985**, *13*, 745. (c) Nagata, Y.; Yokota, H.; Kosuda, O.; Yokoo, K.; Takemura, K.; Kikuchi, T. *FEBS Lett.* **1985**, *183*, 379. (d) Dahlen, P.; Syvanen, A. C.; Hurskainen, P.; Kwiatkowski, M.; Sund, C.; Ylikoski, J.; Soderlund, H.; Lovgren, T. *Mol. Cell. Probes* **1987**, *1*, 159.
- (137) Lubin, A. A.; Plaxco, K. W. *Acc. Chem. Res.* **2010**, *43*, 496.
- (138) Kolpashchikov, D. M. *J. Am. Chem. Soc.* **2005**, *127*, 12442.
- (139) Xu, H.; Wu, H.; Huang, F.; Song, S.; Li, W.; Cao, Y.; Fan, C. *Nucleic Acids Res.* **2005**, *33*, e83.
- (140) (a) Xu, Q. H.; Gaylord, B. S.; Wang, S.; Bazan, G. C.; Moses, D.; Heeger, A. J. *Proc. Natl. Acad. Sci. U.S.A.* **2004**, *101*, 11634. (b) Gaylord, B. S.; Heeger, A. J.; Bazan, G. C. *Proc. Natl. Acad. Sci. U.S.A.* **2002**, *99*, 10954.
- (141) (a) He, Y.; Kang, Z. H.; Li, Q. S.; Tsang, C. H.; Fan, C. H.; Lee, S. T. *Angew. Chem., Int. Ed.* **2009**, *48*, 128. (b) He, Y.; Lu, H.; Su, Y.; Sai, L.; Hu, M.; Fan, C.; Wang, L. *Biomaterials* **2011**, *32*, 2133. (c) He, Y.; Su, Y.; Yang, X.; Kang, Z.; Xu, T.; Zhang, R.; Fan, C.; Lee, S. T. *J. Am. Chem. Soc.* **2009**, *131*, 4434. (d) Resch-Genger, U.; Grabolle, M.; Cavaliere-Jaricot, S.; Nitschke, R.; Nann, T. *Nat. Methods* **2008**, *5*, 763.
- (142) Ho, Y. P.; Kung, M. C.; Yang, S.; Wang, T. H. *Nano Lett.* **2005**, *5*, 1693.
- (143) Lee, J.; Kim, I. S.; Yu, H. W. *Anal. Chem.* **2010**, *82*, 2836.
- (144) (a) Somers, R. C.; Bawendi, M. G.; Nocera, D. G. *Chem. Soc. Rev.* **2007**, *36*, 579. (b) Medintz, I. L.; Mattoussi, H. *Phys. Chem. Chem. Phys.* **2009**, *11*, 17. (c) Song, S.; Qin, Y.; He, Y.; Huang, Q.; Fan, C.; Chen, H. Y. *Chem. Soc. Rev.* **2010**, *39*, 4234. (d) Bau, L.; Tecilla, P.; Mancin, F. *Nanoscale* **2011**, *3*, 121.
- (145) (a) Gao, Y.; Stanford, W. L.; Chan, W. C. *Small* **2011**, *7*, 137. (b) Algar, W. R.; Krull, U. J. *Anal. Chem.* **2009**, *81*, 4113.
- (146) Zhao, X.; Tapec-Dytioco, R.; Tan, W. *J. Am. Chem. Soc.* **2003**, *125*, 11474.
- (147) Zhou, X.; Zhou, J. *Anal. Chem.* **2004**, *76*, 5302.
- (148) (a) Esch, M. B.; Locascio, L. E.; Tarlov, M. J.; Durst, R. A. *Anal. Chem.* **2001**, *73*, 2952. (b) Edwards, K. A.; Baeumner, A. J. *Anal. Chem.* **2007**, *79*, 1806. (c) Gunnarsson, A.; Sjovall, P.; Hook, F. *Nano Lett.* **2010**, *10*, 732.
- (149) Locascio-Brown, L.; Plant, A. L.; Horvath, V.; Durst, R. A. *Anal. Chem.* **1990**, *62*, 2587.
- (150) (a) Wang, J.; Li, J.; Baca, A. J.; Hu, J.; Zhou, F.; Yan, W.; Pang, D. W. *Anal. Chem.* **2003**, *75*, 3941. (b) Baca, A. J.; Zhou, F.; Wang, J.; Hu, J.; Li, J.; Wang, J.; Chikneyan, Z. S. *Electroanalysis* **2004**, *16*, 73. (c) Immoos, C. E.; Lee, S. J.; Grinstaff, M. W. *J. Am. Chem. Soc.* **2004**, *126*, 10814. (d) Lin, L.; Zhou, J.; Zhang, Y.; Lin, Z. *Electroanalysis* **2008**, *20*, 1798. (e) Shiddiky, M. J.; Torriero, A. A.; Zeng, Z.; Spiccia, L.; Bond, A. M. *J. Am. Chem. Soc.* **2010**, *132*, 10053. (f) Martic, S.; Labib, M.; Shipman, P. O.; Kraatz, H. B. *Dalton Trans.* **2011**, *40*, 7264. (g) Fan, C.; Plaxco, K. W.; Heeger, A. J. *Proc. Natl. Acad. Sci. U.S.A.* **2003**, *100*, 9134. (h) Zuo, X.; Song, S.; Zhang, J.; Pan, D.; Wang, L.; Fan, C. *J. Am. Chem. Soc.* **2007**, *129*, 1042.
- (151) (a) Lubin, A. A.; Lai, R. Y.; Baker, B. R.; Heeger, A. J.; Plaxco, K. W. *Anal. Chem.* **2006**, *78*, 5671. (b) Kang, D.; Zuo, X.; Yang, R.; Xia, F.; Plaxco, K. W.; White, R. J. *Anal. Chem.* **2009**, *81*, 9109. (c) Pan, D.; Zuo, X.; Wan, Y.; Wang, L.; Zhang, J.; Song, S.; Fan, C. *Sensors* **2007**, *7*, 2671. (d) Zhang, J.; Song, S.; Wang, L.; Pan, D.; Fan, C. *Nat. Protoc.* **2007**, *2*, 2888. (e) Scrimin, P.; Prins, L. J. *J. Chem. Soc. Rev.* **2011**, *40*, 4488.
- (152) (a) Zhang, J.; Song, S.; Zhang, L.; Wang, L.; Wu, H.; Pan, D.; Fan, C. *J. Am. Chem. Soc.* **2006**, *128*, 8575. (b) Steel, A. B.; Herne, T. M.; Tarlov, M. J. *Anal. Chem.* **1998**, *70*, 4670. (c) Lao, R.; Song, S.; Wu, H.; Wang, L.; Zhang, Z.; He, L.; Fan, C. *Anal. Chem.* **2005**, *77*, 6475.
- (153) Suwansa-Ard, S.; Xiang, Y.; Bash, R.; Thavarungkul, P.; Kanatharana, P.; Wang, J. *Electroanalysis* **2008**, *20*, 308.
- (154) (a) Umek, R. M.; Lin, S. W.; Vielmetter, J.; Terbrueggen, R. H.; Irvine, B.; Yu, C. J.; Kayyem, J. F.; Yowanto, H.; Blackburn, G. F.; Farkas, D. H.; Chen, Y. P. *J. Mol. Diagn.* **2001**, *3*, 74. (b) Drummond, T. G.; Hill, M. G.; Barton, J. K. *Nat. Biotechnol.* **2003**, *21*, 1192.
- (155) (a) Xiao, Y.; Lubin, A. A.; Baker, B. R.; Plaxco, K. W.; Heeger, A. J. *Proc. Natl. Acad. Sci. U.S.A.* **2006**, *103*, 16677. (b) Xia, F.; White, R. J.; Zuo, X.; Patterson, A.; Xiao, Y.; Kang, D.; Gong, X.; Plaxco, K. W.; Heeger, A. J. *J. Am. Chem. Soc.* **2010**, *132*, 14346. (c) Xia, F.; Zuo, X.; Yang, R.; White, R. J.; Xiao, Y.; Kang, D.; Gong, X.; Lubin, A. A.; Vallee-Belisle, A.; Yuen, J. D.; Hsu, B. Y.; Plaxco, K. W. *J. Am. Chem.*

- Soc.* **2010**, *132*, 8557. (d) Liu, N.; Jiang, Y.; Zhou, Y.; Xia, F.; Guo, W.; Jiang, L. *Angew. Chem., Int. Ed.* **2013**, *52*, 1842. (e) Duan, R.; Zuo, X.; Wang, S.; Quan, X.; Chen, D.; Chen, Z.; Jiang, L.; Fan, C.; Xia, F. *J. Am. Chem. Soc.* **2013**, *135*, 4604.
- (156) Ferapontova, E. E.; Gothelf, K. V. *Langmuir* **2009**, *25*, 4279.
- (157) (a) Campbell, C. N.; Gal, D.; Cristler, N.; Banditrat, C.; Heller, A. *Anal. Chem.* **2002**, *74*, 158. (b) Dequaire, M.; Heller, A. *Anal. Chem.* **2002**, *74*, 4370. (c) Zhang, Y.; Kim, H. H.; Heller, A. *Anal. Chem.* **2003**, *75*, 3267. (d) Zhang, Y.; Pothukuchi, A.; Shin, W.; Kim, Y.; Heller, A. *Anal. Chem.* **2004**, *76*, 4093. (e) Zhang, J.; Lao, R.; Song, S.; Yan, Z.; Fan, C. *Anal. Chem.* **2008**, *80*, 9029. (f) Wan, Y.; Zhang, J.; Liu, G.; Pan, D.; Wang, L.; Song, S.; Fan, C. *Biosens. Bioelectron.* **2009**, *24*, 1209. (g) Wan, Y.; Lao, R.; Liu, G.; Song, S.; Wang, L.; Li, D.; Fan, C. *J. Phys. Chem. B* **2010**, *114*, 6703. (h) Miranda-Castro, R.; Lobo-Castanon, M. J.; Miranda-Ordieres, A. J.; Tunon-Blanco, P. *Electroanalysis* **2010**, *22*, 1297. (i) Liu, G.; Wan, Y.; Gau, V.; Zhang, J.; Wang, L.; Song, S.; Fan, C. *J. Am. Chem. Soc.* **2008**, *130*, 6820.
- (158) (a) Kim, E.; Kim, K.; Yang, H.; Kim, Y. T.; Kwak, J. *Anal. Chem.* **2003**, *75*, 5665. (b) Palchetti, I.; Laschi, S.; Marrazza, G.; Mascini, M. *Anal. Chem.* **2007**, *79*, 7206. (c) Miranda-Castro, R.; de-Los-Santos-Alvarez, P.; Lobo-Castanon, M. J.; Miranda-Ordieres, A. J.; Tunon-Blanco, P. *Anal. Chem.* **2007**, *79*, 4050. (d) Lee, A. C.; Dai, Z.; Chen, B.; Wu, H.; Wang, J.; Zhang, A.; Zhang, L.; Lim, T. M.; Lin, Y. *Anal. Chem.* **2008**, *80*, 9402. (e) Miranda-Castro, R.; Lobo-Castanon, M. J.; Miranda-Ordieres, A. J.; Tunon-Blanco, P. *Electroanalysis* **2009**, *21*, 267.
- (159) (a) Dominguez, E.; Rincon, O.; Narvaez, A. *Anal. Chem.* **2004**, *76*, 3132. (b) Zhang, L.; Li, D.; Meng, W.; Huang, Q.; Su, Y.; Wang, L.; Song, S.; Fan, C. *Biosens. Bioelectron.* **2009**, *25*, 368. (c) Xie, H.; Zhang, C.; Gao, Z. *Anal. Chem.* **2004**, *76*, 1611. (d) Chen, X.; Xie, H.; Seow, Z. Y.; Gao, Z. *Biosens. Bioelectron.* **2010**, *25*, 1420. (e) Gao, Z.; Peng, Y. *Biosens. Bioelectron.* **2011**, 3768.
- (160) Wu, J.; Campuzano, S.; Halford, C.; Haake, D. A.; Wang, J. *Anal. Chem.* **2010**, *82*, 8830.
- (161) Pei, H.; Lu, N.; Wen, Y.; Song, S.; Liu, Y.; Yan, H.; Fan, C. *Adv. Mater.* **2010**, *22*, 4754.
- (162) Steel, A. B.; Levicky, R. L.; Herne, T. M.; Tarlov, M. J. *Biophys. J.* **2000**, *79*, 975.
- (163) (a) Authier, L.; Grossiord, C.; Brossier, P. *Anal. Chem.* **2001**, *73*, 4450. (b) de la Escosura-Muniz, A.; Parolo, C.; Maran, F.; Mekoci, A. *Nanoscale* **2011**, *3*, 3350. (c) Syvanen, A. C.; Soderlund, H. *Nat. Biotechnol.* **2002**, *20*, 349.
- (164) (a) Park, S. J.; Taton, T. A.; Mirkin, C. A. *Science* **2002**, *295*, 1503. (b) Li, H.; Sun, Z.; Zhong, W.; Hao, N.; Xu, D.; Chen, H. Y. *Anal. Chem.* **2010**, *82*, 5477.
- (165) (a) Zhang, S.; Zhong, H.; Ding, C. *Anal. Chem.* **2008**, *80*, 7206. (b) Chai, Y.; Tian, D.; Wang, W.; Cui, H. *Chem. Commun.* **2010**, *46*, 7560. (c) Duan, R.; Zhou, X.; Xing, D. *Anal. Chem.* **2010**, *82*, 3099.
- (166) (a) Daniel, M. C.; Astruc, D. *Chem. Rev.* **2004**, *104*, 293. (b) Ghosh, S. K.; Pal, T. *Chem. Rev.* **2007**, *107*, 4797.
- (167) (a) Elghanian, R.; Storhoff, J. J.; Mucic, R. C.; Letsinger, R. L.; Mirkin, C. A. *Science* **1997**, *277*, 1078. (b) Taton, T. A.; Mirkin, C. A.; Letsinger, R. L. *Science* **2000**, *289*, 1757. (c) Wilson, R. *Chem. Soc. Rev.* **2008**, *37*, 2028. (d) Lee, J. H.; Wang, Z.; Liu, J.; Lu, Y. *J. Am. Chem. Soc.* **2008**, *130*, 14217. (e) Lin, Y.; Liu, C.; Chang, H. *Anal. Methods* **2009**, *1*, 14. (f) Boisselier, E.; Astruc, D. *Chem. Soc. Rev.* **2009**, *38*, 1759. (g) Niu, Y.; Zhao, Y.; Fan, A. *Anal. Chem.* **2011**, *83*, 7500. (h) Wang, L.; Liu, X.; Hu, X.; Song, S.; Fan, C. *Chem. Commun.* **2006**, *3780*.
- (168) Alivisatos, P. *Nat. Biotechnol.* **2004**, *22*, 47.
- (169) Zu, Y.; Ting, A. L.; Yi, G.; Gao, Z. *Anal. Chem.* **2011**, *83*, 4090.
- (170) Wang, Y. F.; Pang, D. W.; Zhang, Z. L.; Zheng, H. Z.; Cao, J. P.; Shen, J. T. *J. Med. Virol.* **2003**, *70*, 205.
- (171) Tan, E.; Wong, J.; Nguyen, D.; Zhang, Y.; Erwin, B.; Van Ness, L. K.; Baker, S. M.; Galas, D. J.; Niemz, A. *Anal. Chem.* **2005**, *77*, 7984.
- (172) Xu, W.; Xue, X.; Li, T.; Zeng, H.; Liu, X. *Angew. Chem., Int. Ed.* **2009**, *48*, 6849.
- (173) Li, J.; Deng, T.; Chu, X.; Yang, R.; Jiang, J.; Shen, G.; Yu, R. *Anal. Chem.* **2010**, *82*, 2811.
- (174) (a) Su, X.; Teh, H. F.; Lieu, X.; Gao, Z. *Anal. Chem.* **2007**, *79*, 7192. (b) Garcia, J.; Zhang, Y.; Taylor, H.; Cespedes, O.; Webb, M. E.; Zhou, D. *Nanoscale* **2011**, *3*, 3721. (c) Pinijswan, S.; Shipovskov, S.; Surareungchai, W.; Ferapontova, E. E.; Gothelf, K. V. *Org. Biomol. Chem.* **2011**, *9*, 6352.
- (175) Zhang, N.; Appella, D. H. *J. Am. Chem. Soc.* **2007**, *129*, 8424.
- (176) Li, J.; Song, S.; Liu, X.; Wang, L.; Pan, D.; Huang, Q.; Zhao, Y.; Fan, C. *Adv. Mater.* **2008**, *20*, 497.
- (177) Li, J.; Song, S.; Li, D.; Su, Y.; Huang, Q.; Zhao, Y.; Fan, C. *Biosens. Bioelectron.* **2009**, *24*, 3311.
- (178) Zuo, X.; Peng, C.; Huang, Q.; Song, S.; Wang, L.; Li, D.; Fan, C. *Nano Res.* **2009**, *2*, 617.
- (179) (a) Willner, I.; Shlyahovsky, B.; Zayats, M.; Willner, B. *Chem. Soc. Rev.* **2008**, *37*, 1153. (b) Cheng, X.; Liu, X.; Bing, T.; Cao, Z.; Shangguan, D. *Biochemistry* **2009**, *48*, 7817. (c) He, Y.; Tian, Y.; Mao, C. *Mol. Biosyst.* **2009**, *5*, 238.
- (180) (a) Niazov, T.; Pavlov, V.; Xiao, Y.; Gill, R.; Willner, I. *Nano Lett.* **2004**, *4*, 1683. (b) Pavlov, V.; Xiao, Y.; Gill, R.; Dishon, A.; Kotler, M.; Willner, I. *Anal. Chem.* **2004**, *76*, 2152. (c) Zhou, W. H.; Zhu, C. L.; Lu, C. H.; Guo, X.; Chen, F.; Yang, H. H.; Wang, X. *Chem. Commun.* **2009**, *6845*. (d) Nakayama, S.; Sintim, H. O. *J. Am. Chem. Soc.* **2009**, *131*, 10320. (e) Fu, R.; Li, T.; Park, H. G. *Chem. Commun.* **2009**, *5838*.
- (181) Xiao, Y.; Pavlov, V.; Gill, R.; Bourenko, T.; Willner, I. *ChemBioChem* **2004**, *5*, 374.
- (182) Li, T.; Dong, S.; Wang, E. *Chem. Commun.* **2007**, 4209.
- (183) Kolpashchikov, D. M. *J. Am. Chem. Soc.* **2008**, *130*, 2934.
- (184) Deng, M.; Zhang, D.; Zhou, Y.; Zhou, X. *J. Am. Chem. Soc.* **2008**, *130*, 13095.
- (185) Darius, A. K.; Ling, N. J.; Mahesh, U. *Mol. Biosyst.* **2010**, *6*, 792.
- (186) Neo, J. L.; Aw, K. D.; Uttamchandani, M. *Analyst* **2011**, *136*, 1569.
- (187) (a) Willner, I.; Patolsky, F.; Lichtenstein, A. *Anal. Sci.* **2001**, *17*, i351. (b) Gronewold, T. M.; Baumgartner, A.; Quandt, E.; Famulok, M. *Anal. Chem.* **2006**, *78*, 4865. (c) Cooper, M. A.; Singleton, V. T. *J. Mol. Recognit.* **2007**, *20*, 154.
- (188) Fawcett, N. C.; Craven, R. D.; Zhang, P.; Evans, J. A. *Langmuir* **2004**, *20*, 6651.
- (189) Zhou, X.; O'Shea, S. J.; Li, S. *Chem. Commun.* **2000**, 953.
- (190) Mao, X.; Yang, L.; Su, X. L.; Li, Y. *Biosens. Bioelectron.* **2006**, *21*, 1178.
- (191) (a) He, L.; Smith, E. A.; Natan, M. J.; Keating, C. D. *J. Phys. Chem. B* **2004**, *108*, 10973. (b) Wang, Y.; Zhu, X.; Wu, M.; Xia, N.; Wang, J.; Zhou, F. *Anal. Chem.* **2009**, *81*, 8441. (c) Linman, M. J.; Abbas, A.; Cheng, Q. *Analyst* **2010**, *135*, 2759.
- (192) Wark, A. W.; Lee, H. J.; Qavi, A. J.; Corn, R. M. *Anal. Chem.* **2007**, *79*, 6697.
- (193) D'Agata, R.; Corradini, R.; Grasso, G.; Marchelli, R.; Spoto, G. *ChemBioChem* **2008**, *9*, 2067.
- (194) (a) Fritz, J.; Baller, M. K.; Lang, H. P.; Rothuizen, H.; Vettiger, P.; Meyer, E.; Guntherodt, H.; Gerber, C.; Gimzewski, J. K. *Science* **2000**, *288*, 316. (b) Wu, G.; Ji, H.; Hansen, K.; Thundat, T.; Datar, R.; Cote, R.; Hagan, M. F.; Chakraborty, A. K.; Majumdar, A. *Proc. Natl. Acad. Sci. U.S.A.* **2001**, *98*, 1560. (c) Buchapudi, K. R.; Huang, X.; Yang, X.; Ji, H. F.; Thundat, T. *Analyst* **2011**, *136*, 1539. (d) Hagan, M. F.; Majumdar, A.; Chakraborty, A. K. *J. Phys. Chem. B* **2002**, *106*, 10163. (e) Weizmann, Y.; Patolsky, F.; Lioubashevski, O.; Willner, I. *J. Am. Chem. Soc.* **2004**, *126*, 1073. (f) Mukhopadhyay, R.; Lorentzen, M.; Kjems, J.; Besenbacher, F. *Langmuir* **2005**, *21*, 8400. (g) Shekhawat, G.; Tark, S. H.; Dravid, V. P. *Science* **2006**, *311*, 1592. (h) Ramos, D.; Arroyo-Hernandez, M.; Gil-Santos, E.; Tong, H. D.; Van Rijn, C.; Calleja, M.; Tamayo, J. *Anal. Chem.* **2009**, *81*, 2274. (i) Eom, K.; Jung, H.; Lee, G.; Park, J.; Nam, K.; Lee, S. W.; Yoon, D. S.; Yang, J.; Kwon, T. *Chem. Commun.* **2011**, *48*, 955.
- (195) Biswal, S. L.; Raorane, D.; Chaiken, A.; Birecki, H.; Majumdar, A. *Anal. Chem.* **2006**, *78*, 7104.
- (196) Shu, W.; Liu, D.; Watari, M.; Riener, C. K.; Strunz, T.; Welland, M. E.; Balasubramanian, S.; McKendry, R. A. *J. Am. Chem. Soc.* **2005**, *127*, 17054.

- (197) Su, M.; Li, S.; David, V. P. *Appl. Phys. Lett.* **2003**, *82*, 3562.
(198) (a) Fabris, L.; Dante, M.; Braun, G.; Lee, S. J.; Reich, N. O.; Moskovits, M.; Nguyen, T. Q.; Bazan, G. C. *J. Am. Chem. Soc.* **2007**, *129*, 6086. (b) Banholzer, M. J.; Millstone, J. E.; Qin, L.; Mirkin, C. A. *Chem. Soc. Rev.* **2008**, *37*, 885. (c) Larmour, I. A.; Graham, D. *Analyst* **2011**, *136*, 3831. (d) Prado, E.; Daugey, N.; Plumet, S.; Servant, L.; Lecomte, S. *Chem. Commun.* **2011**, *47*, 7425. (e) Bantz, K. C.; Meyer, A. F.; Wittenberg, N. J.; Im, H.; Kurtulus, O.; Lee, S. H.; Lindquist, N. C.; Oh, S. H.; Haynes, C. L. *Phys. Chem. Chem. Phys.* **2011**, *13*, 11551.
(199) Cao, Y. C.; Jin, R.; Mirkin, C. A. *Science* **2002**, *297*, 1536.
(200) Liu, Y.; Zhong, M.; Shan, G.; Li, Y.; Huang, B.; Yang, G. J. *Phys. Chem. B* **2008**, *112*, 6484.
(201) Hu, J.; Zheng, P. C.; Jiang, J. H.; Shen, G. L.; Yu, R. Q.; Liu, G. K. *Analyst* **2010**, *135*, 1084.
(202) Braun, G.; Lee, S. J.; Dante, M.; Nguyen, T. Q.; Moskovits, M.; Reich, N. J. *Am. Chem. Soc.* **2007**, *129*, 6378.
(203) Zhang, Z.; Wen, Y.; Ma, Y.; Luo, J.; Jiang, L.; Song, Y. *Chem. Commun.* **2011**, *47*, 7407.
(204) Thompson, D. G.; Faulds, K.; Smith, W. E.; Graham, D. *J. Phys. Chem. C* **2010**, *114*, 7384.
(205) Thuy, N. T.; Yokogawa, R.; Yoshimura, Y.; Fujimoto, K.; Koyano, M.; Maenosono, S. *Analyst* **2010**, *135*, 595.
(206) (a) Self, C. H.; Dessi, J. L.; Winger, L. A. *Clin. Chem.* **1996**, *42*, 1527. (b) Kobayashi, N.; Goto, J. *Noncompetitive Immunoassays for Small Molecules with High Sensitivity and Specificity*; Academic Press: San Diego, CA, 2001; pp 139–170.
(207) Ueda, H.; Tsumoto, K.; Kubota, K.; Suzuki, E.; Nagamune, T.; Nishimura, H.; Schueler, P. A.; Winter, G.; Kumagai, I.; Mahoney, W. C. *Nat. Biotechnol.* **1996**, *14*, 1714.
(208) Daniels, D. A.; Chen, H.; Hicke, B. J.; Swiderek, K. M.; Gold, L. *Proc. Natl. Acad. Sci. U.S.A.* **2003**, *100*, 15416.
(209) (a) Zuo, X.; Xiao, Y.; Plaxco, K. W. *J. Am. Chem. Soc.* **2009**, *131*, 6944. (b) Zhang, J.; Wang, L.; Pan, D.; Song, S.; Boey, F. Y.; Zhang, H.; Fan, C. *Small* **2008**, *4*, 1196. (c) Golub, E.; Pelosof, G.; Freeman, R.; Zhang, H.; Willner, I. *Anal. Chem.* **2009**, *81*, 9291. (d) Li, F.; Zhang, J.; Cao, X.; Wang, L.; Li, D.; Song, S.; Ye, B.; Fan, C. *Analyst* **2009**, *134*, 1355. (e) Xia, F.; Zuo, X.; Yang, R.; Xiao, Y.; Kang, D.; Vallee-Belisle, A.; Gong, X.; Heeger, A. J.; Plaxco, K. W. *J. Am. Chem. Soc.* **2010**, *132*, 1252. (f) Xia, F.; Zuo, X.; Yang, R.; Xiao, Y.; Kang, D.; Vallee-Belisle, A.; Gong, X.; Yuen, J. D.; Hsu, B. B.; Heeger, A. J.; Plaxco, K. W. *Proc. Natl. Acad. Sci. U.S.A.* **2010**, *107*, 10837. (g) White, R. J.; Rowe, A. A.; Plaxco, K. W. *Analyst* **2010**, *135*, 589. (h) Wen, Y.; Pei, H.; Wan, Y.; Su, Y.; Huang, Q.; Song, S.; Fan, C. *Anal. Chem.* **2011**, *83*, 7418. (i) Freeman, R.; Liu, X.; Willner, I. *J. Am. Chem. Soc.* **2011**, *133*, 11597.
(210) Stojanovic, M. N.; Prada, P.; Landry, D. W. *J. Am. Chem. Soc.* **2000**, *122*, 2.
(211) Freeman, R.; Sharon, E.; Tel-Vered, R.; Willner, I. *J. Am. Chem. Soc.* **2009**, *131*, 5028.
(212) (a) Du, Y.; Li, B.; Guo, S.; Zhou, Z.; Zhou, M.; Wang, E.; Dong, S. *Analyst* **2011**, *136*, 493. (b) Yang, X.; Huang, J.; Wang, Q.; Wang, K.; Yang, L.; Huo, X. *Anal. Methods* **2011**, *3*, 3. (c) Xu, X.; Zhang, J.; Yang, F.; Yang, X. *Chem. Commun.* **2011**, *47*, 9435. (d) Lin, Z.; Luo, F.; Liu, Q.; Chen, L.; Qiu, B.; Cai, Z.; Chen, G. *Chem. Commun.* **2011**, *47*, 8064. (e) Sharma, A. K.; Heemstra, J. M. *J. Am. Chem. Soc.* **2011**, *133*, 12426.
(213) Lee, J. S.; Han, M. S.; Mirkin, C. A. *Angew. Chem., Int. Ed.* **2007**, *46*, 4093.
(214) Lee, J. S.; Mirkin, C. A. *Anal. Chem.* **2008**, *80*, 6805.
(215) He, S.; Li, D.; Zhu, C.; Song, S.; Wang, L.; Long, Y.; Fan, C. *Chem. Commun.* **2008**, 4885.
(216) (a) Tan, Z. Q.; Liu, J. F.; Liu, R.; Yin, Y. G.; Jiang, G. B. *Chem. Commun.* **2009**, 7030. (b) Wu, Y.; Zhan, S.; Xu, L.; Shi, W.; Xi, T.; Zhan, X.; Zhou, P. *Chem. Commun.* **2011**, *47*, 6027. (c) Liu, D.; Wang, Z.; Jiang, X. *Nanoscale* **2011**, *3*, 1421.
(217) Zhu, Z.; Su, Y.; Li, J.; Li, D.; Zhang, J.; Song, S.; Zhao, Y.; Li, G.; Fan, C. *Anal. Chem.* **2009**, *81*, 7660.
(218) Kong, R. M.; Zhang, X. B.; Zhang, L. L.; Jin, X. Y.; Huan, S. Y.; Shen, G. L.; Yu, R. Q. *Chem. Commun.* **2009**, 5633.
(219) Xu, H.; Gao, S.; Yang, Q.; Pan, D.; Wang, L.; Fan, C. *ACS Appl. Mater. Interfaces* **2010**, *2*, 3211.
(220) (a) Pejcic, B.; De Marco, R.; Parkinson, G. *Analyst* **2006**, *131*, 1079. (b) Perfezou, M.; Turner, A.; Merkoci, A. *Chem. Soc. Rev.* **2011**, *41*, 2606. (c) Ho, J. A.; Zeng, S. C.; Tseng, W. H.; Lin, Y. J.; Chen, C. H. *Anal. Bioanal. Chem.* **2008**, *391*, 479. (d) Zhao, Y.; Ye, M.; Chao, Q.; Jia, N.; Ge, Y.; Shen, H. *J. Agric. Food Chem.* **2009**, *57*, 517. (e) Thiruppathiraja, C.; Saroja, V.; Kamatchiammal, S.; Adaikkappan, P.; Alagar, M. *J. Environ. Monit.* **2011**, *13*, 2782.
(221) Driskell, J. D.; Kwarta, K. M.; Lipert, R. J.; Porter, M. D.; Neill, J. D.; Ridpath, J. F. *Anal. Chem.* **2005**, *77*, 6147.
(222) Agrawal, A.; Zhang, C.; Byassee, T.; Tripp, R. A.; Nie, S. *Anal. Chem.* **2006**, *78*, 1061.
(223) Cao, C.; Dhumpa, R.; Bang, D. D.; Ghavifekr, Z.; Hogberg, J.; Wolff, A. *Analyst* **2010**, *135*, 337.
(224) Driskell, J. D.; Jones, C. A.; Tompkins, S. M.; Tripp, R. A. *Analyst* **2011**, *136*, 3083.
(225) Kale, R. R.; Mukundan, H.; Price, D. N.; Harris, J. F.; Lewallen, D. M.; Swanson, B. I.; Schmidt, J. G.; Iyer, S. S. *J. Am. Chem. Soc.* **2008**, *130*, 8169.
(226) Liu, G.; Mao, X.; Phillips, J. A.; Xu, H.; Tan, W.; Zeng, L. *Anal. Chem.* **2009**, *81*, 10013.
(227) Zhong, H.; Zhang, Q.; Zhang, S. *Chem.—Eur. J.* **2011**, *17*, 8388.
(228) Ambrosi, A.; Castaneda, M. T.; Killard, A. J.; Smyth, M. R.; Alegret, S.; Merkoci, A. *Anal. Chem.* **2007**, *79*, 5232.
(229) Niu, H.; Yuan, R.; Chai, Y.; Mao, L.; Yuan, Y.; Cao, Y.; Zhuo, Y. *Chem. Commun.* **2011**, *47*, 8397.
(230) Du, D.; Wang, J.; Lu, D.; Dohnalkova, A.; Lin, Y. *Anal. Chem.* **2011**, *83*, 6580.
(231) Sardesai, N. P.; Barron, J. C.; Rusling, J. F. *Anal. Chem.* **2011**, *83*, 6698.
(232) Chen, X.; Lin, Y. H.; Li, J.; Lin, L. S.; Chen, G. N.; Yang, H. H. *Chem. Commun.* **2011**, *47*, 12116.
(233) Yuan, T.; Liu, Z.; Hu, L.; Zhang, L.; Xu, G. *Chem. Commun.* **2011**, *47*, 11951.
(234) Baeumner, A. J.; Pretz, J.; Fang, S. *Anal. Chem.* **2004**, *76*, 888.
(235) Aveyard, J.; Mehrabi, M.; Cossins, A.; Braven, H.; Wilson, R. *Chem. Commun.* **2007**, 4251.
(236) Toubanaki, D. K.; Christopoulos, T. K.; Ioannou, P. C.; Gravanis, A. *Hum. Mutat.* **2008**, *29*, 1071.
(237) Mao, X.; Ma, Y.; Zhang, A.; Zhang, L.; Zeng, L.; Liu, G. *Anal. Chem.* **2009**, *81*, 1660.
(238) (a) Edwards, K. A.; Baeumner, A. J. *Anal. Chem.* **2006**, *78*, 1958. (b) Wang, S.; Zhao, X.; Khimji, I.; Akbas, R.; Qiu, W.; Edwards, D.; Cramer, D. W.; Ye, B.; Demirci, U. *Lab Chip* **2011**, *11*, 3411. (c) Roda, A.; Mirasoli, M.; Dolci, L. S.; Buragina, A.; Bonvicini, F.; Simoni, P.; Guardigli, M. *Anal. Chem.* **2011**, *83*, 3178.